

Integrated Building Heating, Cooling and Ventilation Control

Bing Dong

School of Architecture

Carnegie Mellon University

September, 2010

Thesis Committee

Dr. Khee Poh Lam, Professor, Architecture

Dr. Charles Neuman, Professor, ECE

Dr. Burcu Akinci, Professor, CEE

Integrated Building Heating, Cooling and Ventilation Control

A Thesis Submitted
in Partial Fulfillment of the Requirements
for the Degree of Doctor of Philosophy
in Building Performance and Diagnostics
in the School of Architecture
Carnegie Mellon University
Pittsburgh, PA

By

Bing Dong
September, 2010

Copyright Declaration

I hereby declare that I am the sole author of this thesis.

I authorize Carnegie Mellon University, Pittsburgh, Pennsylvania to lend this thesis to other institutions or individuals for the purpose of scholarly research.

I authorize Carnegie Mellon University, Pittsburgh, Pennsylvania to reproduce this thesis by photocopying or by other means, in total or in part, at the request of other institutions or individuals for the purpose of scholarly research.

Dedicated to
my wife Yan Yuan

with Jesus Christ's Love

Acknowledgements

I express my deepest appreciation to Prof. Khee Poh Lam, chair of my PhD thesis committee. Prof. Lam not only guides me through rigorous research, but also leads me in a positive attitude in my daily life. His passion, patience, diligence and wisdom always influences me from the past to the future. He is truly my professor, mentor and friend.

I express my sincerely gratitude to Prof. Charles Neuman. Prof. Neuman taught me everything about the fundamentals of controls. He spent great efforts and countless hours with me to solve control problems in this thesis. His rigorous research attitude and attention to details has substantially improved my research outputs. He is the role model in the fundamental research.

My special thanks go to Prof. Burcu Akinci. She is such a nice person with great respect for her students. Her thoughts and knowledge in Building Information Modeling greatly inspired the topic of “integration” in this thesis. With her advice, this thesis brings the idea of static and dynamic information resources through the control modeling and operation.

I thank many friends that weave into my everyday life and offer my family enormous support. In particular to Prof. Ramesh Krishnamurti for our pool time, Yun Gu, Eugene Ooi, Mei Ru Ooi, Scot Myhr family, ManYu Li, Nianshong Chok, Chunjie Gan, Xiaoqian Jiang, Peng Zheng family, Rui Zhang, Tsung-Hsien Wang, Tajin Biswas, Yuebin Yu, Hu Yang, Erica Cochran, Omer T. Karaguzel, Rongpeng Zhang and Jie Zhao.

Finally, my deepest love and appreciation goes to my wife, Mrs. Yan Yuan. Through my PhD time, we witnessed both the best and worst time in our life. For me to complete my PhD study, her sacrifice is beyond anyone’s imagination.

Abstract

Current research studies show that building heating, cooling and ventilation energy consumption account for nearly 40% of the total building energy use in the U.S. The potential for saving energy through building control systems varies from 5% to 20% based on recent market surveys. In addition, building control affects environmental performances such as thermal, visual, air quality, etc., and occupancy such as working productivity and comfort. Building control has been proven to be important both in design and operation stages.

Building control design and operation need consistent and reliable static and dynamic information from multiple resources. Static information includes building geometry, construction and HVAC equipment. Dynamic information includes zone environmental performance, occupancy and outside weather information during operation.. At the same time, model-based predicted control can help to optimize energy use while maintaining indoor set-point temperature when occupied. Unfortunately, several issues in the current approach of building control design and operation impede achieving this goal. These issues include: a) dynamic information data such as real-time on-site weather (e.g., temperature, wind speed and solar radiation) and occupancy (number of occupants and occupancy duration in the space) are not readily available; b) a comprehensive building energy model is not fully integrated into advanced control for accuracy and robustness; c) real-time implementation of indoor air temperature control are rare. This dissertation aims to investigate and solve these issues based on an integrated building control approach.

This dissertation introduces and illustrates a method for integrated building heating, cooling and ventilation control to reduce energy consumption and maintain indoor temperature set-point, based on the prediction of occupant behavior patterns and weather conditions. Advanced machine learning methods including Adaptive Gaussian Process, Hidden Markov Model, Episode Discovery and Semi-Markov Model are modified and

implemented into this dissertation. A nonlinear Model Predictive Control (NMPC) is designed and implemented in real-time based on Dynamic Programming. The experiment test-bed is setup in the Solar Decathlon House (2005), with over 100 sensor points measuring indoor environmental parameters such as temperature, relative humidity, CO₂, lighting, motion and acoustics, and power consumption for electrical plugs, HVAC and lighting. The outdoor environmental parameters, such as temperature, relative humidity, CO₂, global horizontal solar radiation and wind speed, are measured by the on-site weather station. The designed controller is implemented through LabVIEW.

The experiments are carried out for two continuous months in the heating season and for a week in cooling season. The results show that there is a 26% measured energy reduction in the heating season compared with the scheduled temperature set-points, and 17.8% energy reduction in the cooling season. Further simulation-based results show that with tighter building façade, the cooling energy reduction could reach 20%. Overall, the heating, cooling and ventilation energy reduction could reach nearly 50% based on this integrated control approach for the entire heating/cooling testing periods compared to the conventional scheduled temperature set-point.

Table of Contents

Abstract	i
List of Figures	vii
List of Tables	xii
Nomenclature	xiv
Chapter 1 Introduction	1
1.1 Background and Motivation	1
1.2 Literature Review	5
1.2.1 Model-based Supervisory Control	5
1.2.2 Optimization techniques in the building HVAC controls	11
1.2.3 Occupant detection and behavior prediction in buildings	13
1.2.4 Summary of Literature Review	16
1.3 Research Objective and Approach	16
1.4 Thesis Chapter Overview	18
Chapter 2 Development of the Occupant Behavior Pattern Model	19
2.1 Introduction	19
2.2 Model Development for Detecting Number of Occupants	19
2.2.1 Data Collection	22
2.2.2 Feature Selection	22
2.2.3 Occupancy Estimation Methodology	25
2.3.1.1 Neural Network	25
2.3.1.2 Hidden Markov Model	27

2.2.4 Preliminary Experiment Results	29
2.3 Model Development for Occupancy Duration Estimation	32
2.3.1 Event Detector	33
2.3.2 Episode Discovery	36
2.3.3 Semi-Markov model generation	38
2.3.4 Connections to Building Energy Management	39
2.3.5 Preliminary Experiment Results	41
2.4 Summary	47
Chapter 3 Development of the Building Model	49
3.1 Experiment Setup	49
3.1.1. Overview of HVAC Systems.....	50
3.1.2 Sensor Network.....	53
3.1.2.1 Environmental Sensor Network	54
3.1.2.2 System Sensor Network.....	56
3.2 Building Zone Model.....	57
3.2.1 Model of Zone Air Infiltration.....	57
3.2.2 Model of Wall Heat Transfer.....	58
3.2.3 Model of Zone Heat Transfer	60
3.3 Building HVAC System Model.....	63
3.3.1 Radiant Floor Heating System Model.....	63
3.3.1.1 Model of Radiant Floor Heating.....	64
3.3.1.2 Model of Tankless Water Heater	67
3.3.2 Heat Pump Cooling.....	68
3.4 Parameter Identification.....	69
3.4.1 Objective Function of Optimization	70

3.4.2 Identification Process.....	71
3.5 Validation of the Building Model.....	72
3.5.1 Data Collection	72
3.5.2 Validation Criteria	73
3.5.3 Results and Discussion	73
3.5.3.1 Building thermal properties	73
3.5.3.2 Radiant floor system	79
3.5.3.3 Heat pump system.....	84
3.6 Summary	85
Chapter 4 Integrated Building Control Design and Implementation ...	87
4.1 Optimal Control Design.....	87
4.1.1 Problem Formulation	87
4.1.1.1 Non-linear Model Predictive Control	87
4.1.1.2 Characteristics of Proposed NMPC	91
4.1.2 Optimization Algorithm.....	93
4.1.2.1. Genetic Algorithm	93
4.1.2.2 Dynamic Programming.....	94
4.1.3 Comparisons of Computational Time.....	96
4.1.4 Comparisons of Optimization Results	97
4.2 Optimal Control Implementation.....	98
4.2.1 Overview.....	98
4.2.2 Heating Season.....	99
4.2.2.1 Experiment Setup.....	99
4.2.2.2 Results and Discussion	99
4.2.2.3 Sensitivity Analysis of Heating Controls.....	124

4.2.3 Cooling Season	126
4.2.3.1 Experiment Setup.....	126
4.2.3.2 Results and Discussion	126
4.2.3.3 Sensitivity Analysis of Cooling Controls	136
4.3 Summary	137
Chapter 5 Conclusion.....	138
5.1 Contributions.....	138
5.2 Summary of Findings.....	139
5.3 Future Work	140
References	142

List of Figures

Figure 1.1 Installed units versus system impact on energy consumption in buildings (WBCSD, 2009).....	2
Figure 1.2 Occupant interactions with the surrounding environment.....	13
Figure 2.1 Sensor network layout of the Intelligent Workplace, Carnegie Mellon University.....	21
Figure 2.2 Structure of 2-hidden layer Neural Network used in occupancy detection.....	26
Figure 2.3 Structure of HMM.....	27
Figure 2.4 Occupancy estimation results of bay 13_p2 on March 21 with ANN of 75% accuracy	29
Figure 2.5 Occupancy estimation results of bay 13_p2 on March 21 with HMM of 75% accuracy	29
Figure 2.6 Occupancy estimation results of bay 13 from results from dataset b13_p3 from March 21 to April 3 with HMM of 70% accuracy.....	30
Figure 2.7 Occupancy estimation results of bay 10 from results from dataset b10_p3 from March 27 to April 3 with HMM of 65% accuracy.....	31
Figure 2.8 A holistic view of occupancy duration estimation	33
Figure 2.9 One day example of acoustic events	34
Figure 2.10 Example motion events	35
Figure 2.11 Differences between HMM and SMM.....	38
Figure 2.12 HVAC controls based on pattern recognition	40
Figure 2.13 Test-bed in a conference room	41
Figure 2.14 A one day example results of event detection.....	42
Figure 2.15 Markov model of discovered patterns on 10 minutes maximal window.....	43
Figure 2.16 Semi-Markov model of discovered patterns on 10 minutes maximal window	43
Figure 2.17 Markov model of discovery patterns on patterns	44
Figure 2.18 Semi-Markov model of discovery patterns on patterns.....	44

Figure 2.19 Temperature profile on Summer Design Day (July 21) based on different set points.....	47
Figure 3.1 Exterior view of solar decathlon house 2005 at CMU	49
Figure 3.2 Layout of solar decathlon house.....	50
Figure 3.3 Overview of the energy supply and demand systems in the SD House	51
Figure 3.4 Overview of the sensing infrastructure in solar house	53
Figure 3.5 Environmental sensors in solar house	55
Figure 3.6 Power system measurement	56
Figure 3.7 Heating and cooling system sensors.....	56
Figure 3.8 Wall Heat Transfer Modular	59
Figure 3.9 Thermal network model of solar house test-bed	61
Figure 3.10 Section view of radiant heating floor system	64
Figure 3.11 Water heater temperature rise vs. flow rate.....	67
Figure 3.12 Parameter estimation process	72
Figure 3.13 Model predicted meeting room indoor temperature profile from October 1 to November 29, 2009.....	74
Figure 3.14 Model predicted office room indoor temperature profile from October 1 to November 29, 2009.....	74
Figure 3.15 Model predicted meeting room indoor air temperature profile from October 13 to October 18, 2009.....	75
Figure 3.16 Model predicted office room indoor air temperature profile from October 13 to October 18, 2009.....	75
Figure 3.17 Model predicted meeting room and office indoor air temperature profile on October 18, 2009.....	76
Figure 3.18 Model predicted meeting room indoor air temperature profile from October 1 to October 7, 2009.....	76
Figure 3.19 Model predicted office indoor air temperature profile from October 1 to October 7, 2009.....	77
Figure 3.20 Model predicted floor surface temperature profile from October 1 to November 29, 2009.....	79

Figure 3.21 Meeting room floor surface temperature profile and water flow rate from October 12 to October 18, 2009.....	80
Figure 3.22 Meeting room floor surface temperature profile and water flow rate from October 17 to October 18, 2009.....	81
Figure 3.23 Meeting room floor surface temperature profile and water flow rate from October 21 to October 27, 2009.....	82
Figure 3.24 Results of tankless water heater power consumption validation for one week heating testing period.....	83
Figure 3.25 Meeting room indoor temperature profile during one week cooling testing period.....	84
Figure 3.26 Meeting room cooling energy consumption prediction from July 5 to July 10, 2010.....	85
Figure 4.1 Illustration of NMPC moving horizon control.....	89
Figure 4.2 Overview of the NMPC Design.....	90
Figure 4.3 Nature of the optimal control problem.....	92
Figure 4.4 Schema of GA process in MATLAB/Simulink.....	94
Figure 4.5 Dynamic programming based optimal control.....	95
Figure 4.6 Results of energy optimization comparisons between DP and GA.....	97
Figure 4.7 Overview of optimal control implementation schema.....	98
Figure 4.8 Results of hourly local outdoor air temperature prediction from January 18 to March 19, 2010.....	100
Figure 4.9 Results of hourly local outdoor air temperature prediction from February 1 to February 7, 2010.....	101
Figure 4.10 Results of hourly local outdoor air temperature prediction from February 6 to February 11, 2010.....	102
Figure 4.11 Results of hourly local global horizontal solar radiation prediction from January 18 to March 19, 2010.....	103
Figure 4.12 Results of hourly local global horizontal solar radiation prediction from February 1 to February 7, 2010.....	104
Figure 4.13 Results of hourly local global horizontal solar radiation prediction from February 7 to February 12, 2010.....	105

Figure 4.14 Results of hourly local wind speed prediction from January 18 to March 19, 2010.....	106
Figure 4.15 Results of hourly local wind speed prediction from February 1 to February 7, 2010.....	107
Figure 4.16 Results of hourly local global horizontal solar radiation prediction from March 7 to March 14, 2010.....	108
Figure 4.17 Results of occupancy pattern prediction from January 18 to March 20, 2010	109
Figure 4.18 Results of occupancy pattern prediction from February 1 to February 7, 2010	111
Figure 4.19 Results of occupant pattern prediction on February 1, 2010.....	111
Figure 4.20 Results of occupant pattern prediction from February 7 to February 14, 2010	112
Figure 4.21 Results of occupant pattern prediction on February 11, 2010.....	113
Figure 4.22 Results of occupant pattern prediction from March 16 to March 19, 2010	113
Figure 4.23 Markov model of discovered patterns on 10 minutes maximal window....	115
Figure 4.24 Comparison of energy profile between NMPC and scheduled temperature set-points from January 18 to March 20, 2010	117
Figure 4.25 Temperature profile from February 1 to February 7, 2010	118
Figure 4.26 Comparison of energy profile between NMPC and scheduled temperature set-points of scenario one.....	119
Figure 4.27 Temperature profile from February 1 to February 7, 2010	120
Figure 4.28 Comparison of energy profile between NMPC and scheduled temperature set-points on February 2, 2010.....	121
Figure 4.29 Comparison of energy profile between NMPC and scheduled temperature set-points of scenario two	122
Figure 4.30 Temperature profile from February 7 to February 13, 2010	123
Figure 4.31 Heating energy profile of high occupancy changes on February 5, 2010 ...	124
Figure 4.32 Heating energy profile of moderate occupancy changes on February 4, 2010	125
Figure 4.33 Heating energy profile of low occupancy changes on March 5, 2010	125

Figure 4.34 Results of 15 minutes local outdoor air temperature prediction from July 5 to July 10, 2010.....	127
Figure 4.35 Results of 15 minutes local global horizontal solar radiation prediction from July 5 to July 10, 2010	127
Figure 4.36 Results of 15 minutes local wind speed prediction from July 5 to July 10, 2010.....	128
Figure 4.37 Results of occupancy pattern prediction from July 5 to July 10, 2010	129
Figure 4.38 Results of occupancy pattern prediction on July 6, 2010.....	129
Figure 4.39 Markov model of discovered patterns on 10 minutes maximal window....	130
Figure 4.40 Supply air flow rate with different occupancy level	131
Figure 4.41 Comparison of energy profile between NMPC and scheduled temperature set-points on July 1, 2010	132
Figure 4.42 Energy consumption profile of NMPC from July 5 to July 10, 2010	132
Figure 4.43 Comparison of energy profile between NMPC and scheduled set-point	133
Figure 4.44 Indoor temperature profile based on NMPC from July 5 to July 10, 2010 .	134
Figure 4.45 Comparison of energy profile between NMPC and simulated energy from better envelope.....	135
Figure 4.46 Cooling energy profile of high occupancy changes on July 6, 2010.....	136
Figure 4.47 Cooling energy profile of moderate occupancy changes on July 8, 2010...	136

List of Tables

Table 1.1 Summary of energy saving potentials for different control approaches (Brambley, 2005).....	2
Table 1.2 Information requirements for the design and operation of a model-based building control.....	3
Table 1.3 Summary of main optimization techniques used in building HVAC supervisory controls.....	12
Table 1.4 Comparisons of integrated HVAC control with previous studies	16
Table 2.1 Data collection periods	22
Table 2.2 Investigated features of CO ₂	24
Table 2.3 Information gain with different number of features as output for CO ₂ for the period B13_P1	25
Table 2.4 Summary of occupant number prediction in IW	31
Table 2.5 Definition of important events from sensors	33
Table 2.6 Results of Patterns from MDL and PD.....	42
Table 2.7 Building loads and comfort based on different HVAC set point schedules in the conference room.....	46
Table 3.1 Thermo-physical properties of radiant floor materials	64
Table 3.2 Measured cooling supply air flow rate and temperature.....	69
Table 3.3 Scale Factor Limits for Optimization Search Space.....	71
Table 3.4 Sensitivity analysis of identified building thermal properties	78
Table 3.5 Flow Rate Corresponding to Valve Opening.....	79
Table 3.6 Sensitivity analysis of identified radiant floor thermal properties.....	82
Table 4.1 Definitions for State, Control Variables and Disturbances.....	91
Table 4.2 Comparison of total heating energy consumption and set-point not met hours	118
Table 4.3 Comparison of heating energy consumption and set-point not met hours in scenario one	120

Table 4.4 Comparison of total heating energy consumption of scenario two	123
Table 4.5 Heating energy consumption and daily occupancy changes	126
Table 4.6 Comparison of total cooling energy consumption.....	134

Nomenclature

A_l	Effective air leakage area
C_{air}	Specific heat of the air
C_{out}	Heat capacitance of the external part of the wall
C_{int}	Heat capacitance of the internal part of the wall
$C_{MR_Air_in}$	Heat capacitance of the internal part of the wall in meeting room
C_{oz_in}	Heat capacitance of the internal part of the wall in other zone
$C_{Off_Air_in}$	Heat capacitance of the internal part of the wall in office
$C_{MR_cf_sp}$	Specific heat of concrete floor
C_r	Correction factor due to the impact of indoor furniture
C_s	Stack coefficient
C_w	Wind coefficient
h_{cf}	Overall heat transfer coefficient for floor surface, which includes both radiation and convection
\dot{m}_{MR_cf}	Mass density of concrete floor
m_{fcu}	Air mass flow rate
O_i	<i>ith</i> observation
$P(X_n)$	Probability of X_n
Q_{sol_out}	Solar radiation on the outside surface of the wall
Q_{int_rad}	Internal radiative heat gain absorbed by inside surface of the wall
Q_{FCU_MR}	Load from fan coil unit cooling
Q_{int}	Load from internal heat gain
Q_{inf}	Load from internal infiltration
R_{out}	Outside wall convective heat transfer coefficient
R_{int}	Inside wall convective heat transfer coefficient
R_{wall}	Thermal resistance of the wall
R_{MR_air}	Indoor air convective heat transfer coefficient
$R_{MR_air_f}$	Coefficient of combined effects of radiation and convection between room air and radiant heating floor
R_{MR_cf}	Thermal resistance of the concrete floor in meeting room

R_{oz_MR}	Convective heat transfer coefficient between meeting room and other zone
R_{MR_Off}	Convective heat transfer coefficient between meeting room and office
ΔT	Indoor-outdoor temperature difference
$T_{sur_MR_in}^i$	Surface temperature of the i th internal wall
T_{MR_in}	Room air temperature
\bar{T}_{MR_w}	Temperature around the water tubes
U_{wf}	Water to floor heat transfer coefficient
V_{infl}	Air flow rate from infiltration
V_{wind}	Local wind speed
X_i	i th state in Markov Model
X	A vector of unknown parameters
X_L	Lower bound of unknown parameters
X_u	Upper bound of unknown parameters
α_i	Forward factor
α_{ab_w}	Coefficient of absorbed solar radiation on the external surface of an external wall
β_i	Backward factor
β_{ab_w}	Coefficient of absorbed transmitted solar radiation on the inside surface of an external wall
γ_{ab_w}	Coefficient of absorbed internal heat gain from occupancy and equipment by inside surface of the wall
σ	Stefan-Boltzmann constant
ϵ	Surface total Hemispherical emissivity
μ	Coefficient of transmitted solar radiation absorbed by the concrete floor

1.1 Background and Motivation

Background

Three years ago, the World Business Council for Sustainable Development published the first report on energy efficiency in buildings stating that buildings are responsible for at least 40% of energy use in many countries, energy mostly derived from fossil fuels. Worldwide building energy consumption is expected to grow 45% over the next 20 years (WBCSD, 2007). In the United States, commercial buildings consume almost 17% of national energy use. 76% of the services used by buildings (e.g. heating, cooling, lighting, etc.) are powered by electricity, and these account for 35% of the total electricity consumed nationally (EIA, 2009). Heating, ventilation and air-conditioning (HVAC) systems in commercial buildings account for nearly 37% of the total building energy.

According to the market surveys done by Brambley (2005), building controls can potentially reduce energy consumption significantly in commercial buildings. Table 1.1 demonstrates how a traditional Energy Management and Control System (EMCS) can save between 5 and 15% of a building's energy with an 8 to 10 year return on investment for the system, while occupancy sensors for lighting control can save 20 to 28% energy with 1 to 5 years payback on the initial investment. In addition, one of the objectives of almost every control system is to improve temperature control and provide thermal comfort for occupants. Figure 1.1 further illustrates that HVAC controls have the biggest impact on the building energy consumption, yet with the least installations in buildings.

In addition, the Building Investment Decision Support Tool developed by the Center for Building Performance and Diagnostics at Carnegie Mellon University has identified 20 studies that link improved temperature control to productivity gains, with an average 5.5% productivity increase and a range of other improvements of between 6.2% and 24% (eBIDS, 2010).

Table 1.1 Summary of energy saving potentials for different control approaches (Brambley, 2005)

Control Technology	Technical Market Size [billions ft ²]	Relevant Primary Energy [quads]	Energy Savings [%]	Technical Energy Savings Potential [quads]	Simple Payback Period [years]	Remaining Market Penetration	Market-Achievable Energy Savings [quads]
Energy Management and Control System (EMCS)	33	6.2	5-15%	0.3 – 0.9	8-10	5-10%	0.02-0.09
Commissioning	55	9.8 ^(a)	5-15%	0.5 – 1.5	2-10	3-30%	0.015-0.5
Automatic Fault Detection and Diagnostics (AFDD)/Continuous Commissioning	55	9.8 ^(a)	5-15%	0.5 – 1.5	1-3	15-55% / 6-24%	0.07 – 0.8 / 0.03-0.35
Occupancy Sensors for Lighting Control	50	3.5	20-28%	0.7 – 1.0	1 – 5	0-45%	0-0.45
Photosensor-Based Lighting Control	55	3.9	20-60%	0.8 – 2.3	1 – 7	8-55%	0.08–1.3
Demand Controlled Ventilation (DCV)	55	5.4	10-15%	0.5 – 0.8	2 – 3	15-30%	0.08-0.25

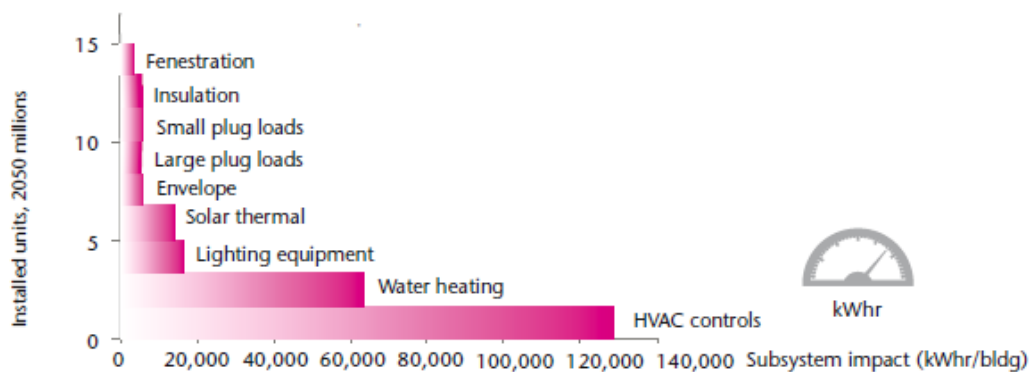


Figure 1.1 Installed units versus system impact on energy consumption in buildings (WBCSD, 2009)

Typical control functions in buildings can be divided into two categories: local control and supervisory control. Local control provides basic control and automation functions, such as ON/OFF control and proportional-integral-derivative (PID) control, that allow

building services to operate properly. Many studies show that local controls can provide thermal comfort and satisfy goals for indoor air quality (Moore and Fisher, 2003; Nassif, et al. 2005; Zhang, et al. 2005). Supervisory control functions are higher level controls that include local control functions while considering whole system characteristics (both HVAC and passive systems), interaction and energy optimization for total building energy saving. Supervisory control functions are developed using the physical model-based method, hybrid method, performance mapping method and data learning approach (Wang, et al. 2008). In the last decade, research has increasingly focused on supervisory control due to higher energy prices and tighter energy supply. This thesis will focus on the hybrid method combining physical model-based method, which is supervisory and set-point control, which is local.

A typical physical model-based method involves using dynamic/static equations to construct control methods, where the equations are based on fundamental thermal dynamics, heat and mass transfer. During the initial control design stage and the later operation stage, both static and dynamic information are needed for a successful model-based control design and online control management of operation as shown in Table 1.2 below.

Table 1.2 Information requirements for the design and operation of a model-based building control

Information Type	Information Elements	
Input Parameters During Control Design Stage		
Geometry Information	Static Information	No. of thermal zones
		No. of doors, windows
		Wall surface area
		Zone volume
		Surface orientation, tilt and azimuth
Construction Information	Static Information	External/internal wall, window and door construction type
		Material properties: thickness, thermal conductivity, specific heat, solar/infrared absorbance
Zone Interior Information	Dynamic Information	Internal gains: No. of occupants, amount of internal equipment
		Indoor temperature set-point, air flow rate, etc.
System Information	Static	HVAC system type (chiller, heat pump, fan coil, etc.) and their physical parameters

	Information	Duct or pipe physical parameters such length
	Dynamic Information	Designed operation information
Weather Information	Dynamic Information	Outside temperature, solar radiation, etc.
Data Resources During Operation		
Static Information	CAD MEP drawings, construction and material manufactures, predefined schedules for HVAC systems, occupancy, lighting, etc.	
Dynamic Information	Real-time HVAC system performance from sensors in systems such as: supply air temperature, supply air flow rate, return air temperature, relative humidity Real-time indoor environmental measures from sensors such as: temperature, RH, CO ₂ , air flow, etc. , and dynamic occupancy information from sensors Dynamic usage of internal equipment from power metering Historical/simulated weather information, onsite weather measurements	

Motivation

This thesis focuses on the integrated building control design and operation. The integration here refers to: 1) the prediction of dynamic occupancy changes and weather information; 2) the optimal control profile which minimizes the energy consumption while maintaining set-point temperature. From the literature review, an integrated building control requires (Braun, 2007; Wang, et al. 2008):

- Correct and consistent static information;
- Available and reliable dynamic information;
- Predictable and robust controller behavior;
- Efficient optimal control algorithm;
- Online implementable.

Unfortunately, there are several issues in the current approach to achieve this goal. These issues include:

- Fragmented static and dynamic information
- Dynamic information such as real-time onsite weather (e.g. temperature, wind speed and solar radiation) and occupancy (number of occupants and occupancy duration in the space) data are not available

- Comprehensive whole building energy prediction model is not fully integrated into advanced controls for accuracy and robustness
- Real-time implementation cases of such control on indoor air temperature are few.

1.2 Literature Review

The literature review is organized into three parts:

1. Model-based supervisory control
2. Optimization techniques in the building HVAC controls
3. Occupancy detection and behavior prediction in buildings

1.2.1 Model-based Supervisory Control

In this thesis, the term model-based control particularly refers to the physical-model based control. In this modeling process, physical models are used to predict the energy/cost and environment performance. The terminology, physical model, begins with the description of a system or process and uses a priori knowledge of the system or process to specify an equation-based model that serves as the basis for overall performance prediction. These models have high performance in prediction and high control reliabilities. Based on this process, this control method can further be divided into two main categories: Equations developed from scratch and equations integrated into existing energy simulation tools.

Developing Equations from Scratch

Many studies in building controls over the last two decades fall into this category and the equations tend to be simplified. Taking the whole building thermal, mass, heat transfer and other factors into equations is too complex and impractical for control design. Simplified models have been shown to greatly improve building energy efficiency

(Henze, et al. 1997; Zaheer-uddin and Zheng, 2001; Zhang and Hanby, 2006; Sane and Guay, 2008).

Kaya, et al.(1982) initially introduced a thermal model based on the equations for an office space along with an index of energy use to develop the optimal control method for one air conditioned zone. The main objective of this study is to demonstrate improvement in control performance and reduction in energy consumption through controlling temperature, humidity, and velocity simultaneously rather than independently. The results indicated that the optimal control strategy can result in reduced energy use.

House, et al. (1991) and House and Smith (1995) developed a systematic standard approach for physical model-based optimal control of building HVAC systems. The detailed plant equations are derived from the principles of conservation of mass and energy, where the interactive of system components, the multi-zone building systems and their interaction were considered. A nonlinear programming technique is used to solve the optimal control problem. Four cases were simulated and the final results show there is a 24% reduction in operation costs compared to the conventional control strategy, while the comfort zone is maintained in only one case.

Kota, et al. (1996) applied the dynamic programming (DP) technique to the optimal control of building HVAC systems. The optimization results were compared with that obtained from a nonlinear programming (NLP) technique using the sequential quadratic programming (SQP) method. The results showed that DP is more efficient compared with NLP for the example problems, while NLP is more robust and can treat constraints on the state variables directly.

Zaheer-uddin and his colleagues completed several studies on the optimal and sub-optimal control of variable-air-volume (VAV) systems in buildings (Zaheer-uddin and Patel 1995; Zheng and Zheer-uddin 1996; Zaheer-uddin and Zheng, 2001). Their simulation results demonstrated that these optimal and sub-optimal control strategies, in

which the multiple control variables were optimized simultaneously using the steepest descent method, can improve the system performance and operational efficiency.

Henze, et al. (1997) paid great attention to the predictive optimal control of building thermal storage systems. In this study, a predictive optimal controller is developed and the performance of the controller validated by simulations. This optimal controller minimized operating costs of the cooling plant over the simulation horizon. An optimal storage charging and discharging strategy is planned at every time step over a fixed 24-hour horizon. The simulation results showed that his optimal controller can achieve significantly better system performance than the conventional controller.

Wang and Jin (2000) presented an optimal control strategy for VAV systems, where the simplified physical models were utilized to predict the overall system performance. Genetic algorithm (GA) was used to solve the optimization problem of multiple control variables. This was the first application of GA in the building HVAC control domain. The simulation results demonstrated that this proposed real time control strategy can improve the overall system energy performance and reduce energy use.

Mendes, et al. (2003) introduced the development of the physical model based on the Matlab/Simulink for building temperature performance analysis with automatic control. They built up a room model based on principles of thermal and mass balance equations with a lumped capacitance approach. A fuzzy logic control (FLC) algorithm was applied and the results show that the new FLC logic has less settling time and a more stable room temperature than the conditional PID controller.

Zhang and Hanby (2006) presented a model-based supervisory control of renewable energy systems. The objective of the control problem was to minimize the net external energy consumption of the system subject to a series of constraints. An evolutionary algorithm was used to seek the optimal and near-optimal control settings. The simulation results indicated that significant improvements in system operations are possible as compare to the existing rule-based control schema. The results also indicated that

significant improvement in execution time will be needed for any future online deployment.

Sane and Guay (2008) presented a real-time dynamic minmax optimization technique over a finite-time horizon applied to the building “demand response” problem. This approach is applied to the peak power demand control problem where electricity consumption and peak power usage in a building has to be controlled in response to real-time pricing. They applied this method to a supervisory control problem for building HVAC control that involves minimization of fixed horizon electric utility cost. The one-day simulation results showed that real-time optimization procedures can provide significant reductions in energy costs.

Some model-based approaches mentioned above (House and Smith, 1995; Zaheer-uddin and Patel 1993; Zheng and Zheer-uddin 1996; Zaheer-uddin and Zheng, 2001) have very detailed physical models. Many parameters in such models require detailed information of the system and building which is a big concern in terms of model built up time and efforts. The parameter identification and performance predictions of these detailed equation-based approaches often require a lot of iterations, which may result in high computational costs and memory demand.

Other approaches mentioned above (Henze, et al. 1997; Wang and Jin, 2000; Mendes, et al. 2003; Zhang and Hanby, 2006; Sane and Guay, 2008) involve ASHRAE thermal network models (ASHRAE, 2009). Such model presents the thermal dynamic and heat transfer process as thermal capacitances and resistances, which is computationally fast and easy to implement online (Wang, et al. 2008). This thesis adopts this approach to build up building zone and system models.

Integrations with Existing Energy Simulation Tools

There are several well-established and empirically validated building energy simulation tools, such as ESP-r (Clarke, 2001), EnergyPlus (Crawley, 1999), TRNSYS (TRNSYS, 2009) and SPARK (Simulation Problem Analysis and Research Kernel) (LBNL, 2006b), which are based on fundamental laws of energy, mass, heat transfer, flow balance, etc. These energy simulation tools, in use for the past two decades, are utilized to predict the energy performance of buildings based on building enclosures, HVAC systems, internal heat gain, occupancy schedules and outside weather. These simulation tools themselves have very limited control functions such as ON/OFF control. Only recently have a few research works started trying to integrate these energy simulation tools with existing control design tools such as MATLAB/Simulink and Dymola.

Clarke (2001) described the development and testing of a prototype simulation assisted controller, in which a detailed simulation program is embedded in real-time control decision making. The prototype system used LabVIEW as the weather data prediction and ESP-r for modeling HVAC system and control design decision support. It pointed out that the predict control, which uses a model in addition to measured data in order to forecast the optimum control strategy to be implemented, could assist in the more efficient operation of building energy management system.

Xu and Haves (2004) presented a hybrid simulation environment for controls testing and training. A real-time simulation of a building and HVAC system was coupled to a real building control system through a hardware interface. A prototype was constructed and tested in which the dynamic performance of both the HVAC equipment and the building envelope was simulated using SPARK. A PID controller was designed to tune room air temperature.

Xing (2004) presented a study on the multiple building load control and optimization using EnergyPlus and genetic algorithm. The second part of his research described three ways of optimizing load control in an aggregation pool: Enumeration, multi-GA and

model-based nonlinear optimization. The results showed that load aggregation offered load diversification opportunities among participants and improved the aggregated load profile. Load shedding later individual load profiles in a way that enhances the aggregation performance

Kummer, et al. (2005) developed and tested an optimal controller for an HVAC system with a high internal gain multi-zone building in TRNSYS type 56. The controller design is based on linear quadratic programming. A PID is cascaded with the optimal controller to compensate for modeling and forecasting errors. This PID adjusted the water supply temperature only.

Yahiaoui, et al. (2005) presented ongoing research on better control modeling in building performance simulation by integrating distributed computer programs. The research focused on the problem of developing run-time coupling of MATLAB and ESP-r over TCP/IP using Internet sockets. The one-day simulation results showed that MATLAB gives better controls over the control function within ESP-r itself.

Henze, et al. (2005) developed a model-based predictive (MPC) controller for a building with active ice storage and passive thermal storage in the building mass, using a 24-hour future horizon, and a 1-hour time-step. TRNSYS was used for the building model and Matlab was used to control the optimization. A subsequent study was conducted by Liu and Henze (2005) to develop a method for automated model calibration to ensure continued accuracy over time. They also worked on the development of a hybrid control system that attempts to incorporate the aspects of continual updating (found in the learning algorithm approach to control) with the simulation-based control approach (Liu and Henze, 2006).

Coffey (2008) presented a flexible software framework for simulation-based supervisory control, along with a modified genetic algorithm developed for use within it, and applied it to a case study of demand response by zone temperature ramping in an office space. Rule-based and simulation-based control variants were studied by using a two-model

configuration (one is acting as the ‘real’ building; the other is being used within the simulation-based control framework). For the case study, simulation-based control was found to perform only slightly better than a logarithmic rule-based approach under ideal conditions, and performed worse under conditions of model or prediction inaccuracies. The results are of use in guiding further research, and the case study itself has been a good test of the software framework.

In summary, these model-based control strategies demonstrated that system energy, environmental performance and system response can be greatly improved. However, very few studies have applied the designed optimal controller in a real building test-bed. The simulation-based supervisory control approach suggests an even longer prediction horizon than detailed equation-based approaches. All these characteristics are barriers for successful real time implementations of optimal control strategies.

1.2.2 Optimization techniques in the building HVAC controls

The discussion of previous research above illustrates the variety of optimization techniques used in building HVAC controls. There are two basic categories for optimization techniques in non-linear HVAC system modeling: the global minimum and the local minimum. The major difference between these two is that nonlinear local optimization techniques always lead to a local optimum and never to a global optimum. Nonlinear local optimization includes direct search and gradient-based approaches, among others, while the nonlinear global optimization includes simulated annealing, evolutionary algorithm, etc. Wang, et al. (2008) and ASHRAE (2007) offer a very detailed literature review on different optimization techniques in the building research domain. Here, only optimization techniques related to building HVAC supervisory controls are reviewed. Table 1.3 shows a detailed review and comparisons among different nonlinear optimization techniques.

Most of these optimization techniques demonstrated their performance for particular applications. Some optimization techniques may only result in a locally optimal solution,

and a globally optimal solution is not always guaranteed. The genetic algorithm (GA) has been attracting growing attention from researchers and has been widely applied in several studies. GA is a result-based method. No derivatives are required during the calculation. This feature makes it possible to solve complicated global optimization problems. However, it needs extensive computational cost and memory demand which is an obstacle for online implementation. There is a need for the future research to improve the computational efficiency and make it feasible for real time implementation.

Table 1.3 Summary of main optimization techniques used in building HVAC supervisory controls

	Techniques	Research Studies	Strength	Weakness
Nonlinear Local Techniques	Direct search	Zaheer-uddin and Zheng, 2001; Xu 2004	Simple and easy to be understood and implemented. No derivatives are required	Often fails to obtain an optimal solution and less computationally efficient
	Sequential quadratic programming	House and Smith 1995; Kota et al. 1996; Sun 2005	Handle a large number of inequality constraints efficiently	Has to start from initial guess values and the speed is affected by its initial values
	Lagrange method	Chang 2004; Sane 2008	Easy to be implemented since Lagrange formula does not depend on the order in which the nodes are arranged	The convergence is not always guaranteed
Nonlinear Global Techniques	Simulated annealing	Flake 1998; Chang et al. 2006	Relatively easy to be implemented	High computational costs and memory demands
	Evolutionary algorithms and genetic algorithm	Henze 1997; Wang et al. 2000; Xing 2004; Kumer 2005; Zhang 2006 and 2007; Coffey 2008	With high generalities and flexibilities, and there are also robust to find the global minimum	Extensive computational costs and memory demands due to high number of fitness evaluations

1.2.3 Occupant detection and behavior prediction in buildings

A fundamental goal of energy efficient and high performance buildings is to facilitate a comfortable, healthy and productive environment for the occupants while maintaining minimum energy consumption. Information regarding the number of occupants in a building space is a key component to achieving this task and is useful for numerous applications, such as lighting control or demand-controlled ventilation. Occupant presence and behavior in buildings has been shown to have large impacts on space heating, cooling and ventilation demand, energy consumption of lighting and space appliances, and building controls (Page, 2007). The impact of occupants' behavior on their working environment can be categorized into several methods of interaction and can be represented as in Figure 1.2. Each interaction is a stochastic process. Occupants emit heat, "pollutants" such as carbon dioxide (CO₂) and odors, and generate sound in the space. These interactions and their effects on the indoor environment can be measured via appropriate environmental sensors.

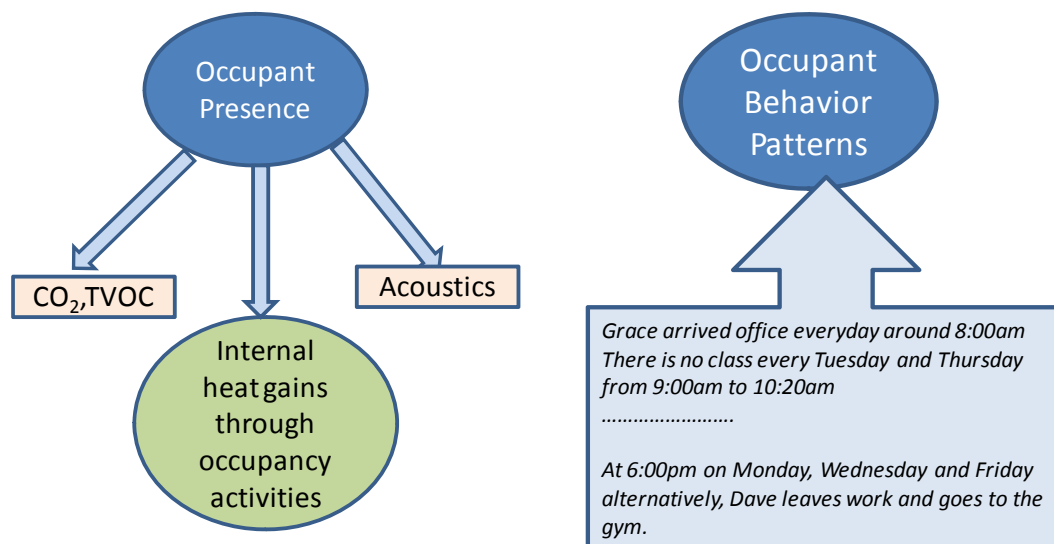


Figure 1.2 Occupant interactions with the surrounding environment

Several stochastic models have been developed to model occupant presence and interactions with space appliances and equipment. Fritsch, et al. (1990) proposed a model

based on Markov chains to model the random opening of windows by occupants. Degelman (1999) developed a Monte Carlo modeling approach for space occupancy predictions based on survey statistics. Reinhart, et al. (2004) determined occupant presence for lighting software by using a simplified stochastic model of arrival and departure. Wang, et al. (2005) applied Poisson distributions to generate daily occupancy profiles in a single-occupied office. Bourgeois, et al. (2006) integrated an occupancy model based on Reinhart's algorithm into ESP-r to investigate lighting use. However, most of the previous occupancy presence models were either tested on a single-person office or presented a specific application such as lighting control. Only recently, Page, et al. (2008) targeted individual occupancy behaviors by developing a generalized stochastic model for the simulation of occupant presence with derived probability distributions based on Markov chains. However, some of the occupant behavior derived from stochastic model was based on the assumption that occupants will interact with different appliances in the space, and the validation was conducted in single-person occupied offices. In addition, current approaches to occupancy detection take place mostly in commercial buildings through the use of passive infrared (PIR) motion detectors. However, motion detectors have inherent limitations when occupants remain relatively still. Moreover, motion detectors alone only provide information regarding the presence or absence of people in a space rather than the number of occupants, information which is highly useful for building control tasks such as demand controlled ventilation (Emmerich, 2001).

Video cameras have also been used to detect indoor human motions. Trivedi, et al. (2000) conducted rigorous experimental investigations on the processing and control modules for the active camera networks and the microphone array which are embedded in an intelligent room. The integrated system has the functionality of human tracking, active camera control, face recognition, and speaker recognition. Lymberopoulos, et al. (2008) developed a system called BehaviorScope for interpreting human activity patterns using a camera network and its application to elder monitoring in assisted living. However, video capture raises privacy concerns and requires large amounts of data storage. Other work has focused on the use of carbon dioxide (CO₂) sensors in conjunction with building

models for estimating the number of people generating the measured CO₂ level (Federspiel, 1997, Wang, et al. 1998). Sufficient models, though, are often not easy to obtain, and extensions to complex or open spaces may be difficult.

Recent research on so-called ‘smart environments’ involves the use of a diverse set of sensors to monitor and infer human activity in a building. Examples include the MIT Intelligent Room (Torrance, 1995), the University of Colorado Boulder Neural Network Adaptive Home (Mozer, 1998), Georgia Tech Aware Home (Lesser, et al. 1999) and the University of Texas at Arlington MavHome (Cook, et al. 2004; Youngblood, et al. 2007). Most of these works focus on behavioral modeling or mobility tracking and do not exploit additional sensing capability for the detection of occupancy numbers. In addition to these test beds, Duong, et al. (2006) used Hidden Semi-Markov models for modeling and detecting activities of daily living such as cooking and eating, and Youngblood, et al. (2007) introduced a new method of automatically constructing Hierarchical Hidden Markov models using the output of a sequential data mining algorithm to control a smart environment. Other research investigates HVAC preconditioning and device automation via mined location and device interaction patterns, and the energy saving potential is estimated through a relatively simple consumption model (Roy, et al. 2007).

In summary, methodologies for the detection of the presence of occupants based on sensor networks have been well established and tested. However, the sensor networks are either as one type of sensor, such as PIR, or video camera which comprises concerns of occupant privacy. In general, occupancy detection that fully exploits information available from low cost, non-intrusive, environmental sensors is an important yet under explored problem in office buildings. Furthermore, the models of occupant behavior patterns for the duration of occupancy within the context of building HVAC controls are very important for the operation of energy efficient buildings, but not explored in the literature review.

1.2.4 Summary of Literature Review

Based on the literature review above, several issues emerge requiring further research in order to achieve better building HVAC control operation. These issues include:

- Very few studies implement the real time optimal control into a real building
- High computational costs and large memory demands are concerns for detailed physical model-based design
- Dynamic occupancy and weather information based on non-intrusive environmental sensor networks are important for the building operation but has not yet been studied

1.3 Research Objective and Approach

Table 1.4 Comparisons of integrated HVAC control with previous studies

Author	Input Information for Control Modeling		Actual Implementation		
	Local Weather Forecasting	Dynamic Occupant Patterns	Real-time	Fully Model-Based	High Computational Speed
Wang, et al. (2000)			√		√
Henze, et al.(1997, 2003, 2005)			√		
Xu (2004)				√	√
Xing (2004)				√	
Sun (2005)			√		
Kummert (2005)			√	√	
Zhang (2006,2007)			√		√
Sane (2008)			√		√
Coffey (2008)			√	√	
Dong (2010)	√	√	√	√	√

Based on the issues highlighted in the literature review, there is a demand for innovative approaches for control design and operation which allows real time implementation with dynamic occupancy schedules and real-time onsite weather information and ultimately reduce energy consumption while maintaining indoor temperature set-points. This motivates the objective of this study to develop integrated heating, cooling and ventilation controls. Comparing to the previous studies, the character of current study is an integration of new, current and previous technologies in HVAC control. Table 1.4 shows the differences between this study and others. The computational costs of those previous studies can be referred to Table 1.3.

The hypothesis of the thesis is:

With the rapid developing of computer and information hardware and software technologies, an integrated building heating, cooling and ventilation control through the prediction of dynamic occupant behavioral patterns and weather information can reduce building energy consumption while still meeting the indoor temperature set-points.

More specifically, the research in this thesis aims to:

- Develop and implement an equation based building model for the Solar Decathlon house test-bed with radiant floor heating and heat pump cooling systems based on fundamental scientific and engineering principles;
- Validate the building model using data from field measurements;
- Develop and implement a data driven model for occupancy behavior patterns;
- Develop and implement a data driven model for weather information (temperature, solar radiation and wind speed) forecasting;
- Implement an real time integrated building HVAC controls in the Solar Decathlon House test-bed based on the prediction of occupancy and weather information ;
- Compare the HVAC energy consumption of proposed integrated control with commonly implemented fixed set-point temperature control strategy.

1.4 Thesis Chapter Overview

This thesis comprises five chapters:

Chapter 1, Introduction: Provides background and motivation of this thesis work. The current research status of the occupancy pattern detection and optimal HVAC control are also introduced. It identifies the research gaps, defines the detailed research objectives and approaches.

Chapter 2, Development of the Occupant Behavior Pattern Model: Presents novel models for: 1) detection number of occupants; 2) duration of the occupancy in the space. These two models have been tested and validated through a large-scale sensor network test-bed setup. In addition, other existing data driven models such as Neural Network are compared with the proposed model.

Chapter 3, Development of the Building Model: Describes the experimental test-bed setup, and first-principle based approaches to develop building zone models and HVAC system models. It also presents the validation results of this building model based on measured field data.

Chapter 4, Integrated Building Control Design and Implementation: Discusses the development of integrated optimal control design with the results from Chapter 2 and 3. It also presents the real-time on-line implementation of the designed controller in the Solar Decathlon house both for heating and cooling seasons. It compares the results with conventional setback temperature control strategies as well.

Chapter 5, Contribution, Conclusion and Future Work: Summaries the major accomplishments achieved in this thesis and conclusions drawn from the work. It also outlines the future directions of research in the area of building HVAC controls.

Chapter 2 **Development of the Occupant Behavior Pattern Model**

2.1 Introduction

Contemporary office buildings commonly experience changes in occupancy patterns and needs due to changes in business practice and personal churns. Hence, it is important to understand and accurately capture the information of such trends for applications in building design and subsequent building operations. Detection of occupancy presence has been used extensively in built environments for applications such as demand-controlled ventilation and security, and occupancy profiles are widely used in building simulations. However, the ability to discern the actual number of people in a space and the occupancy duration are often beyond the scope of current sensing techniques. This chapter presents a study to develop algorithms for occupancy number detection and occupancy duration models based on the analysis of environmental data captured from ambient sensing networks.

2.2 Model Development for Detecting Number of Occupants

To investigate the use of ambient sensors for detecting the number of occupants in an office building, a comprehensive, ubiquitous, environmental sensing test-bed was deployed in the Robert L. Preger Intelligent Workplace (IW) at Carnegie Mellon University. The overall goal of this test-bed is to integrate state-of-the-art IT systems as well as sensing, actuating, and controls technologies to achieve energy efficiency while providing a healthy and productive environment. This test-bed includes distributed sensors for a variety of environmental parameters such as CO₂, total volatile organic compounds (TVOC), small particulates (PM_{2.5}), acoustics, illumination, motion,

temperature, and humidity. In addition to the sensing networks, a video camera network is deployed with one camera in each of selected IW bays. Captured videos can be analyzed by user-assisted software to determine the number of occupants in the space at a given time. This information is used for ground truth occupancy profiles in the analysis.

The contribution of the test-bed lies in the magnitude and diversity of the sensor infrastructure deployed as well as the ability to capture data continuously with very little human intervention. While the aim of the study described here is on the detection of the number of occupants in the building space, this test-bed is an ideal testing environment for a large variety of building technology research areas such as human-centered environmental control, security and energy efficient and sustainable green buildings. In particular, the derived occupancy information can be used as an input for both validating building simulation models and simulating new building or control designs on realistic occupancy profiles.

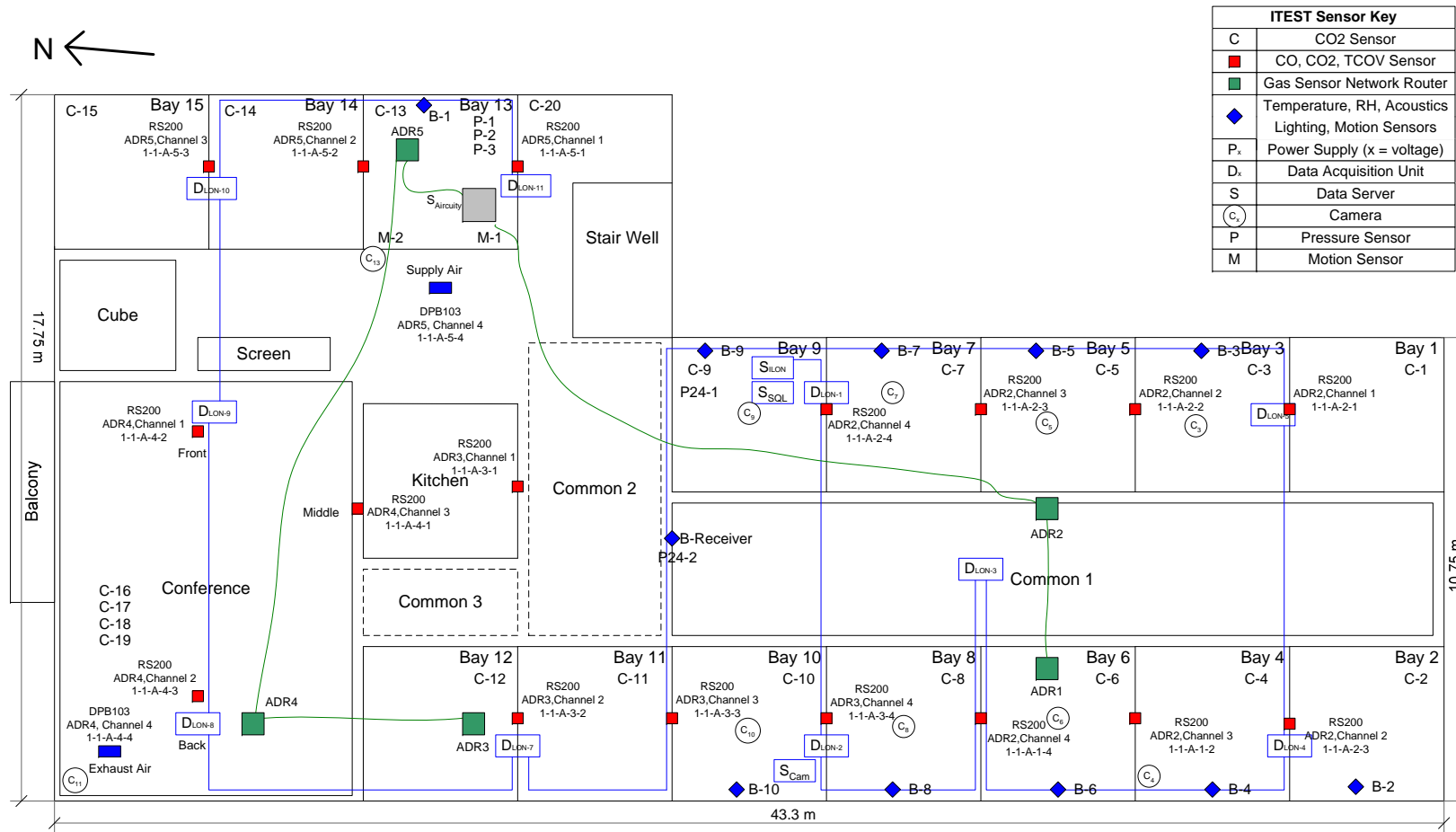


Figure 2.1 Sensor network layout of the Intelligent Workplace, Carnegie Mellon University

2.2.1 Data Collection

Table 2.1 Data collection periods

Dataset	Bay	Starting date	Ending date	# Data points in total
B13_P1	13	01/29/08	03/07/08	21528
B13_P2	13	03/17/08	04/04/08	7705
B13_P3	13	03/27/08	04/03/08	1156
B10_P1	10	01/29/08	03/07/08	20702
B10_P2	10	03/17/08	04/04/08	7555
B10_P3	10	03/27/08	04/03/08	1157

Figure 2.1 shows the sensor network setup in Intelligent Workplace (IW) at Carnegie Mellon University (CMU). Data collection in the IW for this work took place during two continuous periods and in two bays. The time periods are (1) January 29 to March 7, 2008; and (2) March 17, 2008 to April 4, 2008. Occupancy data is recorded on weekdays from 8:00 am to 6:00 pm from the two bays with the most frequent occupancy activity, bays 13 and 10. Table 2.1 lists the details of each dataset and the label for the dataset used throughout the rest of the paper.

2.2.2 Feature Selection

The features of the environmental sensing network are explored to provide the most useful information in the detection and prediction of the occupancy number. To this end, the notion of information gain is implemented, which is a measure of the amount of uncertainty of the input of a system given the value of the output. Here presents a brief overview of the methodology and results of the feature selection analysis; a full report of the details can be found in (Lam, et al. 2009).

Information gain

Mathematically, the relative information gain (RIG) between two random variables x and y is defined as (Mitchell, 1997)

$$RIG(y,x) = \frac{IG(y,x)}{H(y)} \cdot 100\% \quad (2.1)$$

where the mutual information IG is

$$IG(y,x) = H(y) - H(y|x) \quad (2.2)$$

and the entropy $H(y)$ is a measure of the inherent uncertainty of the random variable y :

$$H(y) = \sum_{i=1}^n -p(y_i) \log_2 p(y_i) \quad (2.3)$$

with n is the total number of values the random variable y can take. High entropy corresponds to high uncertainty and vice versa. Information gain is calculated to assess the correlation between occupancy and different sets of features derived from the sensor data. In general, the feature set is comprised of the following features computed for each ambient sensor: the original output, first order difference, second order difference and its difference with outdoor values. For CO₂ and acoustics, a 20 minute moving average value is also considered. The indoor CO₂ level is assumed to be equally contributed by each occupant. A tool (Anderson and Moore, 1998) is employed, which uses an exhaustive search algorithm to check all possible feature combinations from the feature space and then select the most informative combination of features based on the relative information gain.

Results from feature selection

Table 2.2 shows an example of the feature selection analysis on CO₂ data for a particular bay. The features investigated are shown in Table 2.3.

Information gain is computed for increasing numbers of input features and, for each iteration, feature combinations yielding the highest information gain are noted (indicated by the check marks in Table 2.3). This analysis is repeated for each bay, and the number of selections of each feature is totaled to obtain the most informative features for a given sensor. For instance, the three most informative features for CO₂ are found after totaling the selections across all bays to be CO₂_Out, CO₂_FD2 and CO₂_MA_20min.

Table 2.2 Investigated features of CO₂

Feature	Description
<i>CO₂_FD</i>	1st order difference of CO ₂ : CO ₂ (t(i))-CO ₂ (t(i-1))
<i>CO₂_FD2</i>	1st order shifted difference of CO ₂ (CO ₂ (t(i))-CO ₂ (t(i-2)))
<i>CO₂_SD</i>	2nd order difference of CO ₂ : CO ₂ _FD(t(i))-CO ₂ _FD(t(i-1))
<i>CO₂_Diff</i>	1st order difference of CO ₂ difference between indoor and outdoor: CO ₂ _Diff(t(i))-CO ₂ _Diff(t(i-1))
<i>CO₂_Diff_FD</i>	<i>CO₂_Diff_SD</i> (2nd order difference of CO ₂ difference between indoor and outdoor: CO ₂ _Diff_FD(t(i))-CO ₂ _Diff_FD(t(i-1)))
<i>CO₂_MA_20min</i>	20 minutes of moving average of CO ₂ measurement

A similar analysis was conducted combining the three most informative features for a given sensor with those from other sensors. A detailed analysis can be found in (Lam, et al., 2009).

Summarizing the results, thermal performance parameters such as temperature and relative humidity are dominated more by the building heating, cooling, and ventilation systems. The selected features giving the largest information gain are found to be: CO₂, CO₂_Diff, CO₂_FD2

and CO₂_MA_20min acoustics, acoustics_FD2 and PIR. These features are used as inputs to the occupancy estimation methods discussed below. Note that the occupancy estimation methods were also evaluated with additional feature combinations, and those yielding the best results are consistent with the results of Lam, et al. (2009).

Table 2.3 Information gain with different number of features as output for CO₂ for the period B13_P1

CO ₂	CO ₂ _FD	CO ₂ _FD2	CO ₂ _SD	CO ₂ Out	CO ₂ _Diff	CO ₂ _Diff_ FD	CO ₂ _Diff_ SD	CO ₂ _MA_ 20min	Features	RIG(%)
		√		√	√					20
		√		√	√		√			28
		√		√		√	√	√		40
		√	√	√	√	√	√	√		52
√		√	√	√	√		√	√		60
√		√	√	√	√	√	√	√		67
√	√	√	√	√	√	√	√	√		67

2.2.3 Occupancy Estimation Methodology

2.3.1.1 Neural Network

An Artificial Neural Network (ANN) is an interconnected group of artificial neurons that uses a mathematical or computational model for information processing based on a connection approach to computation (Hassoun, 1995).

An ANN of two hidden layers with different combinations of neuron numbers in each hidden layer is tested on the data from the IW. Figure 2.2 shows the structure of the ANN. The neural network applied in this study is used for creating, training, and simulating a fully-connected, feed-forward network. Fully-connected means that each node is connected to all other nodes in the adjacent layers, and feed-forward indicates that information is passed in a single direction from the input to the output nodes.

The learning algorithm employed is the back-propagation, generalized delta method. In this algorithm, the value of the output of the NN is compared to a target value to determine an error. The weights associated with the connection between nodes are then adjusted in a backward direction from the output layer to the input layer in order to minimize this error.

The ANN is implemented using the MATLAB Neural Network Toolbox. The input layer has the most important features obtained from the results of feature selection. The Log Sigmoid function is used as the transfer function in all hidden layers, and a linear function is used in the output layer. Because neural networks are not guaranteed to reach a global solution, training is repeated 10 times, and the output results are averaged.

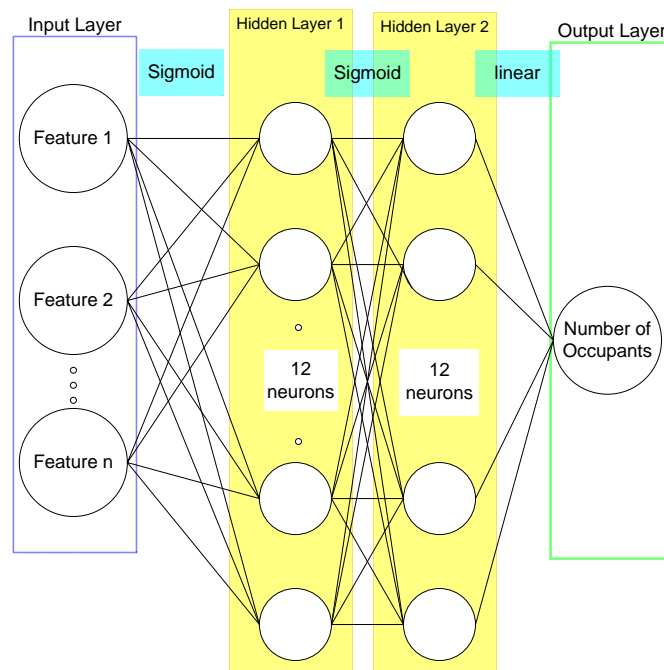


Figure 2.2 Structure of 2-hidden layer Neural Network used in occupancy detection

2.3.1.2 Hidden Markov Model

A hidden Markov model is a statistical model in which the system being modeled is assumed to be a Markov process with unknown parameters, and the challenge is to determine the hidden parameters from the observable parameters. The extracted model parameters can then be used to perform further analysis, for example, for pattern recognition applications. A HMM can be considered to be the simplest dynamic Bayesian network.

In this study, the occupancy number is considered to be a hidden state and the most important features from the sensor network as observations as shown in Figure 2.3. Unlike the NN approach, the HMM method explicitly accounts for temporal correlations between occupancy levels and environmental parameters in consecutive time steps. This temporal information has the potential to greatly improve prediction.

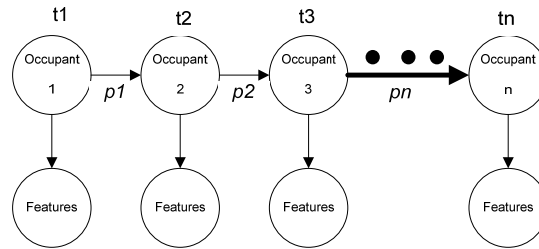


Figure 2.3 Structure of HMM

To train the HMM, the forward and backward algorithm is applied. The update rule is (Rabiner, 1989):

$$(1) \text{Initialize: } \alpha_1(X_1) = P(X_1)P(O_1|X_1) \quad (2.4)$$

Where $O_{1..n}$ are observed sensor values.

(2) For $i=2$ to n ,

$$\alpha_i(X_i) = \sum_{x_{i-1}} P(O_i|X_i)P(X_i|X_{i-1} = x_{i-1}) \alpha_{i-1}(x_{i-1}) \quad (2.5)$$

X_i and X_{i-1} are the number of occupancy in time t and time $t-1$.

(3) Initialize: $\beta_n(X_n) = 1$ (2.6)

(4) For $i = 2$ to n ,

$$\beta_i(X_i) = \sum_{x_{i+1}} P(O_{i+1}|x_{i+1})P(x_{i+1}|X_{i+1})\beta_{i+1}(x_{i+1})$$
 (2.7)

(5) Finally, $P(X_1|O_{1...n}) \propto \alpha_i(X_i)\beta_i(X_i)$ (2.8)

where

α_i *ith* forward probability

β_i *ith* backward probability

X_i *ith* state

O_i *ith* observation.

The final estimation is obtained from Equation (2.8), which is the maximum probability based on the current sensor observations and previous occupancy number.

2.2.4 Preliminary Experiment Results

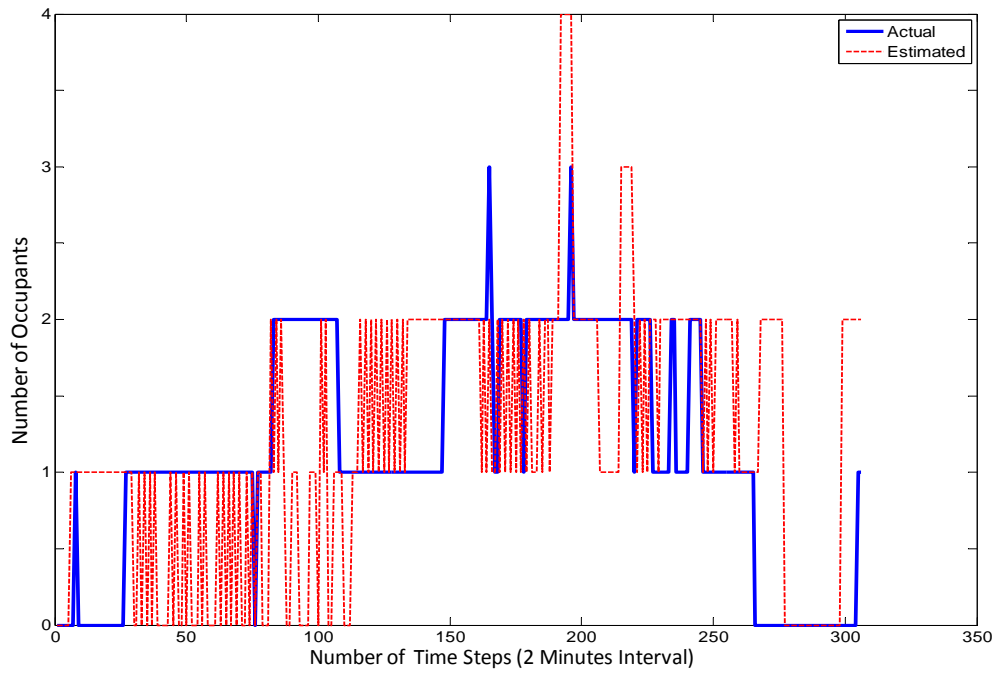


Figure 2.4 Occupancy estimation results of bay 13_p2 on March 21 with ANN of 75% accuracy

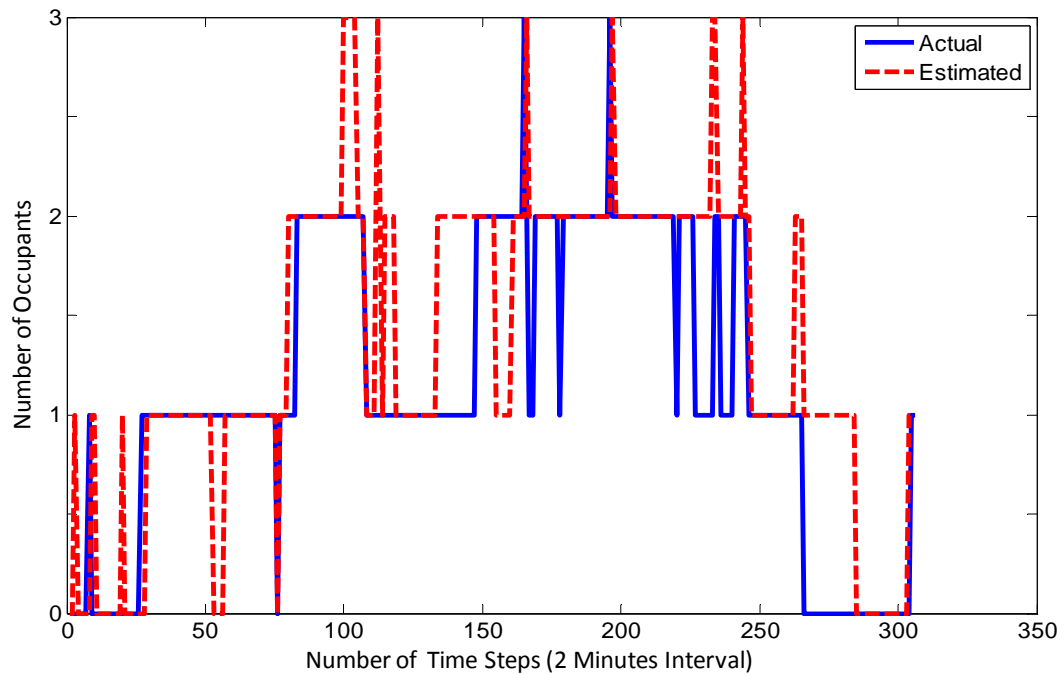


Figure 2.5 Occupancy estimation results of bay 13_p2 on March 21 with HMM of 75% accuracy

Figure 2.4 and Figure 2.5 show the results from the ANN and HMM analysis, respectively. Data for one day (March 21) is used for testing, and the remaining dates are used for training. The x axis corresponds to the number of time steps (2-minute interval), and the y axis the number of occupants in the space. The solid line is the actual occupancy profile and the red dotted line is the estimation. ANN generates rather noisy occupancy estimates with frequent fluctuations. This can in part be attributed to the ANN assumption that each data point is independent and identically distributed, which is not always accurate. This is particularly true with respect to parameters such as CO₂ because of the strong temporal correlations inherent in CO₂ measurements. The HMM approach is more well suited to account for these temporal correlations because of the dynamic Markov properties.

Figure 2.6 and Figure 2.7 show one week estimation results from bays 13 and bay 10, respectively. The testing period is from period P3 as shown in Table 2.1 and the training period is obtained by combining the P1 and P2 periods. In total, there are 1156 data points. Accuracies for Figures 2.6 and 2.7 are 70% and 65%, respectively. While these numbers appear somewhat low, the profiles illustrate that the estimations track changes in occupancy fairly well. The estimated profiles also present a “smoothed” version of the true occupancy profile.

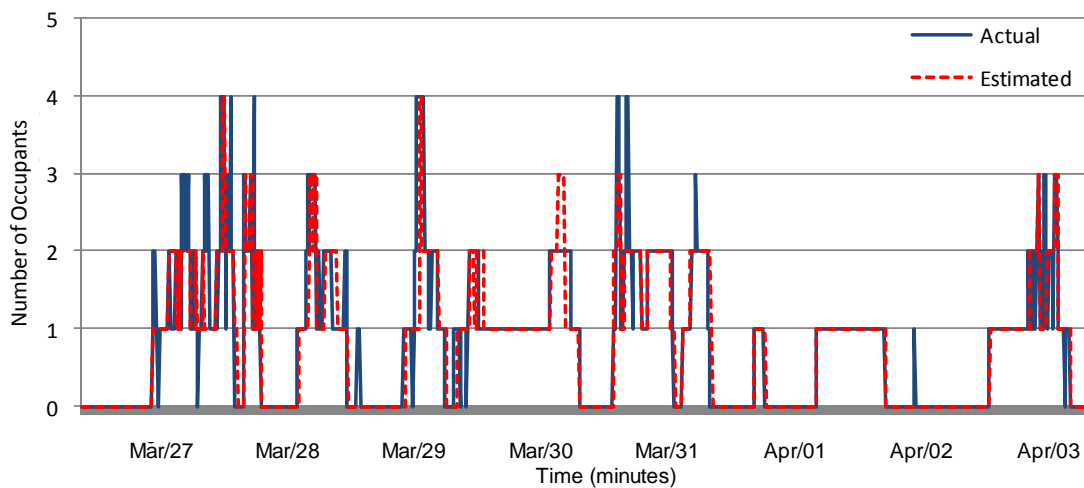


Figure 2.6 Occupancy estimation results of bay 13 from results from dataset b13_p3 from March 21 to April 3 with HMM of 70% accuracy

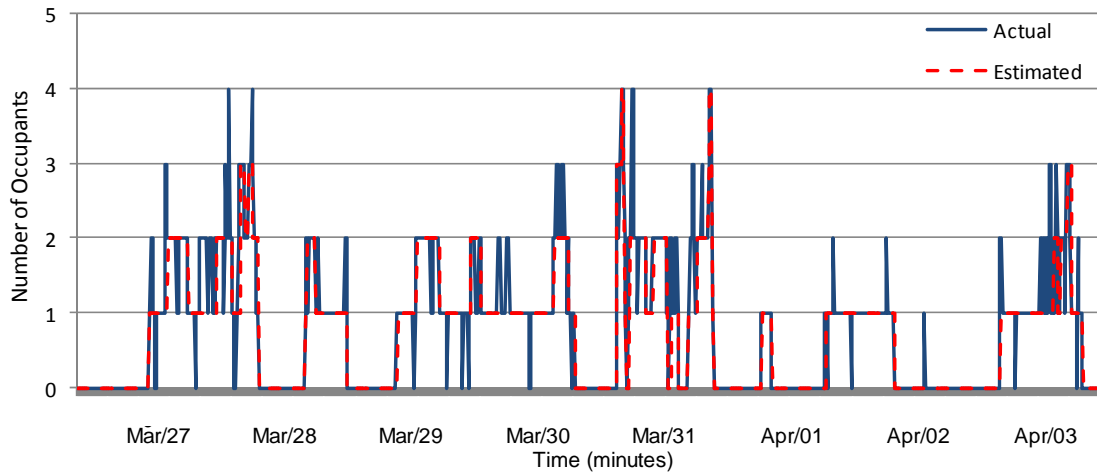


Figure 2.7 Occupancy estimation results of bay 10 from results from dataset b10_p3 from March 27 to April 3 with HMM of 65% accuracy

Table 2.4 Summary of occupant number prediction in IW

Dataset	Bay	Match (%)	Not-Match (%)
B13_P1	13	65	35
B13_P2	13	72	28
B13_P3	13	70	30
B10_P1	10	68	32
B10_P2	10	70	30
B10_P3	10	65	35

Table 2.4 presents a summary table from the results of occupant number prediction. In summary, the HMM estimates occupant numbers successfully for 70% of the testing period, but ignoring abrupt fluctuations of short duration. From the perspective of an occupancy-based HVAC control scheme, this behavior is sufficient because the abrupt changes are rather insignificant. This test-bed has a comprehensive sensor network covering possible sensors that can be installed in buildings. The methods are based on information theory and rigorous mathematical models. It is believable that the model developed here can be applied to any building with the same sensor network setup.

2.3 Model Development for Occupancy Duration Estimation

The objective here is to develop and implement unsupervised algorithms for ambient sensor-based modeling and prediction of user behavior within the context of intelligent buildings and connect the derived user behavioral patterns to building energy and comfort management. The approach is based on the work of Youngblood, et al. (2007) in that a behavioral pattern model is constructed by mining sensor events for significant patterns (Episode Discovery), and then a Markov model is generated from the resulting patterns. However, three additional contributions to the model are introduced here:

- 1) Integration of a rich environmental sensor network with acoustics, temperature, relative humidity, CO₂ and motion detection etc. into the data-driven model of occupancy behavioral patterns.
- 2) Incorporation of occupancy duration into the Semi-Markov Model to capture behavioral transitions over larger time scales as well as energy related events.
- 3) Development of a formal method to connect the discovered patterns with energy and thermal comfort management in buildings, demonstrated through simulation using measured data. In particular, a comparative analysis is conducted between using a dynamic occupancy schedule versus a conventional temperature set-point schedule in EnergyPlus simulation.

Figure 2.8 illustrates the overall approach, comprising: (1) sensor event detection method; (2) frequency pattern detection using Episode Discovery, minimum description length (MDL), period detection (PD) and energy weighting factors; (3) a Semi-Markov Model for occupancy duration models.

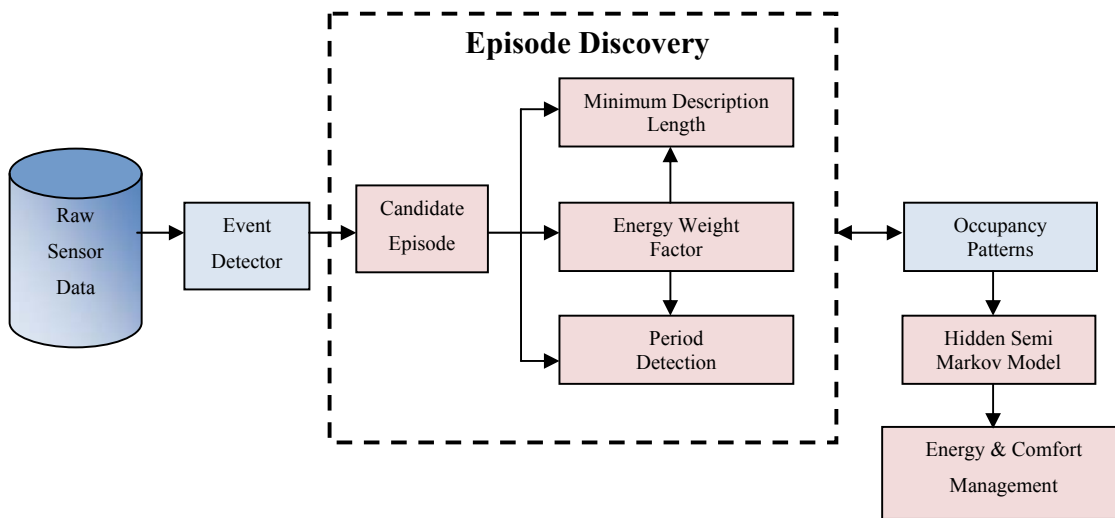


Figure 2.8 A holistic view of occupancy duration estimation

2.3.1 Event Detector

The detection of events comes from a variety of different measured sensor data. Each single event is denoted with a code and an episode as a sequence of codes. Table 2.4 shows code assignments. An example of an episode may be “*agghkjhk...*”. All parameter values used in the definitions are determined empirically for the test-bed environment used in this study.

Table 2.5 Definition of important events from sensors

Sensors	State Transitions	Code	Sensors	State Transitions	Code
Acoustics	1. Low acoustics	a	CO ₂	1. Increasing	g
	2. Loud acoustics	b		2. Decreasing	h
Illumination	1. Off-On	c	Temperature	1. Increasing	i
	2. On-off	d		2. Decreasing	j
Motion	1. Off-on (motion)	e	Relative Humidity	1. Increasing	k
	2. On-off (no motion)	f		2. Decreasing	l

a. Acoustics

The acoustics sensor outputs a calibrated percentage of the acoustics level in the space. Figure 2.9 shows an acoustics profile example for a typical day in a conference room. The acoustic events are categorized into two types: (1) ventilation noise or background noise, defined as an acoustics level between 15% and 20% that is accompanied by at least a 5% increase from the previous level (event ‘*a*’); (2) human activity (e.g., voice or door opening/closing), defined as an acoustics level above 20% accompanied by at least a 10% increase from the previous level (event ‘*b*’). A smoothing method based on a root mean square approach is implemented to reduce noise (Smaton and McHugh, 2006).

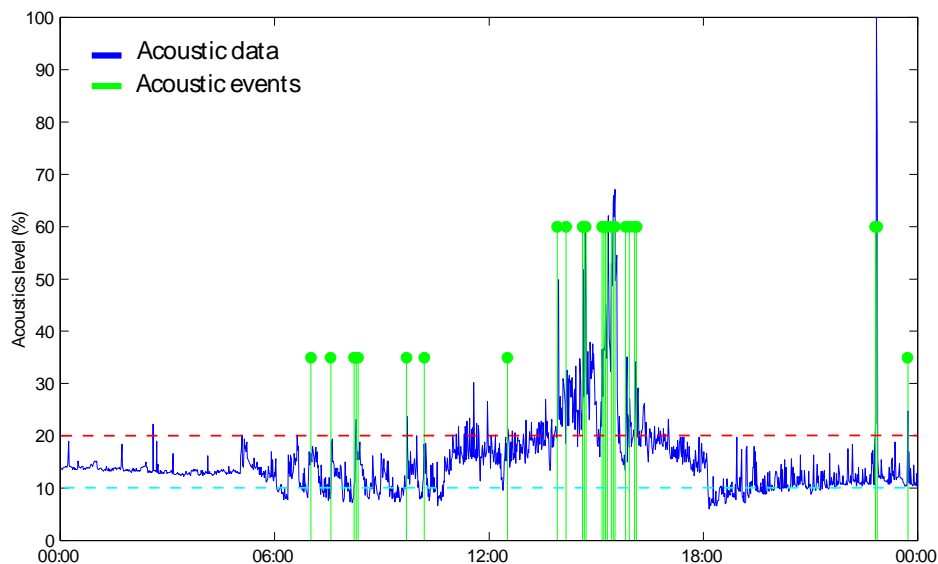


Figure 2.9 One day example of acoustic events

b. Lighting

Lighting events are defined as: (1) light turned on (event ‘*c*’); (2) light turned off (event ‘*d*’).

c. Motion

Motion sensor events are defined in the obvious way for a binary motion sensor with an event each for motion switching (1) on (event ‘*e*’) and (2) off (event ‘*f*’). However, to avoid capturing

high frequency fluctuations that occur naturally when occupants are inside the room and to obtain a more informative signal, a 10 minute time window is used to smooth the signal. A motion off event must be followed by no motion activity within this window. Figure 2.10 shows an example motion profile and the accompanying events.

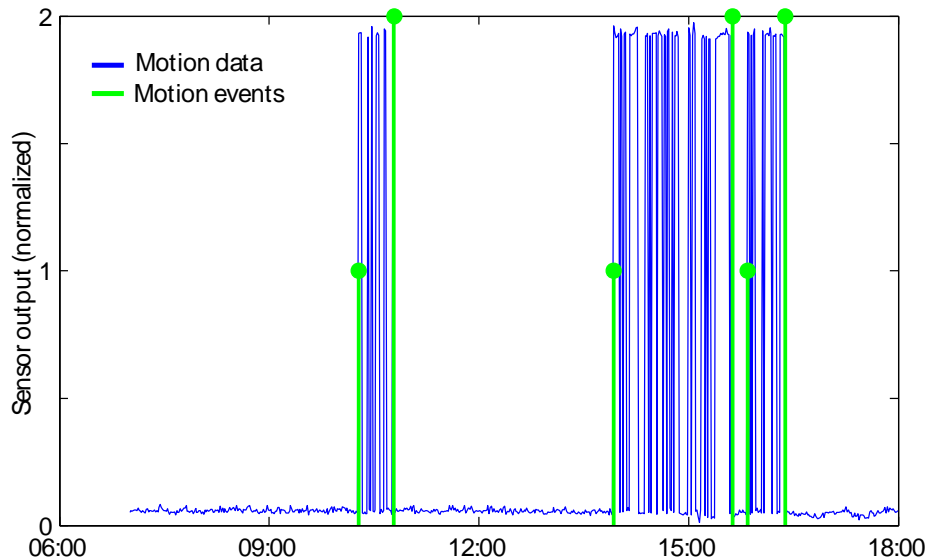


Figure 2.10 Example motion events

d. Carbon Dioxide

According to the results from Lam et al. (2008), an increase of 50 ppm CO₂ level in 10 minutes is found to have high correlation with human presence. This, however, clearly depends on the location of the sensor; in this study, the CO₂ sensor is located above the conference table in the center of the room at roughly nose level. The events are then defined as: (1) CO₂ increase of 50 ppm in a 10 minute time window (event ‘g’); (2) CO₂ decrease of 50 ppm in 10 minutes (event ‘h’).

e. Temperature and relative humidity

In a room without windows such as the conference room test-bed, individual human-based temperature fluctuations are minimal or on vary slow time scales. Large changes in temperature (1 °C) in a short time frame (10 minutes) are more likely associated with high energy activities

such as large group presence, the HVAC system being turned, or a projector. Hence, the events for temperature are defined as (1) 1 °C increase in 10 minutes (event ‘*i*’); (2) 1 °C decrease in 10 minutes (event ‘*j*’). Relative humidity fluctuates very little under the test-bed conditions unless there are occupants inside the space or the HVAC system brings in outside air. Hence RH events are defined as: (1) 10% increase in 10 minutes (event ‘*k*’); (2) 10% decrease in 10 minutes (event ‘*l*’).

2.3.2 Episode Discovery

Episode Discovery (Heierman, et al. 2004) is the process of discovering significant patterns in the data sequence by first generating candidate sequences and then pruning this set to obtain a final set of important sequences. Time series sensor event sequences generated according to the author’s definitions in the previous section are mined for potentially significant candidate episodes using a sliding time window. Briefly, in every episode window, the event codes are ordered according to the time of occurrence. If the codes happen at the exact same time, they are ordered by alphabetical order for consistency. For each episode window, all possible subsets of the episode are generated. The generation of these subsets as additional candidates accounts for fluctuations in event order or the occurrence of spurious events. For example, if the episode pattern in a 3 minutes time window is $\{c,e,f,g,d\}$, then the candidate episode patterns are $\{\text{null}\}$, $\{c,e,f\}$, $\{g,d\}$ and so on. However, to make this problem more tractable and avoid considering the superset of the episode as candidates, subsets are pruned using the following rule (Heierman et al., 2004). The subset candidates of a candidate episode that have the same episode occurrences as the parent episode do not need to be generated as candidates. An example resulting candidate episode is ‘*cef*’, which, for our event definitions, corresponds to ‘light on’ followed by ‘motion on’ and ‘motion off’ and is most likely representative of someone entering a room.

After candidate episodes are generated, significant episodes to be included in the behavioural model are determined using the minimum description length (MDL) criteria and periodicity (PD) as described below. In addition, since the focus is on energy consuming behaviour, a weighting

factor is used in both the MDL and PD steps to increase the importance of episodes containing high energy impact events, namely, lighting, temperature, and humidity events.

Minimum description length

The intent of MDL is to discover event patterns that have the largest compression ratio which best represent the original input stream. Event patterns may be thought of as a code table for encoding the original input sequence. The optimal code table is the one that minimizes both the size of the code table plus the length of the encoded original sequence. A brief algorithm is shown below (for a detailed algorithm, see Bathoorn, 2006):

Let candidate episodes $\Theta = \{P_1, P_2, \dots, P_n\}$, where P_n is the n^{th} episode.

1. Ordering Θ according to

a. Length; b. Frequency

2. Compress (Θ)

CodeTable = allSinglePatterns;

minSize = computeSize(CodeTable)

for each $P_i \in \Theta$

CodeTable.add(P_i)

newSize = computeSize(CodeTable)

if newSize < minSize

minSize = newSize;

else

CodeTable.remove(P_i)

return CodeTable

Periodicity detection

Often, behaviours with the most utility for building automation systems are those that exhibit some periodicity. In a time series data set D_{org} , a symbol s or an episode p is said to be periodic with a period l , if s or p exists every l time step. Episode periodicity is computed using a convolution-based approach, where the time series is shifted l positions and the shifted series D_{new} is compared with D_{org} (Mohamed, et al., 2005). This tantamount to conducting a frequency spectrum analysis using a Fourier transform. Detailed algorithm information can be found in Mohamed et al. (2005).

2.3.3 Semi-Markov model generation

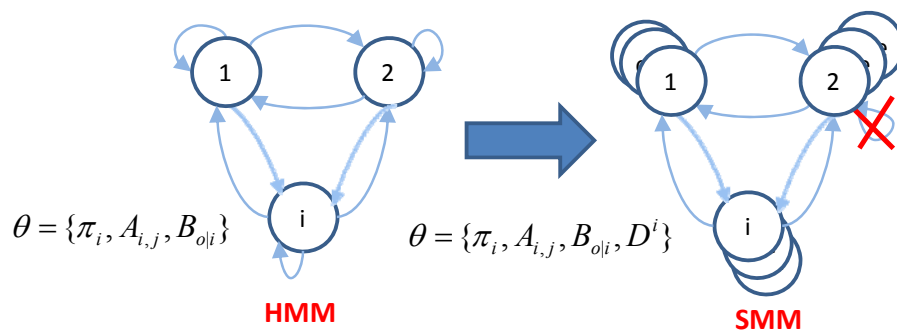


Figure 2.11 Differences between HMM and SMM

A Semi-Markov Model (Figure 2.11) allows for duration in each state before transitioning to the next state (Murphy, 2002). In standard HMM, a set of parameters θ is learned, where π_i is the initial probability matrix, A_{ij} is the state transition probability from state i to state j , and $B_{o|i}$ is the observation matrix. In SMM, in addition these, the state i is not hidden and cannot have a transit to itself. In other words, an additional parameter D^i is learned, which is a duration model. As pointed out by Duong et al. (2006), D^i could be modeled as multinomial distribution in the case of non-parametric modelling or as a distribution in the exponential family. In this study, D^i is modeled as the exponential distribution, consistent with the previous study (Duong, et al. 2006).

$$D_m^i \stackrel{\Delta}{=} \Pr(m | \lambda) = \lambda e^{-\lambda m} \quad (2.9)$$

$$E[X] = \lambda^{-1} \quad (2.10)$$

After learning the parameter λ , the expected duration, given a random variable X , is the reciprocal of λ . In this study, as in Youngblood, et al. (2007), each discovered important pattern is treated as a state in the Markov model. The Semi-Markov Model is learned using a forward-backward algorithm (Yu and Kobayashi 2003). In this current approach, states are not considered hidden. Hence, $B_{o|t}$ is explicitly defined and does not require a learning process.

2.3.4 Connections to Building Energy Management

A dynamic occupancy schedule with expected durations is developed from the behavioral pattern recognition results. This dynamic schedule, as described below, can be connected with a building energy and comfort management system (BECMS) through dynamic real-time temperature and ventilation set point inputs. The BECMS can then make decisions according to the dynamic schedule. In order to test the practicality of this approach, the dynamic schedule is coupled with EnergyPlus, a widely used energy simulation tool (Crawley, et al. 1999).

There are several current approaches in the literature for modeling occupancy within the context of energy simulation. Claridge, et al. (2001) suggested that occupancy diversity profiles might be derived from lighting diversity profiles through establishing a strong correlation between observed occupancy levels. However, other studies suggested diversity profiles generate misleading information when occupancy-sensing lighting controls are used (Degelman, 1999). Bourgeois, et al. (2006) developed a sub-hourly occupancy-based control (SHOCC) coupled with the ESP-r simulation program. SHOCC tracks individual instances of occupants and occupancy-controlled objects such as blinds. However, its application is limited with lighting controls.

In this preliminary analysis stage, the dynamic schedule is used toward lighting and HVAC controls. The control strategy utilizes the learned Markov model of behaviour and takes advantage of the fact that some patterns such as ‘*ecfdef*’ only last briefly, corresponding to commonly found scenarios where users step into the conference room to, for example, make a cell phone call. In situations such as this, the HVAC system does not need to meet the temperature set point and ventilation rate. Figure 2.12 illustrates the coupling of an HVAC control strategy with occupancy pattern recognition.

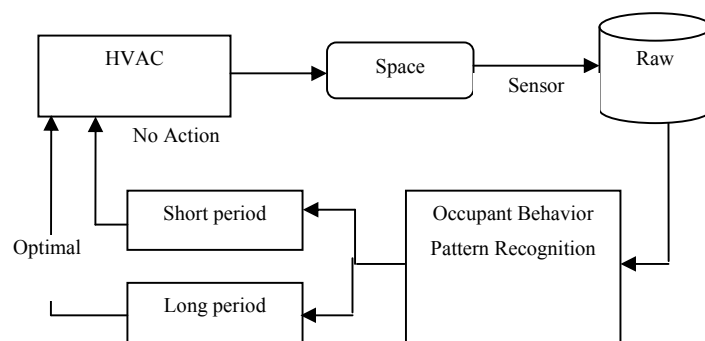


Figure 2.12 HVAC controls based on pattern recognition

The term “dynamic schedule” refers to the time and state-dependent use of the Markov model in the HVAC and lighting control strategy. The system monitors sensor events to determine the current state of the environment as given by the Markov model. If an entry state (e.g., one involving lights turning on) is identified, the system computes the most probable duration of occupancy based on the model and responds accordingly. The control strategy is updated as the detected state changes. Because our emphasis here is on illustrating the utility of data-driven behavioral modeling for energy management rather than on controller design, the author implemented a simple occupancy-dependent on/off control; however, more advanced controllers can achieve better performance by utilizing the duration information contained in the model. For our simulation, a software link between the dynamic schedule and EnergyPlus is used so that the time dependent schedule can be generated automatically from pattern recognition.

2.3.5 Preliminary Experiment Results

The preliminary experiment is conducted in a conference room in a commercial building in Pittsburgh. Data is collected every one minute from June 1 to June 30, 2008. Figure 4 shows a picture of the conference room and its installed sensors. The results are two parts: 1) Occupancy behavior patterns; 2) Dynamic occupancy-based energy management.

Occupant behavior patterns

Figure 2.14 illustrates an example day of sensor events generated according to the definitions described in Table 2.5. Event numbers on the y axis indicate which event occurred for the given sensor according to the codes in Table 2.2. For example, at 5:40am, the temperature decrease event (Event_2 for the temperature decrease event) occurred when the air conditioning system turned on. As is typical with most days in the conference room, numerous motion and acoustic events occur from 10:00am to 11:00am when the room is active with meetings. At 11:00 pm, a custodian enters the room, generating lighting and acoustics (vacuum cleaner) event



Figure 2.13 Test-bed in a conference room

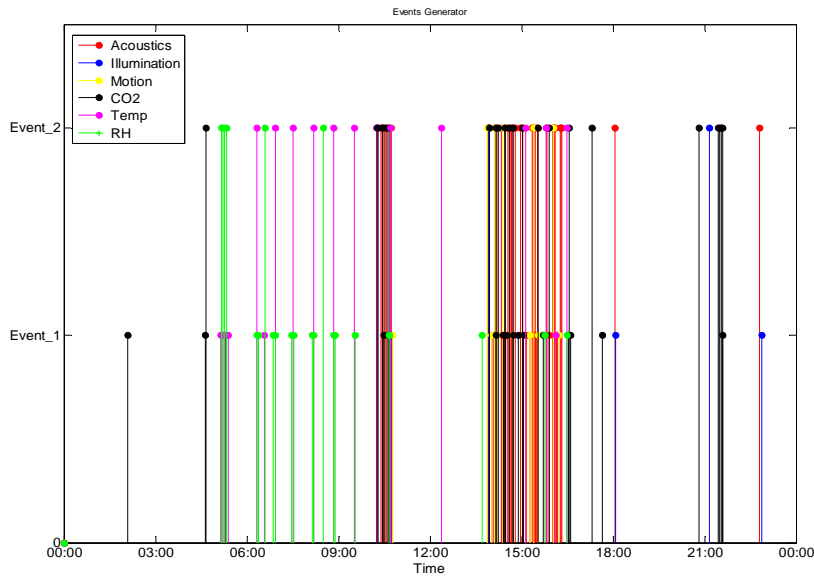


Figure 2.14 A one day example results of event detection

Based on a time window of 10 minutes, a summary of important patterns resulting from the MDL and PD selection criteria are shown in Table 2.6. It is noted here that the MDL component discards some very long patterns due to highly infrequent occurrence (once every week or every few days). The final set of important patterns is those resulting from both MDL and PD.

Table 2.6 Results of Patterns from MDL and PD

	# of Patterns	Longest Pattern	Most Comp. Pattern	Other Patterns
MDL	9	<i>bebdf (22)</i>	<i>cedf (19)</i>	<i>dfcedf, bebdf, ebbdf, fefe, aa, ghg, gge</i>
PD	8	<i>ebbfe(24)</i>	<i>bg (84)</i>	<i>bgfb, feg, hbe, aec, fhd</i>

The exponential family of distribution functions is used to model the durations associated with the discovered patterns. This is consistent with other work in speech recognition (Russell, 1985) and occupancy of single-person offices (Wang, et al. 2005). Figures 2.15 and 2.16 show the resulting semi-Markov model of important patterns. Event code letters are as defined in Table 2.2. Figure 2.15 shows a standard Markov model with numbers on the arcs indicating the

transition probability between states, Transitions with relatively low probabilities (less than 15%) are not shown. Parentheses indicate number of occurrences of the pattern in the training period. As an example, state “*ecf*” has a 25% transition probability to state “*eb*” and a 24% probability to state “*def*”, with “*ecf*” occurring 22 times, “*eb*” 37 times and “*def*” 15 times during the month. Figure 7 shows the results of including duration in the model. Each duration distribution is denoted as $X\sim(time)$, where *time* is the expected duration for the exponential model. For example, “*ecf*” has an expected duration of 30 minutes before it transitions to state “*eb*” and 10 minutes before transiting to state “*def*”. The dotted line indicates a typical 75 minute meeting scenario where an occupant enters the room, triggers the motion sensor “*e*”, turns on the light “*c*”, and sits down, triggering the motion off “*f*”. The occupant continues to stay in the room, generating acoustics “*b*” and moving around generating motion “*e*”. Upon leaving, the occupant turns off the light “*e*”, moves towards the door “*e*” and finally departs “*f*”. Another possible duration path is on average 138 minutes, representing a longer meeting.

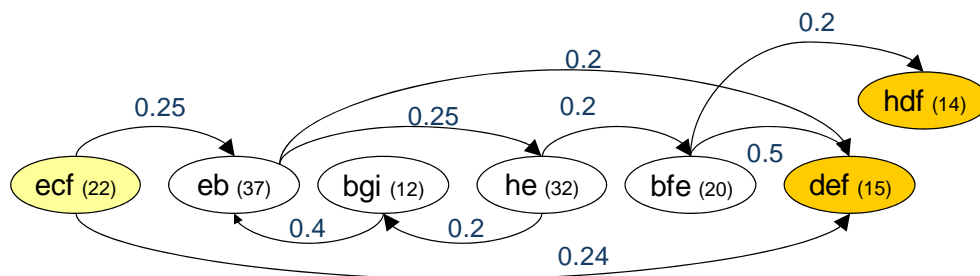


Figure 2.15 Markov model of discovered patterns on 10 minutes maximal window

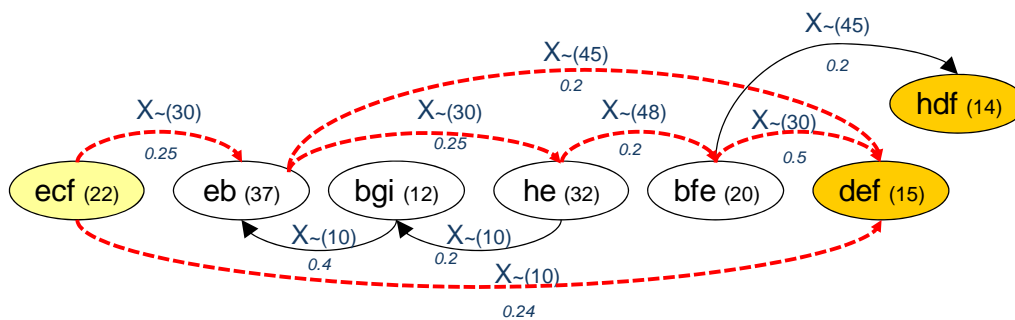
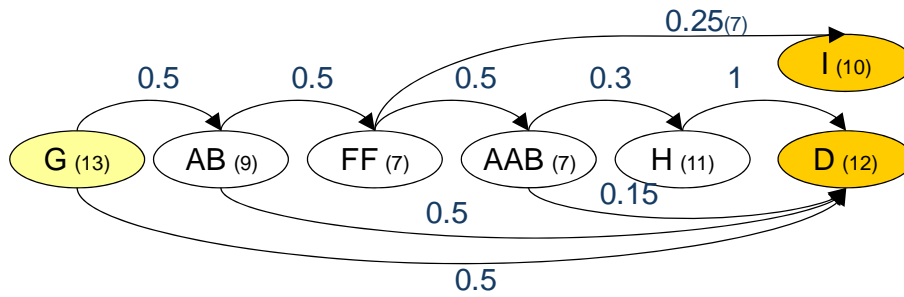


Figure 2.16 Semi-Markov model of discovered patterns on 10 minutes maximal window



A: 'eb' → stay B: 'he' → stay G: 'ecf' → enter E: 'bfe' → stay K: 'ged' → leave
 D: 'hdf' → leave I: 'def' → leave H: 'ag' → stay F: 'hj' → HVAC

Figure 2.17 Markov model of discovery patterns on patterns

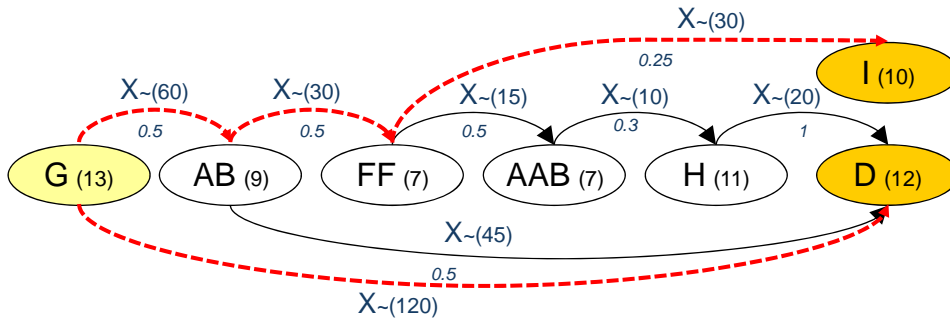


Figure 2.18 Semi-Markov model of discovery patterns on patterns

Additional models representing longer time scales may be generated by considering a pattern such as 'ecf' as a new event 'G' and repeating the pattern discovery process (Youngblood, et al. 2007). Results are shown in Figure 2.17 to Figure 2.18 for the resulting model of this approach using a maximal window of two hours.

Dynamic occupancy-based energy management

In order to evaluate the energy saving effects and thermal comfort conditions based on dynamic scheduling strategies from the occupant behavioral patterns, the energy usage of four different set point strategies are compared. These four possible HVAC set point schedules, and their advantages and disadvantages are:

1. Fixed system schedule set point at 24 C from 7:00am to 6:00pm.
 Advantage: simplicity for facility manager

Disadvantage: High Energy Cost. No need to maintain 24 °C when there are no people present

2. *Outlook schedule based on company outlook (Barney and Lynne, 2007)*

Advantage: exact meeting schedule and possible meeting duration

Disadvantage: Many meetings occur spontaneously with no pre-scheduling in Outlook

3. *Occupancy (Motion) sensor based*

Advantage: Simplicity

Disadvantage: No motion occurs if occupants are relatively still in the room. Also, motion is triggered if an occupant enters the room in the middle of the meeting, generating spurious events.

4. *Dynamic occupancy schedule*

Advantage: Dynamic temperature set point; an explicit meeting duration model; Automatic lighting control when zero occupancy; Save energy and maintain comfort

Disadvantage: Need for additional sensors

All schedules have a night setback temperature of 30 °C, and, aside from the fixed-point schedule, all have a daily setback of 27 °C at 7:00 am. A lower temperature set-point of 24 °C during the day is set when the room is considered occupied.

EnergyPlus simulations with three zones are conducted: a simple conference zone of size 3 x 6 m² faces east, a “Resistive” zone before the conference zone, and a North zone. We focus on evaluating controller performance in the conference zone (the other zones are kept at fixed standard operation schedules). Building loads are calculated from June 1 to August 31, 2008,

with TMY-3 Pittsburgh weather data. The true occupancy profile used for the simulation is taken from an “occupancy counter box” (see Figure 2.9) deployed in the conference room that allows occupants to keep track of the number of people in the room at all times by pushing up or down buttons. Table 2.7 shows the results from EnergyPlus in terms of total building loads for the three months.

Table 2.7 Building loads and comfort based on different HVAC set point schedules in the conference room

	Fixed	Outlook	Motion	Dynamic
Total Cooling Loads (kWh)	5483	4050	3794	3833
Total Lighting (kWh)	1150	880	872	872
Total (kWh)	6633	4930	4666	4705
Duration When Comfort Not Met (ASHRAE-55) (hour/day)	0.63	3.26	2.38	1

Table 2.7 shows that while the fixed schedule achieves very good comfort conditions (with very little time when comfort is not met), it is very energy inefficient. The Outlook schedule does not perform well because meetings are often either shorter than scheduled or even cancelled, leaving the HVAC system running with no one present. The largest total saving is from the motion-based approach. However, this comes with a sacrifice in occupant comfort because of times when occupants are present with little or no motion, causing the HVAC system to revert to the higher, less comfortable daily setback temperature. The dynamic schedule, which is derived from the data-driven pattern model, achieves energy saving comparable to that of the motion-based approach, but with a less amount of time when comfort is not achieved. The one hour per day of temperature set-point not met arises mostly from short visits to the meeting room (approximately 10 minutes) that are not worthwhile and not effective to start the cooling.

Figure 2.19 shows a daily indoor temperature profile from these four different set point schedules. The outlook schedule for the given day is: 9:15am~10:30am and 1:45pm~3:30pm. All

three non-fixed set point schedules reach the daily setback temperature at 7:00am as scheduled. Beginning at 7:00am, the temperature profiles behave differently according to the different set point strategies. Interestingly, during lunch time, the motioned-based schedule still tried to meet the set point despite only short visits to the conference room during that time.

The result from this section is only a preliminary test run for the developed occupant behavior pattern algorithm. A more comprehensive experiment is implemented in the Solar Decathlon house and results are discussed in Chapter 4.

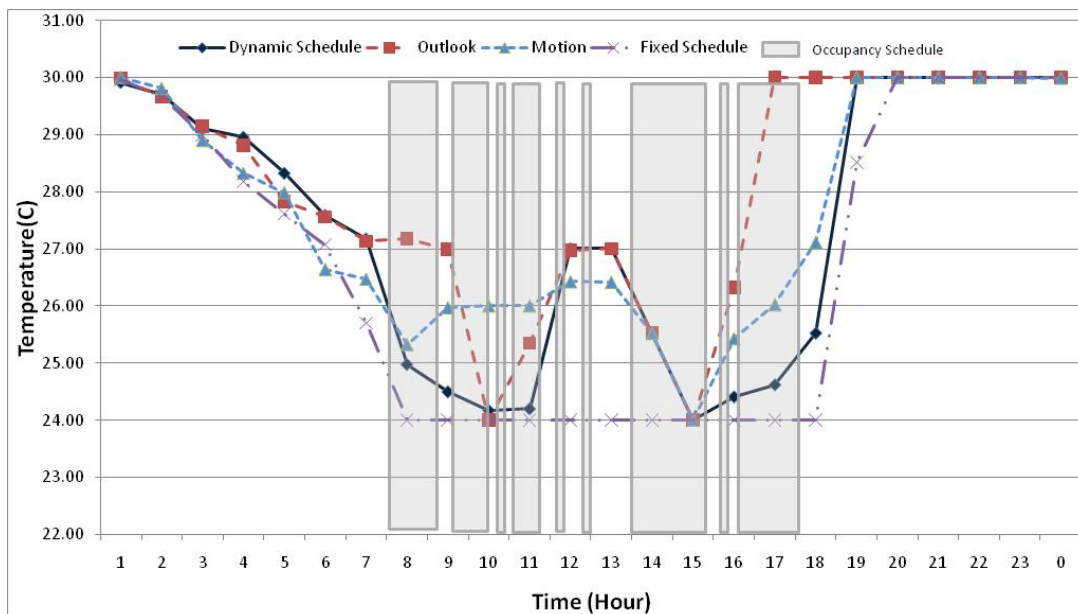


Figure 2.19 Temperature profile on Summer Design Day (July 21) based on different set points

2.4 Summary

This chapter presents methods for occupancy number estimation and occupancy duration prediction based on environmental sensor networks. Both results have accuracy as high as 75%. In addition, through simulation the energy-saving utility of using a data-driven model of occupant behavior for energy management is demonstrated. Ambient sensing data such as lighting, acoustics, CO₂, temperature, and relative humidity are incorporated into an event-based

pattern detection algorithm used for modeling occupant behavior toward HVAC system control. Furthermore, a connection of the learned behavioral model with energy control systems is illustrated through the generation of a dynamic occupancy schedule. Such a dynamic schedule is generated from a conference room environment equipped with a wireless sensor network and tested as an input to an HVAC control system in an EnergyPlus simulation. Compared with other alternative occupancy-based control strategies, the results of the dynamic schedule show significant energy saving with minimal comfort sacrifice. The algorithms developed in this chapter are integrated with predictive controls in Chapter 4.

Chapter 3 Development of the Building Model

3.1 Experiment Setup

The experiment is setup in the Solar Decathlon 2005 house, which has a typical office setup with a meeting room and several office workstations, as shown in Figure 3.1 below. The house is facing exactly South with a tilted wall at 14 degree off the vertical line, which has the least direct sun into the space. The upper roof is equipped with a solar thermal system, which did not function at all during the heating experiment time. The office room is occupied by a single occupant. The meeting room has both regular meetings and classes for graduate students. All HVAC equipment and appliances are easy to access. It serves as a living lab for graduate level researches.



Figure 3.1 Exterior view of solar decathlon house 2005 at CMU



Figure 3.2 Layout of solar decathlon house

3.1.1. Overview of HVAC Systems

Figure 3.3 shows the overview of the energy supply and demand systems in the solar house. PV and solar thermal are two main energy supply systems. Electric instant water heater, energy recovery ventilation, fan coil and heat pump are main energy demand side systems.

Heating system

The heating system in this study is called hydronic radiant floor heating system (HRFHS). The radiant floor heating system ideally consists of six main components if all components are functioned: the solar thermal collector, heat transfer/storage tank, instant water heater, radiant floor, the heating zone (room), and the system controls. In this study, only instant water heater is considered and implemented as the heating source of the water. As shown in Figure 3.3, HRFHS of the Solar Decathlon House has two loops which are the main loop (where thermal tank, instant water heater, and inlet and outlet nodes for supply and return pipes are connected in series) and three different secondary loops serving each different thermal zone of the building (meeting

room, office, and bathroom). There is a single main pump on the main loop and the other three pumps are serving the three thermal zones. Secondary loops are closed loops by the use of three-way valves which mix the return water from each room to each supply pipe.

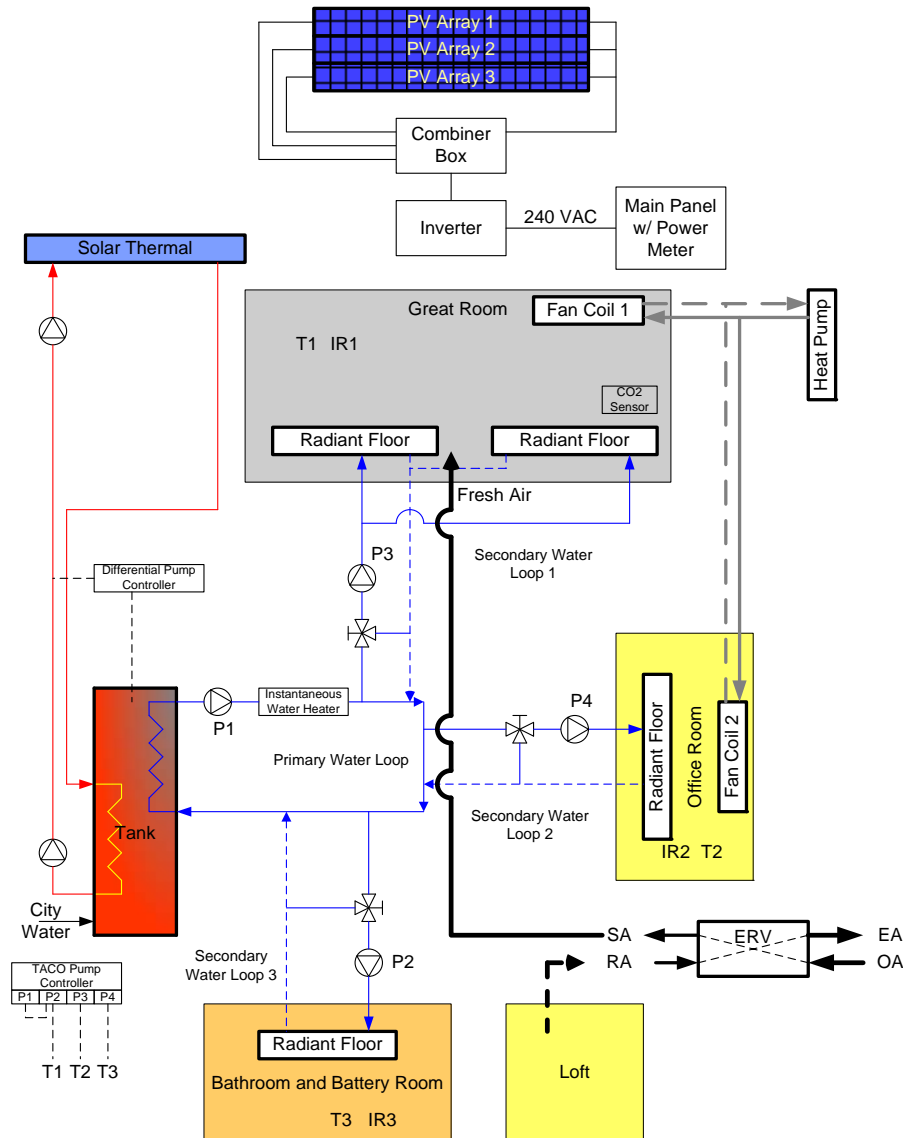


Figure 3.3 Overview of the energy supply and demand systems in the SD House

The thermal tank of the system is also connected to a solar collector which is acting as an auxiliary system to the operation of instant water heater. Due to the fact that each secondary water loop is connected to each other in series, the thermal conditions inside one room (e.g., meeting room) has an effect on the required supply water temperature for the next coming room

(e.g., office room). As a result, the main water supply temperature should be regulated taking into account of all three different thermal zones and their supply and return temperature differences. In this study, only meeting room is a controlled zone.

An electric instantaneous (tankless) hot water heater provides the heat source for supply water. This water heater, model SH-5 manufactured by SEISCO, is connected in series with the solar thermal loop. The SH-5 is rated at 5kW, and runs on a standard 240 VAC circuit. Advanced micro-processing contributes to extremely efficient operation of the unit, with one agency rating it at over 99% efficient. When no additional heating required, the water simply passes through the heater passively.

Cooling system

The cooling system uses multi-split fan coil units manufactured by Mitsubishi, Mr. Slim, MXZ series. As shown in Figure 3.3, it has two components, indoor fan coil units and outdoor air to air heat pump. Office and meeting room have one indoor fan coil unit independently. The user can control the temperature set-point and fan speed by using a remote infrared controller. The variable speed heat pump provides a constant supply air temperature at varying flow rate.

Ventilation system

The ventilation system is an Energy Recovery Ventilation (ERV) EV300 from RenewAir Inc. It supplies constant air to the great room (meeting room) only in the amount of 295cfm. The return duct is placed in the upper loft space. Basically, it takes outside air and return air, having them to exchange energy in the core part, and supplies the heated or cooled air into the space. The expected efficiencies are 61% ~75% in winter and 45%~60% in summer.

3.1.2 Sensor Network

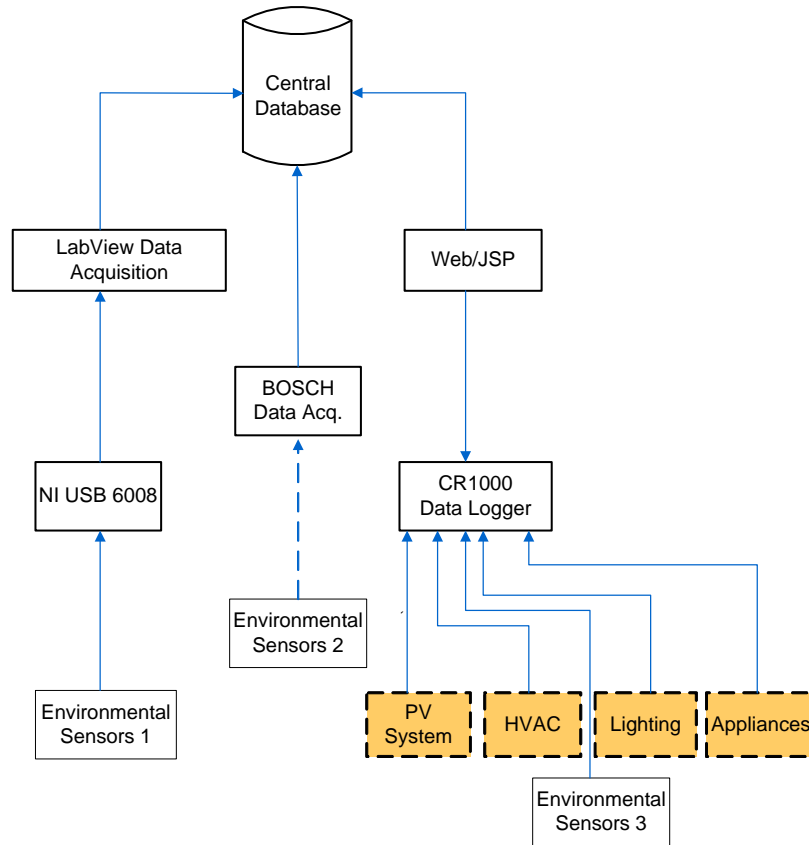


Figure 3.4 Overview of the sensing infrastructure in solar house

The house is equipped with a complex sensor network to measure and retrieves as much operational information as possible. Figure 3.4 shows the overall sensor infrastructure. Basically, there are three independent sensor networks.

- LabVIEW based data acquisition system (DAQ), called “environmental sensor 1”. All sensors are connected with DAQ and signals are transferred and stored through LabVIEW.
- A wireless environmental sensor network, donated by BOSCH RTC, Pittsburgh.
- Campbell Scientific CR1000 data logger system. This system not only measures the environmental performance variables, but also the system operations including PV, HVAC, lighting and appliances.

All sensor data is finally integrated into a central database. Since different sensor networks have their own timestamps, they have to be synchronized in the central database.

3.1.2.1 Environmental Sensor Network

The three environmental sensor networks are described below. LabVIEW based sensor network measures indoor temperature at different heights, RH and both indoor and outdoor CO₂ levels with a sampling of one minute. The CO₂ sensors are manufactured by TelAir. Most of the temperature sensors in “environmental sensor 1” are made with LM 35DZ. As shown in Figure 3.5, mean radiant temperature is measured with a black globe.

The BOSCH wireless sensor network measures temperature, RH, lighting, acoustics and motion with a sampling time of one minute. All the other information is preparatory.

CR1000 measures indoor temperature sensors, outdoor local weather station (temperature, RH, wind speed, pyranometer) and power metering for every electricity consumer, with a sampling time of five seconds. All the temperature sensors are from Omega engineering, type T sensor. The temperature and RH probe is HMP50-50, Campbell Scientific. Every indoor temperature sensor from Omega engineering has a radiation shell to exclude the effect from radiation and measure the pure air temperature.



TeleAir CO2 Sensor



Temperature Sensor



RH and Temperature Probe



Floor Surface Temperature Sensor



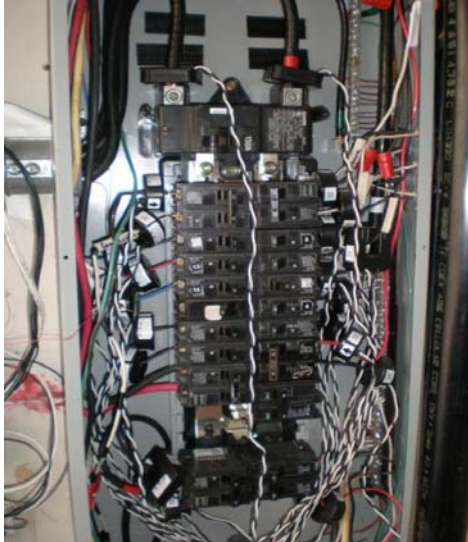
Mean Radiant Temperature Sensor



BOSCH Wireless Mote

Figure 3.5 Environmental sensors in solar house

3.1.2.2 System Sensor Network



CTs inside Power Distribution Board



WattsNode connecting with CTs

Figure 3.6 Power system measurement

Figure 3.6 shows the power consumption measurement in the SD house. For each switch in the power distribution board, the power consumption is measured. The power generated by PV system is also measured through measuring the AC and DC side of inverter.



Surface temperature sensors of radiant floor system



Temperature and RH sensors for fan coil

Figure 3.7 Heating and cooling system sensors

Figure 3.7 shows the heating and cooling system sensors. For radiant floor heating system, the supply and return pipe surface temperature and water flow to each branch are measured. The pipes are well insulated so that the surface temperature of the copper pipes is assumed to be the same as water temperature. In addition, the floor surface temperature is also measured as shown in Figure 3.4. For cooling system, the supply air temperature and RH is measured at the outlet of the indoor fan coil. The supply air flow rate has three stages and measured by a portable flow meter before the experiment period.

3.2 Building Zone Model

The building zone model represents the thermal dynamics interaction between the indoor and outdoor environment. It mainly includes wall and roof heat transfer, zone air infiltration and solar radiation impacts. It describes how outdoor environment changes can affect the indoor environment changes and the HVAC systems as well.

3.2.1 Model of Zone Air Infiltration

Based on the model of Sherman and Grimsrud (1980), which uses the effective air leakage area, the airflow rate from infiltration is calculated according to:

$$V_{infl} = A_l \sqrt{C_s \Delta T + C_w V_{wind}^2} \quad (2.11)$$

where,

A_l	Effective air leakage area [m ²]
C_s	Stack coefficient [-]
ΔT	Indoor-outdoor temperature difference [°C]
C_w	Wind coefficient [-]
V_{wind}	Local wind speed [m ³ /s]

V_{inft} Air flow rate through infiltration [m^3/s]

According to the ASHRAE fundamentals Chapter 16, $C_s = 0.015$ for a one story basic house and $C_w = 0.0065$ is for a one story house with “Typical shelter caused by other buildings across street from building under study”.

The energy flux due to the infiltration and window opening are calculated as below:

$$Q_{inf} = C_{air}V_{inft}\Delta T \quad (3.8)$$

where,

C_{air} Specific heat of the air [$J/Kg \cdot K$]

Q_{inf} Energy flux due to the infiltration [W]

3.2.2 Model of Wall Heat Transfer

A surface temperature sensor is installed on the inside surface of the east and west façade. The east wall is modeled as standard two capacitances and three resistances (2C3R) model (ASHRAE thermal network model) as shown in Figure 3.8.

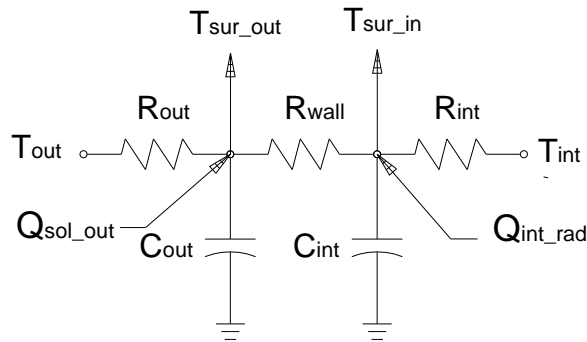


Figure 3.8 Wall Heat Transfer Modular

The relationship of solar radiation and internal heat gain is defined as below, one purpose of system identification is to find α_{ab_w} , β_{ab_w} and γ_{ab_w} .

$$Q_{sol_out} = \alpha_{ab_w} Q_{sol} \quad (3.9)$$

$$Q_{int_rad} = \beta_{ab_w} Q_{sol} + \gamma_{ab_w} Q_{int} \quad (3.10)$$

where

- γ_{ab_w} Coefficient of absorbed internal heat gain from occupancy and equipment by inside surface of the wall
- α_{ab_w} Coefficient of absorbed solar radiation on the external surface of an external wall
- β_{ab_w} Coefficient of absorbed transmitted solar radiation on the inside surface of an external wall

According to the relationship between thermal resistance and capacitance described in Figure 3.8, the thermal network model can be written as:

$$C_{out} \frac{dT_{sur_out}}{dt} = \alpha_{ab_w} Q_{sol} + \frac{T_{out} - T_{sur_out}}{R_{out}} - \frac{T_{sur_out} - T_{sur_in}}{R_{wall}} \quad (3.11)$$

$$C_{in} \frac{dT_{sur_in}}{dt} = \beta_{ab_w} Q_{sol} + \gamma_{ab_w} Q_{int} + \frac{T_{sur_out} - T_{sur_in}}{R_{wall}} - \frac{T_{sur_in} - T_{in}}{R_{int}} \quad (3.12)$$

where

R_{out}	Outside wall convective heat transfer coefficient [K.m ² /W]
R_{int}	Inside wall convective heat transfer coefficient [K.m ² /W]
R_{wall}	Thermal resistance of the wall [K.m ² /W]
C_{out}	Heat capacitance of the external part of the wall [J/m ³ ·K]
C_{in}	Heat capacitance of the internal part of the wall [J/m ³ ·K]
Q_{sol_out}	Solar radiation on the outside surface of the wall [W]
Q_{int_rad}	Internal radiative heat gain absorbed by inside surface of the wall [W]

The roof heat transfer model takes the same approach as described above, which is not described in detail here.

3.2.3 Model of Zone Heat Transfer

Meeting room and office room have at least one person during day time. The main heating source is from radiant heating floor. The cooling source is from a fan coil unit. Figure 3.9 below shows the thermal network in these two zones. Each wall is simulated as 2R3C model as discussed above. The internal zone including the loft, mechanical room, bathroom and entrance room is simulated as 2R3C model, which is adopted from Wang et al. (2002). All resistances and capacitances are assumed to be time invariant. The thermal storage effect of window is neglected and represented as a resistance only. There is a door between office and meeting room, which is

represented as a resistance as well. Office and meeting rooms are decomposed to identify independently.

The calculation of solar radiation on specific building surfaces is presented in Lam (2004). This calculation is used for the system identification.

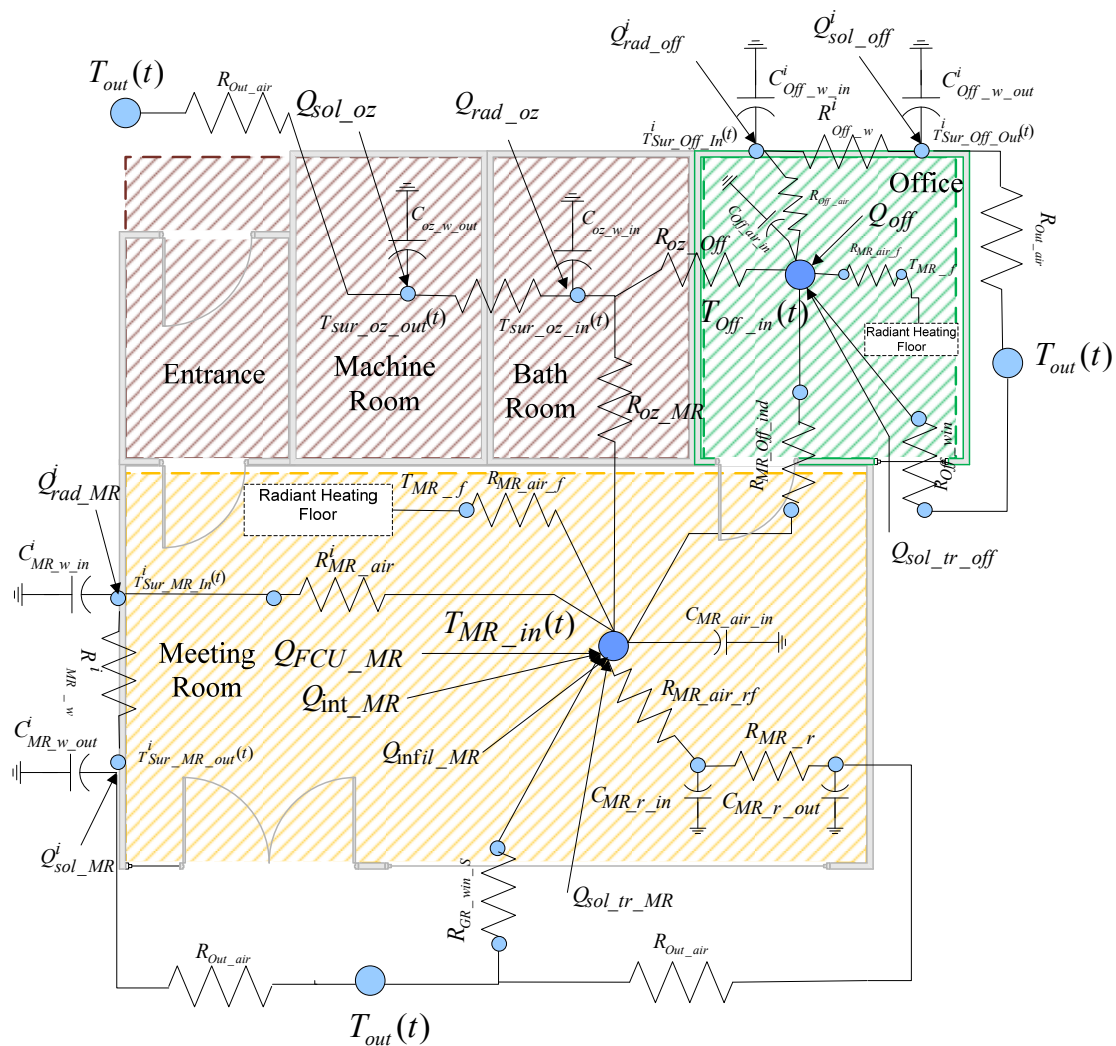


Figure 3.9 Thermal network model of solar house test-bed

The heat transfer for meeting room is represented with the following differential equation:

$$\begin{aligned}
C_{MR_Air_in} \frac{dT_{MR_in}}{dt} &= Q_{FCU_MR} + Q_{int_MR} + \epsilon Q_{inf_MR} + \sum_{i=1}^n \frac{T_{sur_MR_in}^i - T_{MR_in}}{R_{MR_air}} \\
&+ \frac{T_{MR_sur_f} - T_{MR_in}}{R_{MR_air_f}} + \frac{T_{sur_oz_in} - T_{MR_in}}{R_{Oz_MR}} + \frac{T_{Off_in} - T_{MR_in}}{R_{MR_Off}} \\
&+ \frac{T_{Sur_MR_win} - T_{MR_in}}{R_{MR_air}}
\end{aligned} \tag{3.13}$$

The heat transfer for lumped other zones is:

$$\begin{aligned}
C_{oz_out} \frac{dT_{sur_oz_out}}{dt} &= \alpha_{oz} Q_{sol} + \frac{T_{out} - T_{sur_oz_out}}{R_{out_air}} - \frac{T_{sur_oz_out} - T_{sur_oz_in}}{R_{oz_w}}
\end{aligned} \tag{3.14}$$

$$\begin{aligned}
C_{oz_in} \frac{dT_{sur_oz_in}}{dt} &= \beta_{oz} Q_{sol} + \gamma_{oz} Q_{int} + \frac{T_{sur_oz_out} - T_{sur_oz_in}}{R_{oz_w}} \\
&- \frac{T_{sur_oz_in} - T_{MR_in}}{R_{Oz_MR}}
\end{aligned} \tag{3.15}$$

The heat transfer for office zone is:

$$\begin{aligned}
C_{Off_Air_in} \frac{dT_{off_in}}{dt} &= Q_{FCU_off} + Q_{int_off} + \epsilon Q_{inf_off} \\
&+ \sum_{i=1}^n \frac{T_{sur_off_in}^i - T_{off_in}}{R_{off_air}} + \frac{T_{off_sur_f} - T_{MR_in}}{R_{off_air_f}} \\
&+ \frac{T_{sur_oz_in} - T_{off_in}}{R_{oz_off}} + \frac{T_{off_in} - T_{off_in}}{R_{off_MR}} \\
&+ \frac{T_{sur_off_win} - T_{off_in}}{R_{off_air}}
\end{aligned} \tag{3.16}$$

Where n is number of external façades include roof, i is the i th external façade, T is the temperature, C and R are capacitance and resistance, subscripts sur, in, out, f, rf, oz indicate surface, indoor, outdoor, floor, roof and other zone respectively. To smoothing the later model parameter identification, the coefficient of combined effects of radiation and convection from radiant heating floor is represented by $R_{off_com_f}$ and $R_{MR_co_f}$, instead of fourth order calculation. Q_{FCU} is the cooling from fan coil unit. Q_{int} is the internal heat gain from occupancy, office equipment etc. Q_{inf} is the heat or loss through infiltration and natural ventilation.

3.3 Building HVAC System Model

3.3.1 Radiant Floor Heating System Model

A radiant floor for meeting room has 0.089 thick exposed concrete slabs of 21.6 m². Office room has a hardwood (oak) floor covering (with 7.6m² exposed-area) that sits on a concrete slab. Hot water is circulated through the 0.0127m diameter PEX (cross-linked polyethylene) tubes which are embedded in the middle of concrete slabs of meeting room and located underneath the timber flooring of office room. The office room has a single loop of PEX tubes with total length of 47m, whereas, meeting room has two loops of PEX tubes (assumed to be in identical layout) with a total length of 107.2m.

3.3.1.1 Model of Radiant Floor Heating

Figure 3.10 shows the floor section view and its thermal circuit model to model the radiant heating process. This process involves heat conductivity within the concrete; heat convection and radiation with surrounding air; radiation from floor to other surfaces; and transmitted solar radiation through the window. Basic thermal properties of radiant floor material and tube are listed in Table 3.1 (Engineering ToolBox, 2009).

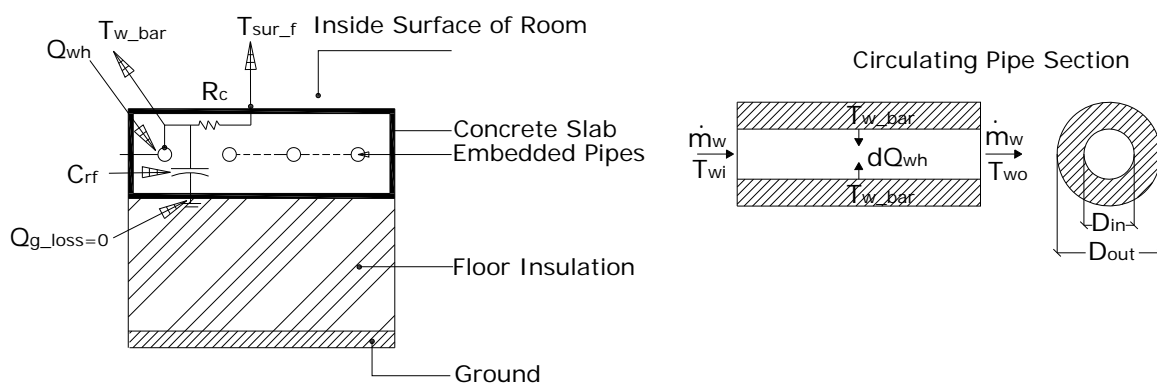


Figure 3.10 Section view of radiant heating floor system

Table 3.1 Thermo-physical properties of radiant floor materials

RFHS Material	Density (kg/m ³)	Specific Heat (J/kg·K)	Conductance (W/m·K)
Concrete	2200	840	1.700
Oak (hardwood)	720	1260	0.160
PEX tubing	950	2301	0.502

The floor concrete slab is modeled as a thermal capacitance with a resistance as shown in Figure 3.10. Since the floor is well insulated, the heat loss through the ground is assumed to be 0. Equations (3.17) to (3.20) describe the detailed heat transfer model.

$$\begin{aligned} \dot{m}_{cf} C_{MR_{cf,sp}} \frac{dT_{MR_{sur_f}}}{dt} \\ = h_{cf} A_f (T_{MR_{in}} - T_{MR_{sur_f}}) + \frac{\bar{T}_{MR_w} - T_{MR_{sur_f}}}{R_{MR_{cf}}} + \mu_{MR} \dot{Q}_{sol} \end{aligned} \quad (3.17)$$

$$\dot{m}_{cf} C_{MR_{cf,sp}} \frac{d\bar{T}_{MR_w}}{dt} = \dot{m}_{MR_w} C_{pw} (T_{MR_{wi}} - T_{MR_{wo}}) + \frac{T_{MR_{sur_g}} - \bar{T}_{MR_w}}{R_{MR_{cf}}} \quad (3.18)$$

$$\dot{m}_{cf} C_{MR_{cf,sp}} \frac{T_{MR_{sur_g}}}{dt} = \frac{\bar{T}_{MR_w} - T_{MR_{sur_g}}}{R_{MR_{cf}}} \quad (3.19)$$

$$T_{MR_{wo}} = T_{MR_{wi}} + (T_{MR_{sur_f}} - T_{MR_{wi}}) \left(1 - e^{-\frac{U_{wf} \pi D_p}{\dot{m}_{MR_w} C_{pw}} L_p}\right) \quad (3.20)$$

where

\bar{T}_{MR_w}	Temperature around the water tubes [°C]
$T_{MR_{wi}}$	Inlet water temperature of radiant floor system [°C]
$T_{MR_{wo}}$	Outlet water temperature of radiant floor system [°C]
$\dot{m}_{MR_{cf}}$	Mass density of concrete floor [kg/m ³]
$C_{MR_{cf,sp}}$	Specific heat of concrete floor [kJ/kg·K]
μ	Coefficient of transmitted solar absorbed by the concrete floor [-]
U_{wf}	Water to floor heat transfer coefficient [W/m ² ·K]
h_{cf}	Overall heat transfer coefficient for floor surface [-]
D_p	Diameter of water tubes [m]

h_{cf} includes both radiation and convection. It is defined as

$$h_{cf} = h_{rf_cov} + h_{cf_rad} \quad (3.21)$$

where

$$h_{cf_rad} = 4\sigma\epsilon C_r (T_{cf_s} + 273.15)^3 \quad (3.22)$$

σ Stefan-Boltzmann constant, which is $5.670 \cdot 10^{-8}$ [J/K⁴.m².s]

ϵ surface total Hemispherical emissivity, which is 0.91 [-]

C_r correction factor due to the impact of indoor furniture [-]

Convection from horizontal plates facing downward when heated (or upward when cooled) is a special case. Therefore, there are two parts for convection, named natural and forced, respectively (ASHRAE, 2009).

$$h_{cf_cov_n} = 2.31|T_{air} - T_{cf_s}|^{0.31} \quad (3.23)$$

$$Nu = \frac{h_{cf_cov_f} D}{\lambda} = 0.037 Re^{0.8} Pr^{0.6} \quad (3.24)$$

where

Nu Nusselt number

Pr Prandtl number

Re Reynolds number

λ Fluid conductivity

D Characteristic length

3.3.1.2 Model of Tankless Water Heater

Ideally, when the energy provided by the solar thermal collector system is not adequate to heat the water for the radiant floor system, an electric instantaneous (tankless) hot water heater provides the additional temperature rise. In this study, the solar collector is not in operation. Hence, this tankless water heater is the only hot water heat source.

Figure 3.11 shows the performance curve of temperature rise vs. flow rate (GPM). The data is from manufacture data sets. The cubic polynomial equation is found to be the best fit for these data with R^2 of 0.985. The curve shows, at the fixed power rate, the slower the water flow, the higher the temperature rise.

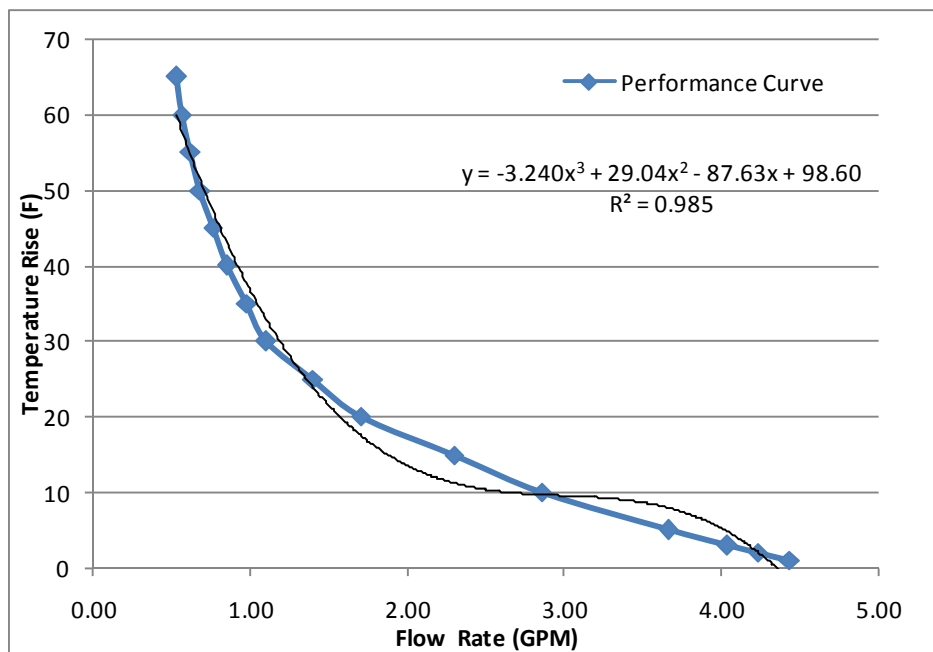


Figure 3.11 Water heater temperature rise vs. flow rate

The total energy to heat the water at each time step is calculated as:

$$\dot{Q}_{hw} = (T_{hw,s} - T_{hw,r})\dot{m}_w C_{pw} \quad (3.25)$$

where $T_{hw,s}$ and $T_{hw,r}$ are the supply and return water temperature of tankless water heater, respectively. \dot{m}_w is the total water flow rate.

The heater efficiency (Eff_{heater}) is defined as the ratio of the hot water energy to the electric input energy

$$Eff_{heater} = \frac{Q_{hw}}{Q_{elec}} \quad (3.26)$$

$$Q_{elec} = \frac{Q_{hw}}{Eff_{heater}} = \frac{(T_{hw,s} - T_{hw,r})\dot{m}_w C_{pw}}{Eff_{heater}} \quad (3.27)$$

3.3.2 Heat Pump Cooling

The cooling equipment in the solar house is provided by a multi-split fan coil unit from Mitsubishi Electric Inc. It is a refrigerant cooling with outside air to air heat pump. Hence, the total amount of cooling energy into the space can be represented by:

$$Q_{fcu} = C_{air} \dot{m}_{fcu} (T_{air,s} - T_{MR,in}) \quad (3.28)$$

$$E_{cooling} = \frac{\alpha_{hp} Q_{fcu}}{COP} \quad (3.29)$$

where

\dot{m}_{fcu}	Air mass flow rate [m ³ /s]
$T_{air,s}$	Supply air temperature [°C]
COP	Coefficient of performance of heat pump [-]
α_{hp}	Correction factor for heat pump energy consumption [-]
Q_{fcu}	Fan coil cooling load [W]
$E_{cooling}$	Cooling energy consumption [W]

Based on the onsite measurement, the supply air temperature is observed to be constant at certain flow rate which is shown in Table 3.2 below.

Table 3.2 Measured cooling supply air flow rate and temperature

Flow Rate (m³/s)	Temperature (°C)
0.08	15.5
0.12	13.5
0.19	11.5

3.4 Parameter Identification

It is important to investigate how the onsite data logger can help to identify the material thermal properties when it is difficult to find out existing building construction materials, although the materials properties could be reached by manufactures if the materials were known. Hence, identification of wall thermal properties is presented below. The assumptions for this calculation are: a) wall surface temperature, indoor air temperature and radiative heat gain on the inside surface of the wall are uniformly distributed; b) indoor convective heat transfer coefficient is not changing with time.

There are several parameter identification methods in the literature and can be divided into two main categories: black-box and grey-box. Mechaqrance and Zouak (2002) developed a neural network auto regressive with exogenous input (NNARX) model to predict the indoor temperature of a residential building. The summed square error is close to 0.9. Recently, Jimenez, Madsen and Andersen (2008) presented the application of the IDENT Graphical User Interface of MATLAB to estimate thermal properties of building thermal components from outdoor dynamic testing, imposing appropriate physical constraints and assuming linear and time invariant parametric models. A follow-up study by Jimenez et al. (2009) presented different system identification approaches to find the U value of a given building component. However, this black-box approach requires a long period of training to improve the performance accuracy.

In addition, the black-box may have more complex model structure than lower-order models such as gray-box models, which make the model analysis difficult.

With these disadvantages of the black-box model, there are some other studies on developing and validating grey-box model. Braun and Chaturvedi (2002) developed a thermal network model for transient building load prediction. This inverse grey-box model needs one week of data to train with rich zone temperature variations or two to three weeks of data to train with limited zone temperatures variations. The model error can be limited within 2% with simulation data and 9% with on-site data. Wang and Xu (2006) developed a simplified model of the building thermal load on heat transfer of building envelope and internal mass. The parameters of building thermal network models for building envelope are determined by frequency characteristic analysis; the parameters of thermal network models for lumped internal mass are identified with generic algorithm. McKinley and Aleyne (2008) presented an alternative approach using optimization search process (hill climbing algorithm) to identify building thermal model parameters and loads based on site measurement.

In this study, considering this problem as a constrained nonlinear optimization, the subspace trust region solver based on the interior-reflective Newton method (Coleman and Li, 1996) is chosen. It is available in the MATLAB 2009b Optimization Toolbox.

3.4.1 Objective Function of Optimization

The simulated indoor and wall surface temperatures from the above equations are used to compare with the measured temperature. The optimized parameters are the resistances, capacitances and coefficients of infiltration and solar radiation. The objective function J is defined as (Neuman, C., personal communication, March 13, 2009):

$$J = \min_{\mathbf{x}} \|\mathbf{f}(\mathbf{x})\|_2^2 = \min_{\mathbf{x}} \frac{(f_1^2 + f_2^2 \dots + f_n^2)}{n} \quad (3.30)$$

S.T. $\mathbf{X}_L < \mathbf{X} < \mathbf{X}_u$

where

$$f_n(x) = T_{predict}^n - T_{measured}^n \quad (3.31)$$

- n Number of measured data points [-]
- $T_{predict}$ Predicted air temperature [°C]
- $T_{measured}$ Measured air temperature [°C]
- X Vector of unknown parameters [-]
- X_L Lower bound of unknown parameters [-]
- X_u Upper bound of unknown parameters [-]

Since most of the parameters are physical parameters which should be bounded in certain ranges, the lower and upper bound are based on their initial engineering guess values. Table 3.3 below shows the scale factor for different type of physical parameters.

Table 3.3 Scale Factor Limits for Optimization Search Space

Parameters	Minimum	Maximum
C_{out}	$0.5 C_{initial}$	$2C_{initial}$
C_{in}	$0.1 C_{initial}$	$0.5C_{initial}$
R	$0.5R_{initial}$	$1.5R_{initial}$
α	0.01	1
β	0.01	1
γ	0.01	1
ϵ	0.01	1

3.4.2 Identification Process

The parameter estimation process (PEP) is shown in Figure 3.12. The process starts from the wall and roof heat transfer PEP. Measured wall and roof surface temperature, indoor, outdoor temperature and solar radiation on the surface are the inputs. Wall and roof thermal properties

are the outputs. The estimated wall and roof parameters with measured zone temperature and solar radiation will be the inputs for Meeting Room and Office Room PEP. The uncertain parameters of radiant floor heating system include floor slab thermal properties, floor absorbed solar radiation and surface radiant and convective heat transfer coefficients.

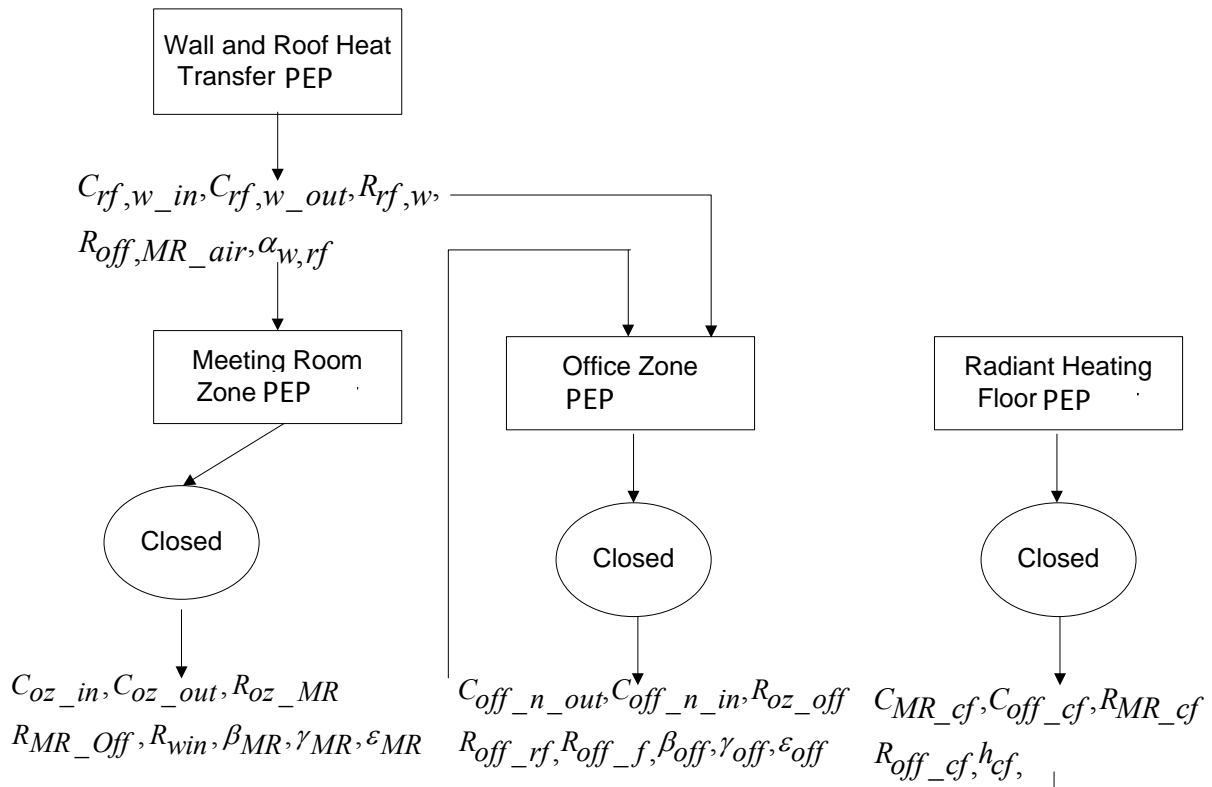


Figure 3.12 Parameter estimation process

3.5 Validation of the Building Model

3.5.1 Data Collection

The data is continuously collected every one minute or one and half minutes (depending on the network legacy) since April 28, 2009. The minimum training and testing days are five days and one day, respectively.

3.5.2 Validation Criteria

The evaluation function for the accuracy of model validation in this study is the Root Mean Square Error (RMSE). RMSE quantifies the deviations of predicted values from measured values over the whole measurement period. It is defined as

$$RMSE = \sqrt{\frac{1}{n} \sum_{t=1}^n (A_t - P_t)^2} \quad (3.32)$$

where

n Total number of data points

A_t Measured data points

P_t Predicted data points.

3.5.3 Results and Discussion

3.5.3.1 Building thermal properties

a. Overview

Figure 3.13 and 3.14 show model predicted indoor air temperature for two continuous months from October 1 to November 28, 2009, in Meeting Room and Office Room, respectively. The overall RMSEs are 0.55 and 0.76, respectively. There are weeks which have smaller RMSE than the average value, called scenario one, and higher RMSE, called scenario two. Each week is selected to represent each scenario and discussed later. In addition, some days do not have data at all due to the failure of the data acquisition system.

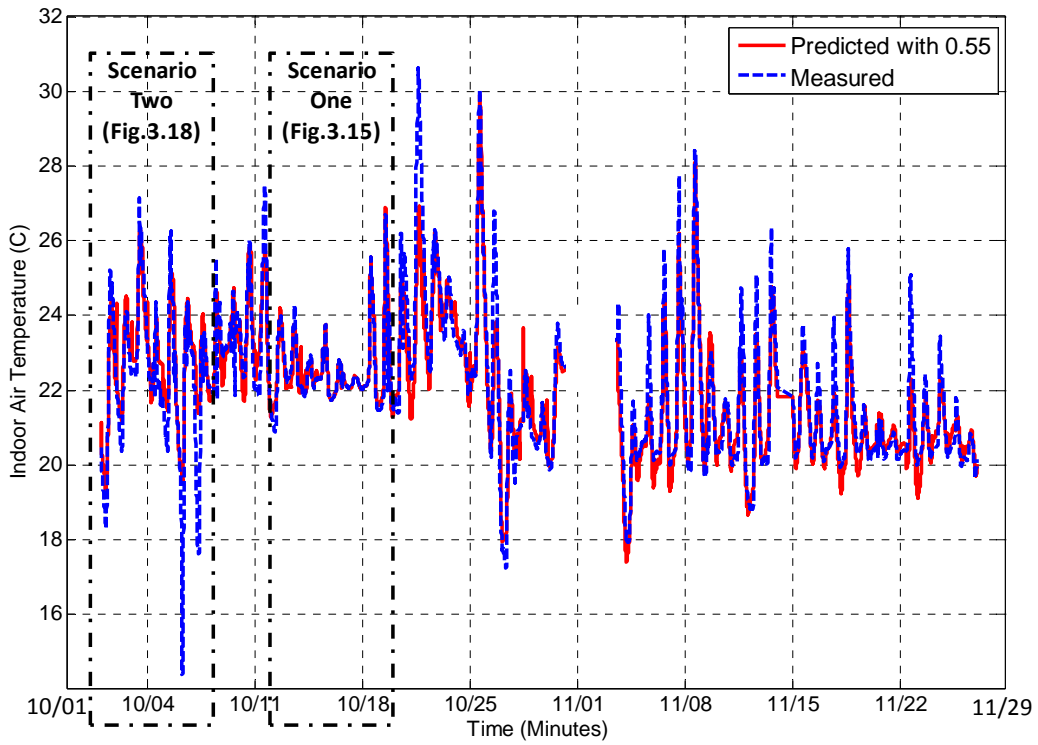


Figure 3.13 Model predicted meeting room indoor temperature profile from October 1 to November 29, 2009

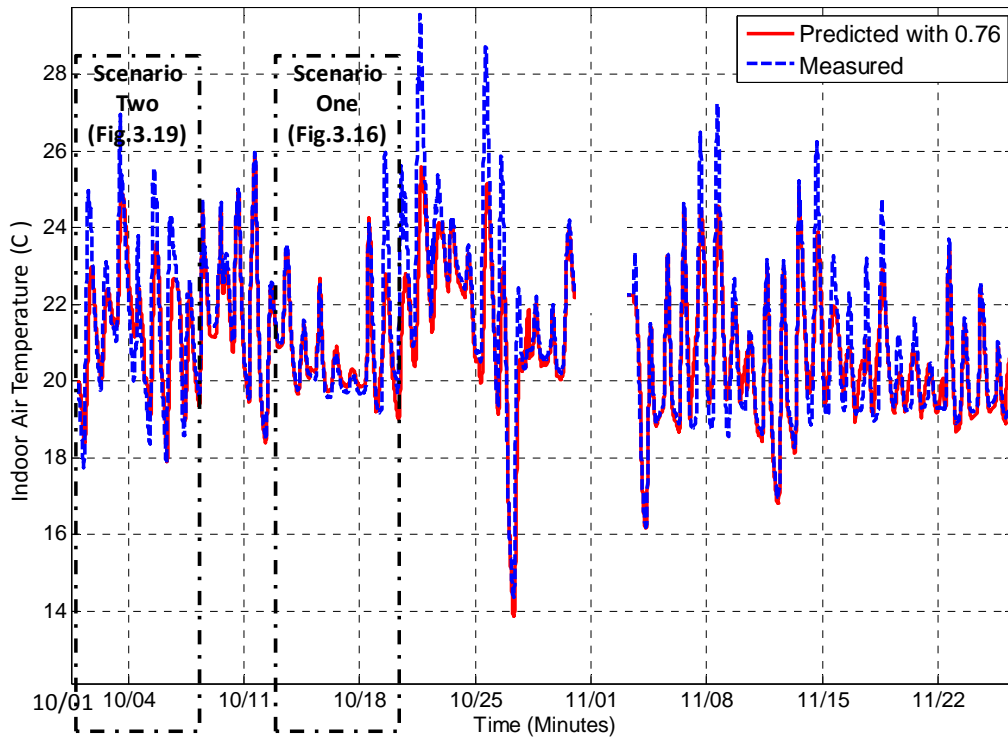


Figure 3.14 Model predicted office room indoor temperature profile from October 1 to November 29, 2009

b. Scenario One

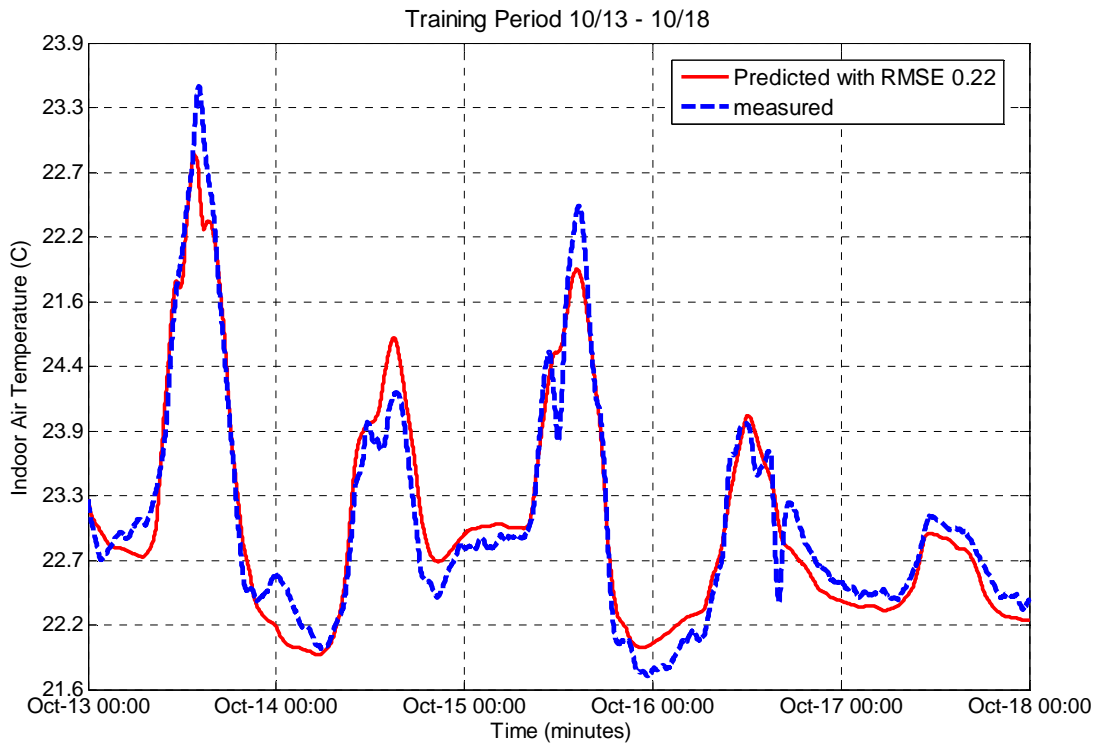


Figure 3.15 Model predicted meeting room indoor air temperature profile from October 13 to October 18, 2009

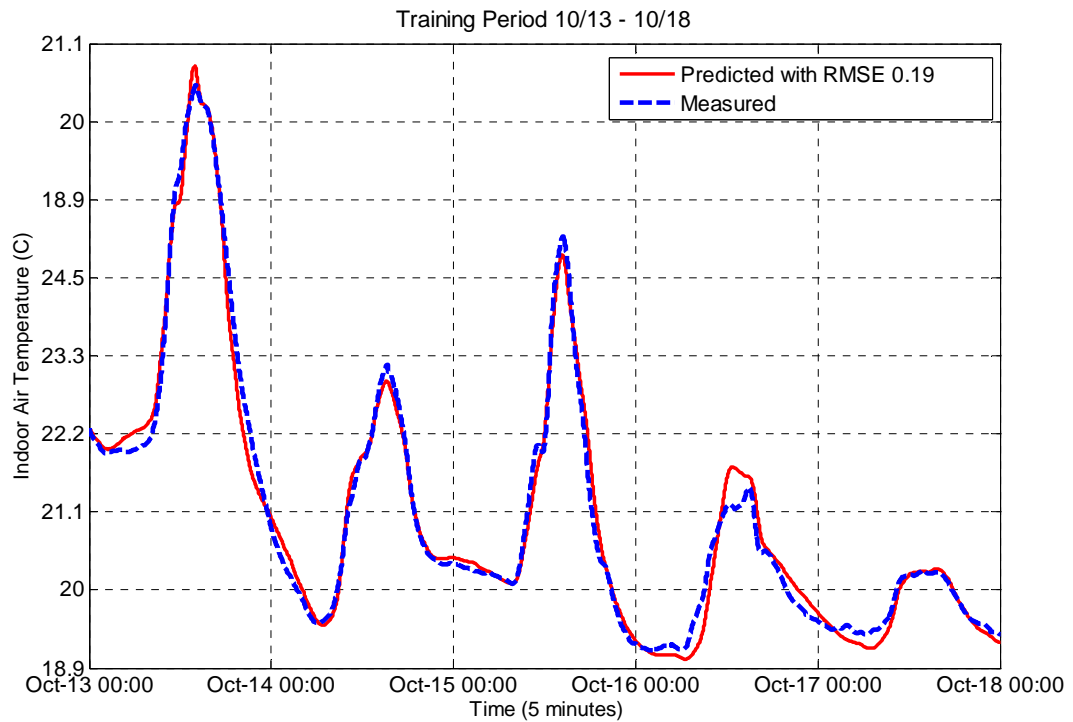


Figure 3.16 Model predicted office room indoor air temperature profile from October 13 to October 18, 2009

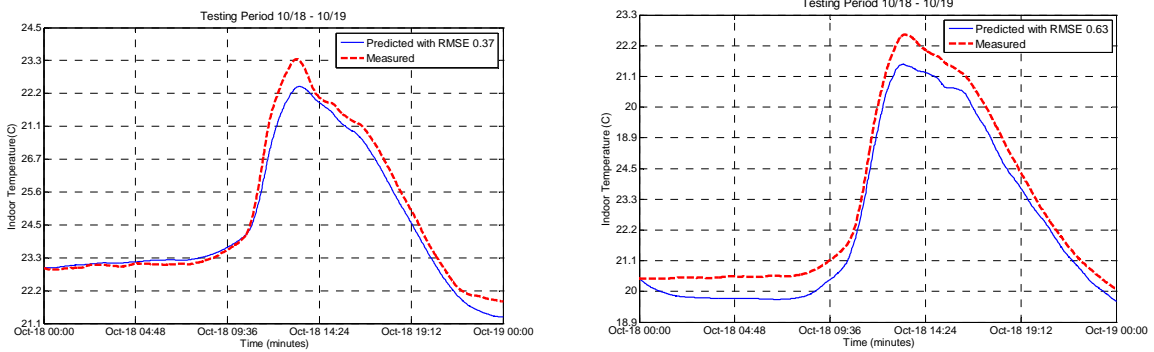


Figure 3.17 Model predicted meeting room and office indoor air temperature profile on October 18, 2009

Figures 3.15 to 3.16 show Scenario One where the RMSEs of model predicted indoor air temperature are 0.22 and 0.19 for Meeting Room and Office Room, respectively. The predicted temperature tracks well with the measured one. In addition, the predicted daily temperature shows that the prediction performance is better at night than during day time because of less disturbances such as solar radiation as shown in Figure 3.17.

c. Scenario Two

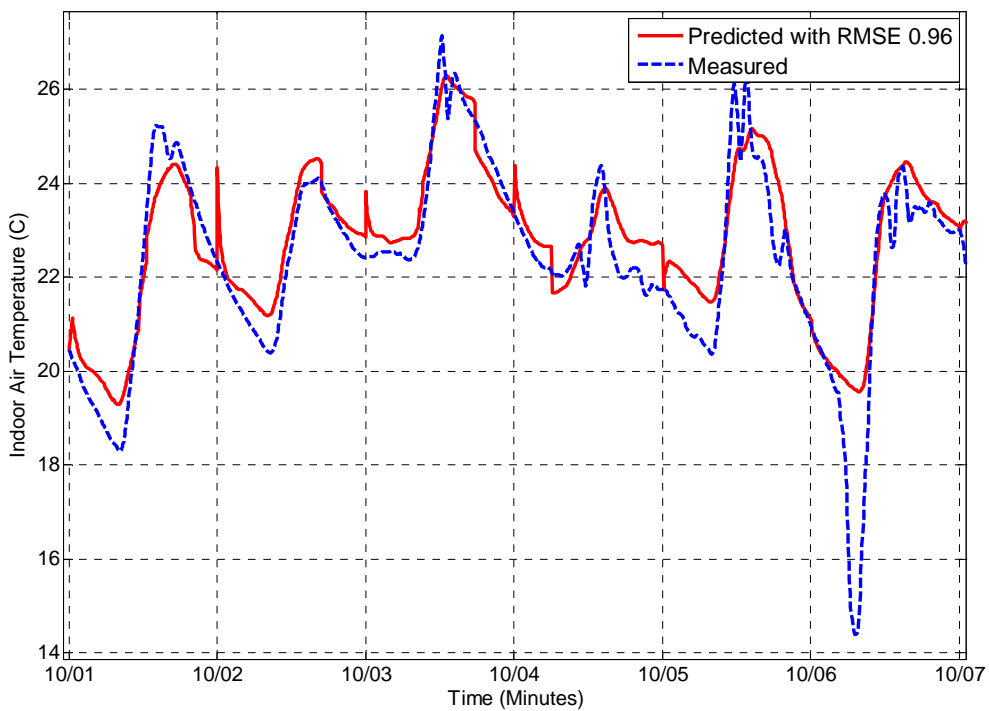


Figure 3.18 Model predicted meeting room indoor air temperature profile from October 1 to October 7, 2009

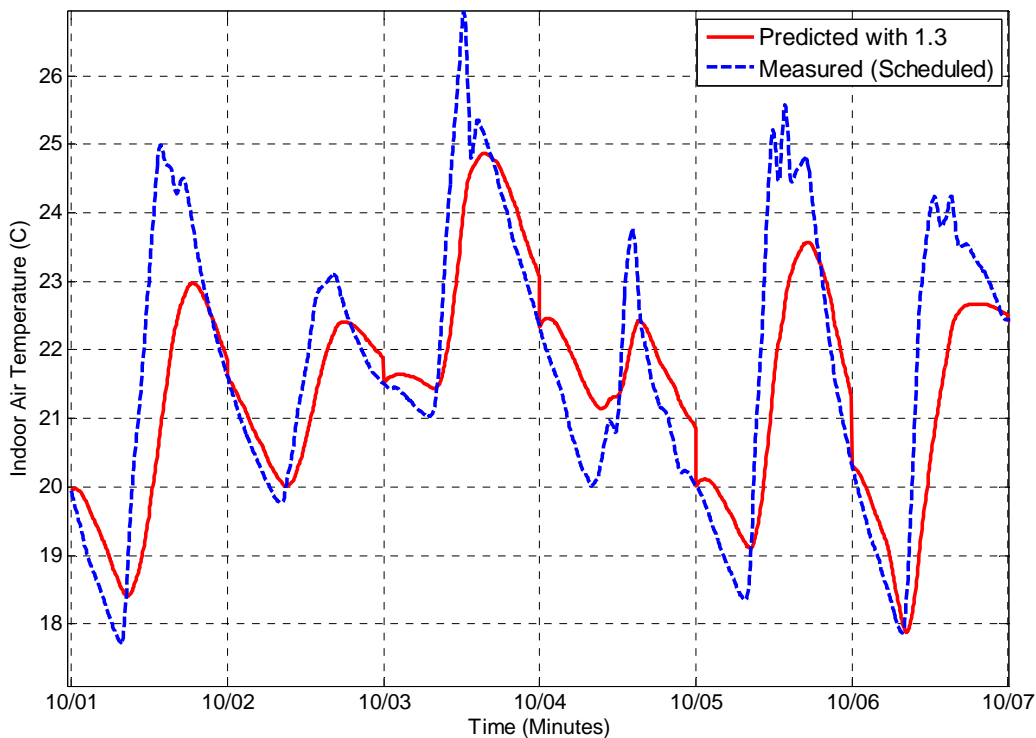


Figure 3.19 Model predicted office indoor air temperature profile from October 1 to October 7, 2009

Figures 3.18 to 3.19 show Scenario Two where the RMSEs of model predicted indoor air temperature are 0.96 and 1.3 for meeting and office room, respectively. The prediction did not perform well, possibly because this week is during the seasonal transition period, where the daily temperature has a huge difference (30%~40%) with night temperature, particularly for the office space. In addition, during the middle of some days, the measured temperature raised much higher than predicted one. The previous learned solar radiation coefficients may not be applied in this case. Figure 3.18 also shows a sudden temperature decreases on October 6 in meeting room, while office room does not. This could be a failure of temperature sensor in meeting room.

In conclusion, the building zone model predicts the indoor air temperature with RMSE of 0.55 when the temperature is relatively stable and does not change more than 8 °C from day time to night time.

d. Sensitivity Analysis

Table 3.4 Results of sensitivity analysis on identified building thermal properties

Parameters	Identified		Parameters	Identified	
	Mean	Deviation		Mean	Deviation
$R_{wall_East}, R_{wall_west}$	0.5 [K.m ² /W]	0.0618	C_{MR_in}	$1.2355 \cdot 10^6$ [J/m ³ .K]	$1.182 \cdot 10^3$
R_{MR_air}	0.3 [K.m ² /W]	0.1	C_{MR_out}	$7.4106 \cdot 10^7$ [J/m ³ .K]	$1.42 \cdot 10^3$
R_{oz_MR}	0.28 [K.m ² /W]	0.1	C_{oz_in}	$1.0475 \cdot 10^6$ [J/m ³ .K]	$2.15 \cdot 10^4$
R_{MR_Off}	0.1 [K.m ² /W]	0.046	C_{oz_out}	$1.0475 \cdot 10^7$ [J/m ³ .K]	$3.04 \cdot 10^3$
R_{off_air}	0.2 [K.m ² /W]	0.15	$C_{MR_air_in}$	$1.7781 \cdot 10^5$ [J/m ³ .K]	$1.40 \cdot 10^3$
$R_{MR_air_f}$	0.03 [K.m ² /W]	0.01	$C_{off_air_in}$	$4.627 \cdot 10^4$ [J/m ³ .K]	$3.10 \cdot 10^2$

Table 3.4 shows the sensitivity analysis of identified parameters. The most sensitive parameter is the one with the largest deviation from the mean value. The physical parameters, such as the wall thermal resistances and capacitances, change only within 10% of the mean value. The overall heat transfer coefficients for room air, floor to room air and wall to room air change more than 30% from the mean value. It means that these coefficients are sensitive to the response of the model. When input training data changes, they need to be re-identified.

3.5.3.2 Radiant floor system

Thermal Properties

a. Overview

Table 3.5 shows the different flow rates for different valve opening options. In the system identification study, the flow rate for both meeting room and office room are fixed at highest position. The actual measured flow rate is highest at 7.8 gpm.

Table 3.5 Flow Rate Corresponding to Valve Opening

Stage	Speed	Flow Rate	Power	Current
1	Low	1.87 gpm	60 W	.55 A
2	Medium	5.80 gpm	80 W	.66 A
3	High	8.79 gpm	87 W	.75 A

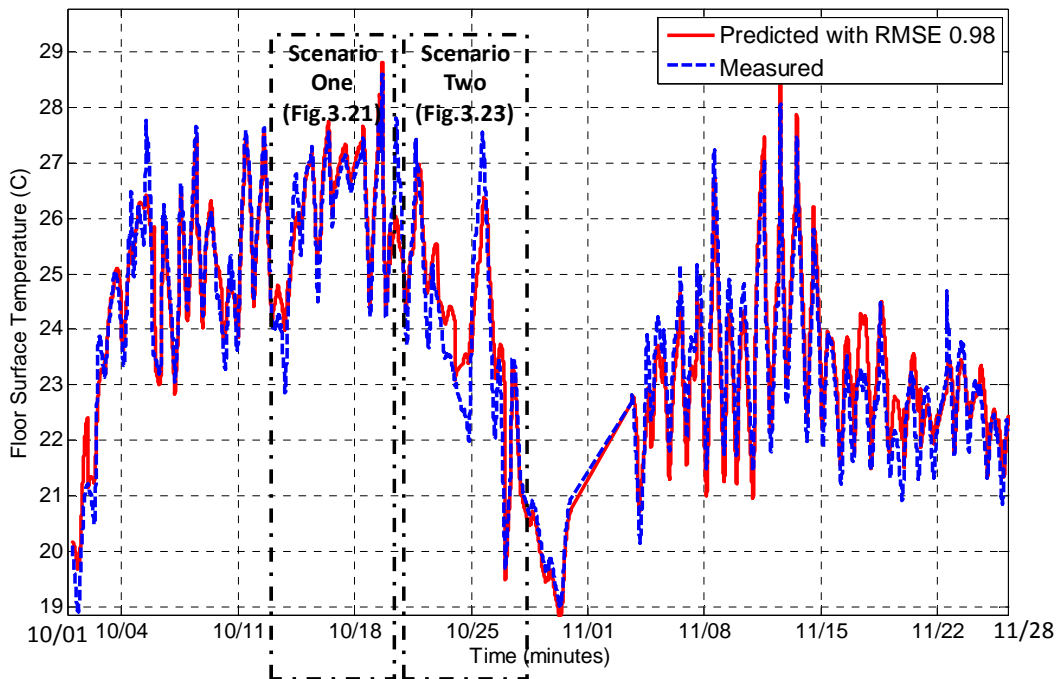


Figure 3.20 Model predicted floor surface temperature profile from October 1 to November 29, 2009

Figure 3.20 shows the model predicted floor surface temperature profile from October 1 to November 29, 2009, with RMSE of 0.98. Two scenarios are selected to present different model prediction accuracies.

b. Scenario One

Figure 3.21 shows the results of a week testing with RMSE of 0.8. The floor surface temperature follows the measured one well, whether the pump is at on or off status. Figure 3.22 shows a one day result of predicted floor surface temperature compared to measured ones. The RMSE of predicted surface temperature is 0.25, although the pump remains on and off all the time and creates a lot of variations.

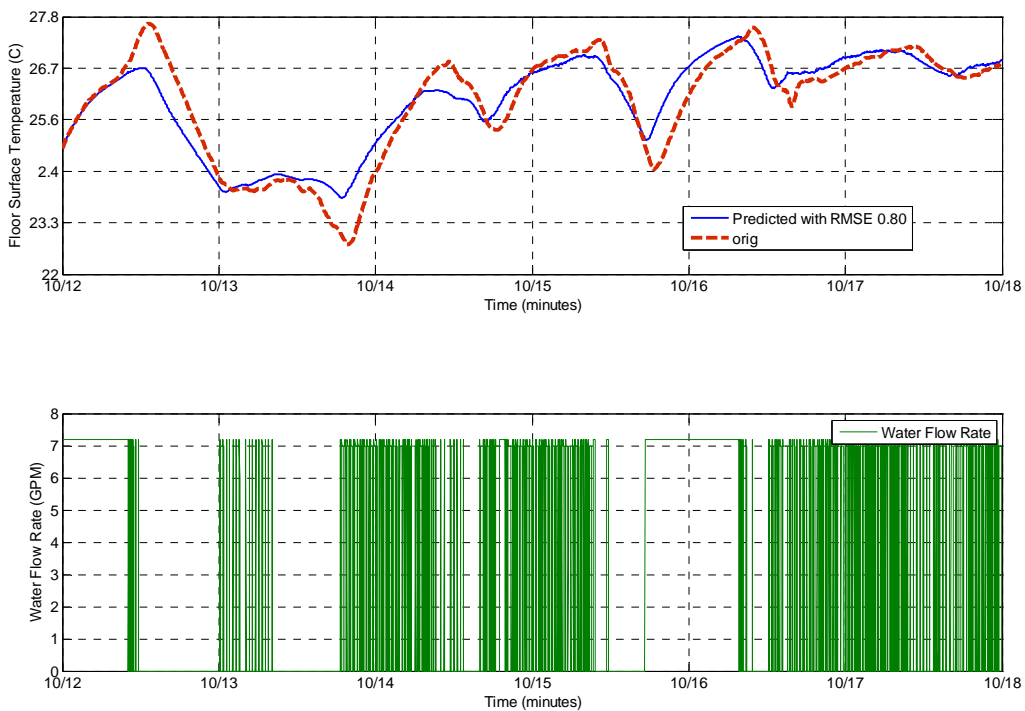


Figure 3.21 Meeting room floor surface temperature profile and water flow rate from October 12 to October 18, 2009

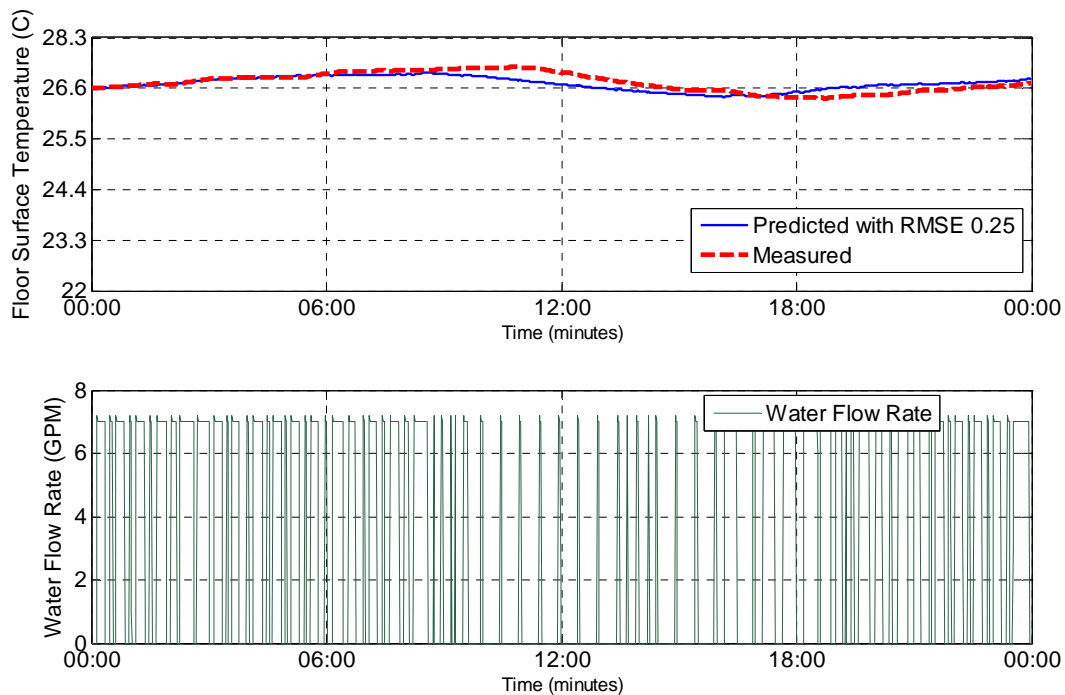


Figure 3.22 Meeting room floor surface temperature profile and water flow rate from October 17 to October 18, 2009

b. Scenario Two

In this scenario, the heating activities only happen on three days. When there is no heating activity, the prediction accuracy of the floor surface temperature is with relatively high RMSE of 1.2. The reason could be the assumption that the energy loss from the water tube through insulation slab to the ground is 0. When there is no heating activity for more than one day, the measured temperature decreases faster than the predicted one.

In conclusion, the radiant floor heating model predicts the floor surface temperature with RMSE of 0.8 when there are continuous heating activities. The prediction accuracy of the model starts degrading when there is no heating activity for more than one day.

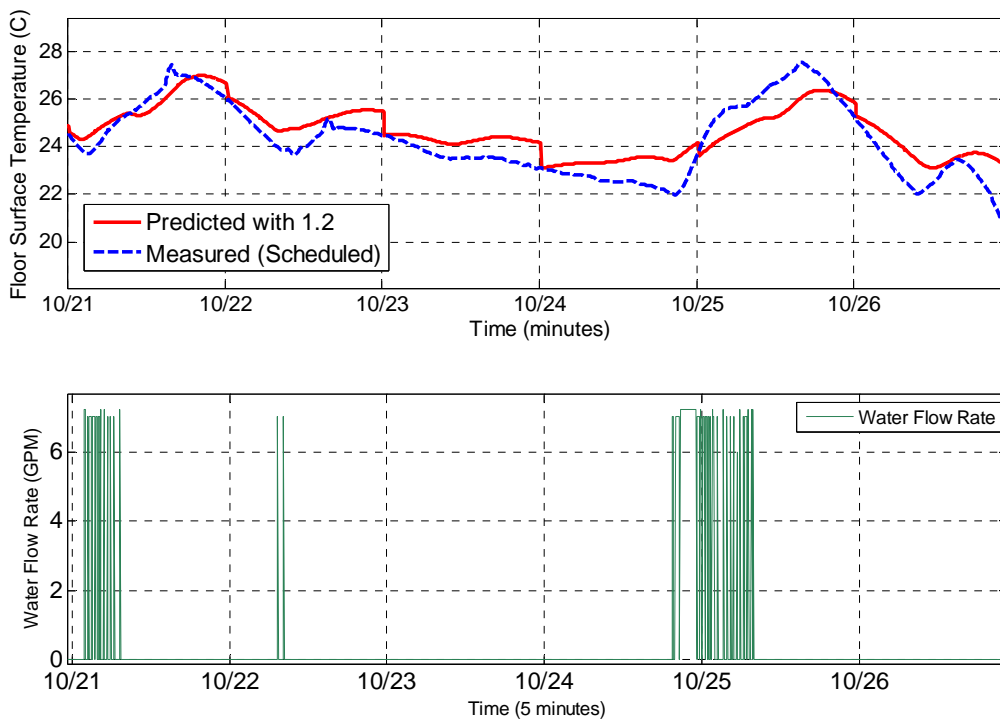


Figure 3.23 Meeting room floor surface temperature profile and water flow rate from October 21 to October 27, 2009

d. Sensitivity Analysis

Table 3.6 Results of sensitivity analysis on identified radiant floor thermal properties

Parameters	Identified		Parameters	Identified	
	Mean	Deviation		Mean	Deviation
h_{cf}	30 [W/K.m ²]	10	β_{cf}	1.5[-]	0.06
$C_{MR,cf}$	$1.98 \cdot 10^5$ [J/m ³ ·K]	$2.03 \cdot 10^3$	γ_{cf}	0.35[-]	0.01
$R_{MR,cf}$	0.13 [K·m ² /W]	0.01	Cr	0.3[-]	0.004

Table 3.6 shows the sensitivity analysis of identified radiant floor thermal properties. The coefficients of absorbed solar radiation and internal heat gain are relatively stable compared to the overall heat transfer coefficients, h_{cf} , from floor surface to room air. It is affected by indoor

air temperature, amount of solar radiation into the space and absorbed internal heat gain by slabs. h_{cf} has to be identified once a new set of training data is available.

Tankless water heater power consumption

Figure 3.21 shows the validation of tankless water heater energy consumption model on one week measured data including water flow rate, supply and return water temperature. It is found that the RMSE is 0.38 and the predicted energy consumption tracks well with the measured one. The efficiency of the water heater is found to be 90%.

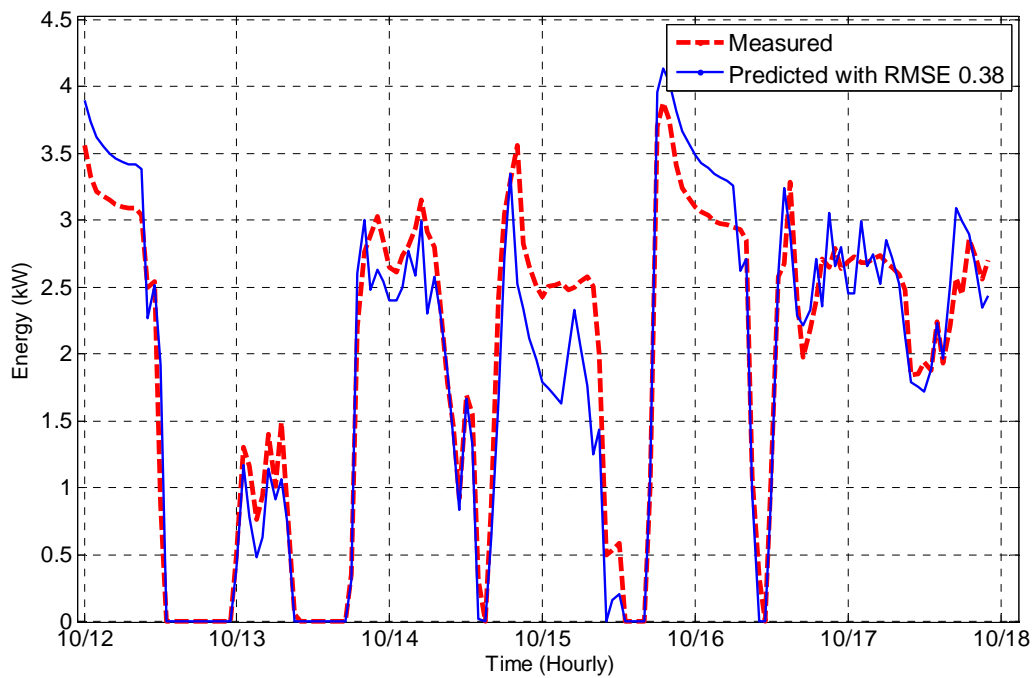


Figure 3.24 Results of tankless water heater power consumption validation for one week heating testing period

3.5.3.3 Heat pump system

Indoor air terminal units

The modeling of indoor air terminal units is simplified as an evaporative cooling process. Figure 3.25 shows during one week of cooling period, the model predicted indoor air temperature tracks well with measured temperature. However, the result in terms of RMSE is not as good as the one during heating season. This is because the indoor temperatures response more quickly to the HVAC system during cooling season.

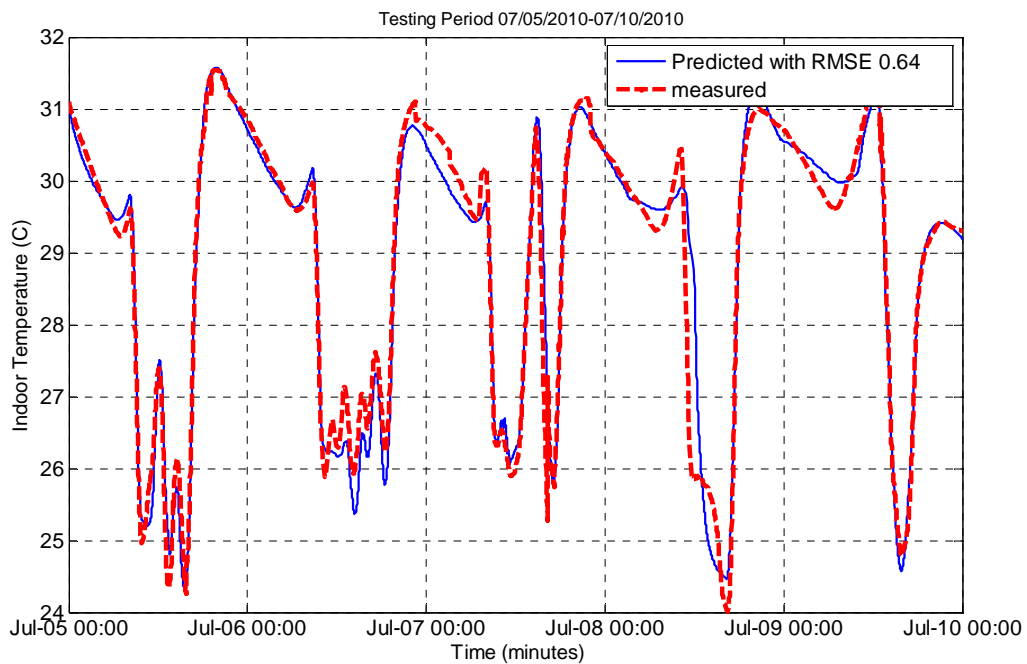


Figure 3.25 Meeting room indoor temperature profile during one week cooling testing period

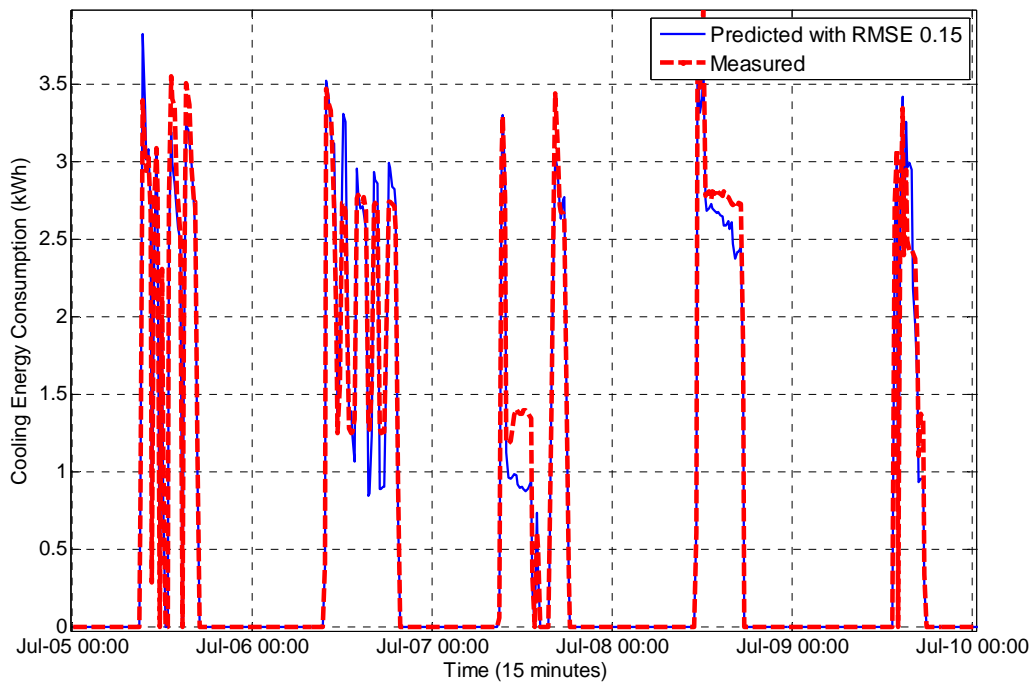


Figure 3.26 Meeting room cooling energy consumption prediction from July 5 to July 10, 2010

Heat pump energy consumption

Figure 3.26 shows the predicted and measured cooling energy consumption for one week. The identified parameter is coefficient of performance of heat pump (COP), which is 2.5 in this study. The manufacture data shows the COP is 3.1. Considering this unit has been installed and used for 5 years, a COP of 2.5 should be a good estimate. Figure 3.26 suggests that the model prediction performs weak when the system started, stopped and when the fan speed changed.

3.6 Summary

In this chapter, a baseline building model including both spaces and HVAC systems is developed and validated based on continuous measured data. This building model is built upon the first principle of thermal dynamics and heat transfer. The zone model is based on ASHRAE thermal network models. The radiant heating floor system model is a steady-state model which considers both heat convection and radiation exchange with room air temperature. The heat pump cooling

system is modeled as a typical evaporative cooling process. The validation results show that the predicted room air temperature in both heating and cooling season is within RMSE of 0.8 compared to measured data. During the heating season transition period, the RMSE from the model prediction ranges from 0.98 to 1.3. Surface temperature prediction of the concrete slab from radiant floor model is within RMSE of 1. When there is no heating activity for more than one day, the radiant floor heating model predicts higher temperature than measured ones, with RMSE of 1.2. The water heater energy consumption is with RMSE of 0.38. The heat pump energy consumption is with RMSE of 0.5. Based on the results above, the baseline model for the whole building including zone and system models is accurate and applicable to the integrated building control in Chapter 4.

Chapter 4 Integrated Building Control Design and Implementation

4.1 Optimal Control Design

4.1.1 Problem Formulation

The optimization of building energy consumption has been studied both based on well established simulation tools such as EnergyPlus and TRNSYS with BuildOpt (Wetter, 2005) for building early design stage and ASHRAE simplified heat balance models (Wang, et al. 2001 and Henze, et al. 2004) for real time optimal control implementation. However, very few studies show the integration of real-time weather information into the real time implementation (Ma, et al. 2009). Almost no previous study shows the integration of the real-time occupancy information to the HVAC control. In this thesis, the real-time weather and occupancy information are integrated into the traditional optimal control for building HVAC systems.

4.1.1.1 Non-linear Model Predictive Control

The general optimization problem in continuous time is (Camacho, et al. 2003):

$$\text{Minimize } J = \int_{t_i}^{t_f} \varphi(x(t), y(t), u(t), d(t)) dt \quad (4.1)$$

$$\text{Subject to } f(\dot{x}(t)) = g(x(t), y(t), u(t), d(t)) \quad (4.2)$$

$$x^L \leq x(t) \leq x^U \quad (4.3)$$

$$u^L \leq u(t) \leq u^U \quad (4.4)$$

$$y^L \leq y(t) \leq y^U \quad (4.5)$$

$$x(t_0) = X_0 \quad (4.6)$$

$$x(t_f) = X_f \quad (4.7)$$

$$t \in [t_i, t_f] \quad (4.8)$$

where φ is the cost function of electricity and gas. $f(\dot{x}(t))$ is a function based on the heat transfer and thermal dynamics of building space and HVAC systems which can be referred in Chapter 3, $x(t) \in \mathcal{R}^{nx}$ is the vector of state variables, X_0 is a vector of initial values and X_f is a vector of final values; $u(t) \in \mathcal{R}^{nu}$ is the vector of control variables; $y(t) \in \mathcal{R}^{ny}$ is the vector of algebraic variables. x^L , u^L and y^L are lower bounds of u and x , while x^U , u^U and y^U are upper bounds; $d(t)$ is the vector of disturbances.

In this thesis, a non-linear model predictive control (NMPC) is designed following Magni, et al. (2003) and implemented in the test bed. The optimization problem becomes:

$$\Psi_h(x_t) \quad \min_u \quad \sum_{t=1}^h \varphi(x_t, y_t, u_t, d_t) \quad (4.9)$$

$$\text{Subject to } x_{t+1} = g(x_t, y_t, u_t, d_t) \quad t = 1 \dots, h \quad (4.10)$$

$$x^L \leq x_t \leq x^U \quad t = 1 \dots, h \quad (4.11)$$

$$x^L \leq x_t \leq x^U \quad t = 1 \dots, h \quad (4.12)$$

$$u^L \leq u_t \leq u^U \quad t = 1 \dots, h \quad (4.13)$$

$$y^L \leq y_t \leq y^U \quad t = 1 \dots, h \quad (4.14)$$

$$x_1 = X_0 \quad (4.15)$$

The specific problem $\Psi_N(x_t)$ presented above is a discrete time formulation of the general problem defined in Equation (4.1). Figure 4.1 below further illustrates the NMPC applied in this thesis. The general problem for HVAC control is an infinite time horizon control problem. It is converted into a finite time control problem with a moving horizon h at each time step. At current time t , the initial conditions $x_t = x_0$ are obtained as inputs into the plant model. At the

same time, the optimization problem defined by Equations. (4.9)-(4.15) is solved. The results are the optimal control profile $u(t|t)$ for HVAC systems and corresponding room temperature set-point $y(t|t)$. However, only the first step from t to $t+1$ of calculated u_t is actually executed, which is defined in u_t^* . Once x_{t+1} is known at the next time step, the prediction horizon is shifted forward by one time step and problem $\Psi_h(x_{t+1})$ is solved again to find u_{t+1} . The new $u(t+1|t+1)$ is in principle different from $u(t+1|t)$ because of the additional new information available. During the heating season, the moving time horizon h is defined as 24 hours because the response time of radiant floor heating system is slow. However, during the cooling season, the moving horizon h is defined as 3 hours (Coffey, 2008) because heat pump cooling is air-based system and responds much faster than the radiant floor system.

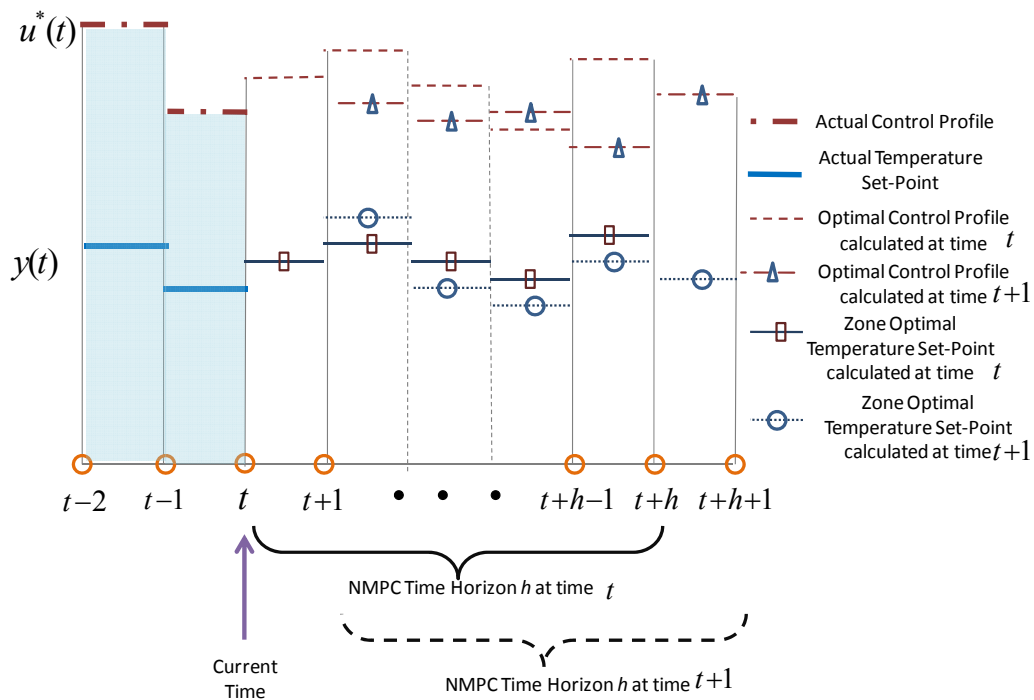


Figure 4.1 Illustration of NMPC moving horizon control

Figure 4.2 shows the overall NMPC design. The plant model are building thermal zone model and building HVAC system model which are defined in Chapter 3. The disturbances are from real-time outdoor weather condition and indoor occupancy activities. X_0 is a vector of initial values and X_f is a vector of final values. The NMPC is constructed based on plant model and disturbances model and solved by dynamic programming. The output control signals are ideally

implemented through a local PID controller, where the control signal should be tuned based on disturbances received in real-time and track the optimized control set-point as close as possible. In this study, the controller design is in MATLAB and implemented through LabVIEW to local actuators directly on the relays of pumps.

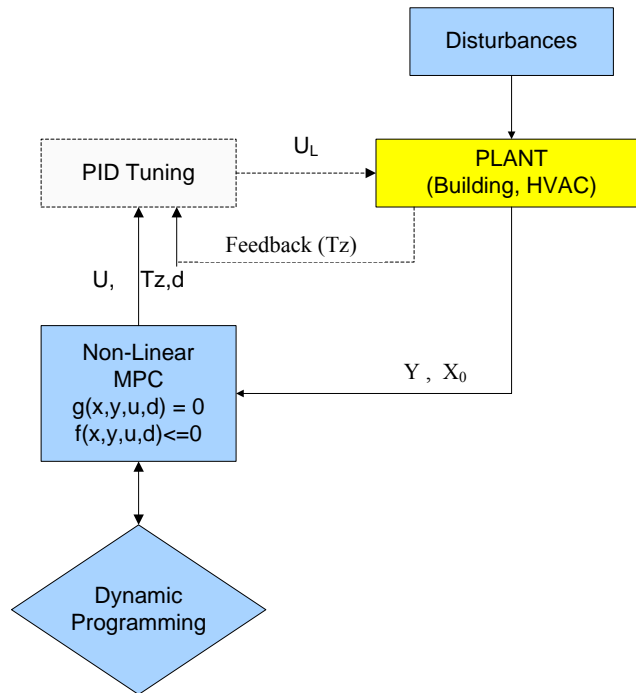


Figure 4.2 Overview of the NMPC Design

Table 4.1 describes $x(t)$, $u(t)$ and $d(t)$ which are state, control and disturbance variables in this optimal control problem. Particularly during modeling, the control variables are water temperature rise and water flow rate for heating, while supply air flow rate for cooling in the model. During the actual implementation, the control variables are different because of the limitations of hardware. Detailed heat transfer equations and other definitions have been provided in Chapter 3.

Table 4.1 Definitions for State, Control Variables and Disturbances

Name	Definition	Name	Definition
State Variables x(t)			
T_{MR_in}, T_{Off_in}	Meeting room and office indoor air temperature	$T_{MR_sur_f}, T_{off_sur_f}$	Meeting room and office floor surface temperature
$T_{sur_MR_in}^i, T_{sur_off_in}^i$	Meeting room and office wall inside surface temperature	$T_{Sur_MR_win}, T_{Sur_off_win}$	Meeting room and office floor window surface temperature
$\bar{T}_{MR_w}, \bar{T}_{off_w}$	Hot water tube's surface temperature	$T_{hw,s}, T_{hw,r}$	Supply and return water temperature
Model Control Variables u(t)			
ΔT_{hw}	Hot water temperature rise	$T_{air,s}$	Supply air temperature
\dot{m}_w	Water flow rate	\dot{m}_{fcu}	Air flow rate of fan coil unit
Implemented Control Variables			
$SetT_{heat} = f(\dot{m}_w, \Delta T_{hw})$	Indoor heating temperature set-point	$SetT_{cool} = f(\dot{m}_{fcu}, T_{air,s})$	Indoor cooling temperature set-point
		\dot{m}_{fcu}	Air flow rate of fan coil unit
Disturbances D(t)			
$Q_{int_off_MR}$	Internal heat gain	\dot{Q}_{sol}	Solar radiation
$Q_{in_off_MR}$	Infiltration heat gain/loss	T_{out}	Outside temperature

4.1.1.2 Characteristics of Proposed NMPC

Before solving this problem, the analysis of the nature of this problem is necessary. Figure 4.3 shows an example of the measured outputs, disturbances and control signal. Although the indoor air temperature fluctuates, the wall surface temperature tends to be constant. To model and design a controller for such kind of system is a challenge task. As Underwood (1999) pointed out, the main characteristics of such a complex system are:

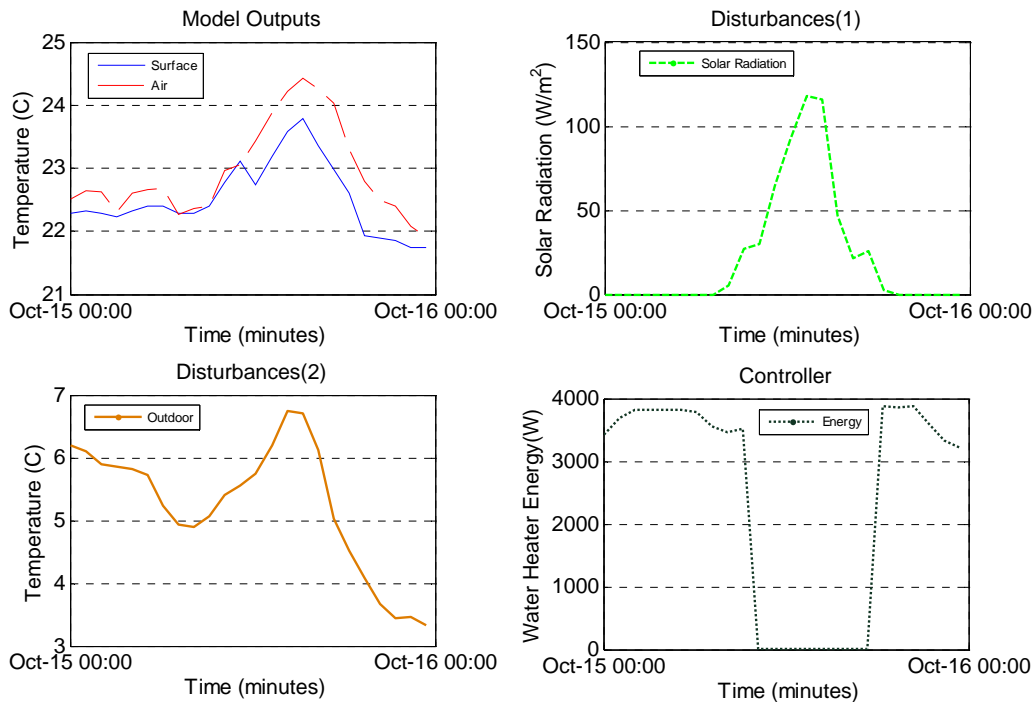


Figure 4.3 Nature of the optimal control problem

- **Stiffness**

The response time of indoor temperature and wall surface temperature could be in a different time magnitude.

- **Nonlinear Differential Algebra Equations (DAE) equations (>50)**

The heat balance equations for indoor/outdoor environment, heating, cooling and ventilation are nonlinear DAEs. Particularly, heat exchange in the form of convection and radiation are commonly described as nonlinear DAEs.

- **Mixed On/Off and continuous control signal**

Some of the given control equipment only accept on/off control signals such as motor controller operable windows. Some accept continuous signals such as variable frequency drive pump to control water flow.

- **Disturbances are dynamic**

The disturbances to the system come from the outside temperature, wind, solar, inside electrical equipment, occupancy and lights. Most of these disturbances vary from time to time. As shown in Figure 4.10, solar radiation could vary from 0 to 120w/m² in a day time with an overcast sky.

4.1.2 Optimization Algorithm

In Chapter 2, a detailed literature review is conducted on optimization methods. Based on the nature of this problem described in Section 4.1.1.2, genetic algorithm and dynamic programming are the two most suitable optimization algorithms, which are further illustrated and discussed in this section, to solve the NMPC problem.

4.1.2.1. Genetic Algorithm

The genetic algorithm is based on natural evolution and selection of species. It starts with a population with a certain number of individuals with different states in the search space. In each generation, the individuals are evaluated with the fittest reproducing and continue with the next generations through fitness-based selection. The selection and/or invention of genetic operators are problem-specific and heavily depend on experience. As the process continues, the population converges to better individuals, which gives a higher likelihood of achieving global optimum. GA has been applied widely in building energy optimizations because of two reasons (Xing, 2004; Wetter, 2005):

- 1) The optimization does not require a smooth cost function which makes the discontinuity in controller parameters possible;
- 2) It is a population-based search which makes the multi-objective optimization possible;

However, GA also requires a huge number of function evaluation which causes high computation time and memory. In this thesis, the Genetic Algorithm Solver in Global Optimization Toolbox 3.0 in MATLAB 2009b (The MathWorks, 2010a) is used. An evaluation function and several other parameters such as creation, fitness scaling, selection, crossover and mutation have to be provided. Since the building model is constructed in Simulink, the MATLAB modifies the inputs into Simulink and get outputs such as total heating energy consumption from the Simulink model as the fitness value for further optimization iterations.

The schema of the GA used in this thesis is described in Figure 4.4. The number of generations is set dynamically based on different optimization time horizons.

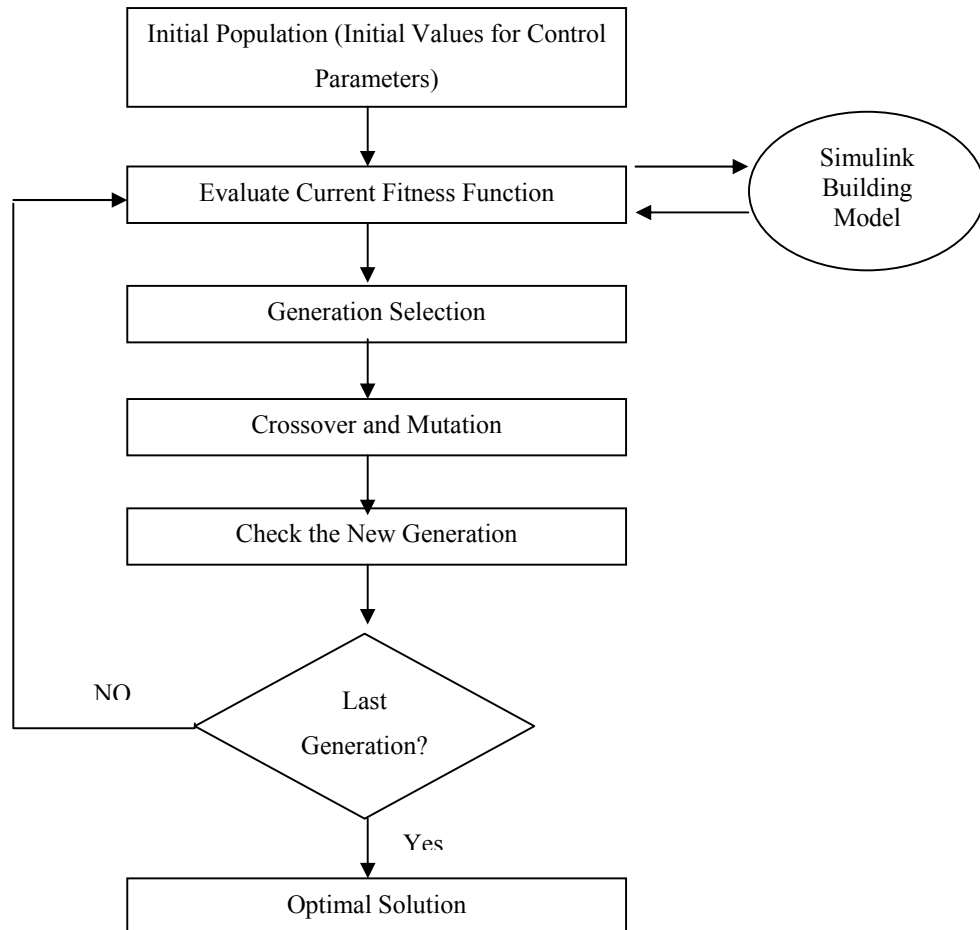


Figure 4.4 Schema of GA process in MATLAB/Simulink

4.1.2.2 Dynamic Programming

Dynamic Programming (DP) is a very powerful algorithmic paradigm in which a problem is solved by identifying a collection of sub-problems and tackling them one by one, smallest (one time step) first, using the answers to small problems to help to figure out larger ones, until the whole time horizon is solved. It comes from Bellman's principle of optimality (Bellman and Kalaba, 1965). It has been widely implemented in building HVAC real time controls (Rink and Li, 1995; Chen, 2001; Braun, 2003; Yu and Dexter, 2009). The optimization problem defined in Equation (4.9) can be re-constructed as below:

$$J^*[X(t), t] = \min_{u(t-1)} \{ \varphi(X(t), u(t-1), d(t), y(t)) + J^*[X(t+1), t+1] \} \quad (4.16)$$

Where $J^*[X(t), t]$ is the minimum energy consumption at time t based on sequence of optimal control profile defined in $u_t^* = \{u^*(t-1), u^*(t), \dots, u^*(h-1)\}$.

The above DP equation shows that the future decision is determined indirectly through the future system states $X(t+1)$. Figure 4.5 illustrates the implementation of DP-based optimal control. The current minimum energy consumption $J^*[X(t), t]$ at time t can be determined by the current cost function $\varphi(X(t), u(t-1), d(t), y(t))$ and future optimal cost function $J^*[X(t+1), t+1]$, which is determined at time $t+1$. This also brings an important computational feature of dynamic programming. The calculation of the cost function $J^*[X(t), t]$ and all possible control actions at time t should be stored until the last time step $t+h$ in order to find out the optimal cost profile. This will increase a significant amount of computer storage. Finally, the problem becomes find a shortest energy consumption path and is solved based on Dijkstra's algorithm (Weiss, 2007).

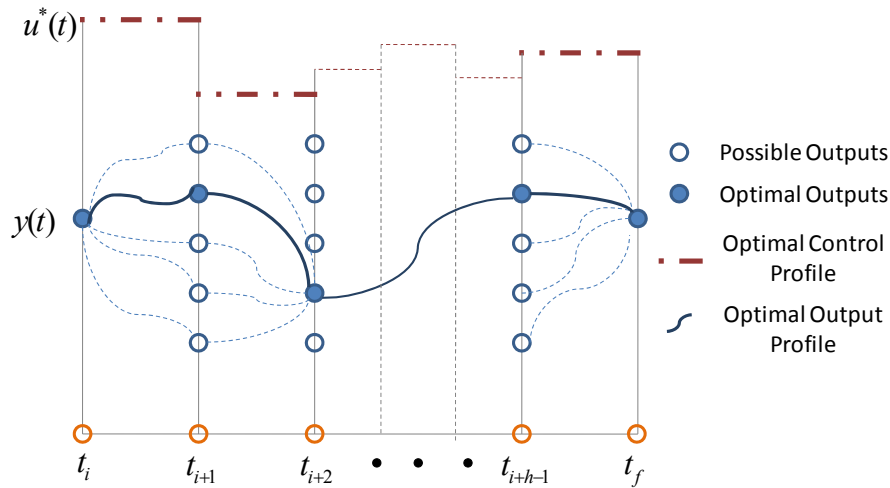


Figure 4.5 Dynamic programming based optimal control

4.1.3 Comparisons of Computational Time

The computational dimension depends on the number of time steps and the constraints. In this study, the prediction time horizon during the heating season is 24 hours and 3 hours for cooling season. The time step is 1 hour and 15 minutes, respectively. For each temperature set-point, considering ranges 15~21 °C for heating and 24~30 °C for cooling, there are 7 possible values. Over the whole prediction horizon, there are 7^{24} possible configurations during heating season and 7^{12} during cooling season. This is a challenge for the real time implementation of NMPC.

The computational time of evolutionary algorithms (EA) including GA has been studied in a few simple cases (Ejebn, et al. 1999; Droste, et al. 2002; Wegener, et al. 2002). Rudolph (1998) gave a comprehensive survey of the theoretical work up to 1997 and provided an $O(n \log n)$ upper bound for the (1 + 1) EA using the 1-bit-flip mutation for ONE-MAX problem. (1 + 1) EA means the population size is 1. Only recently, He and Yao (2001; 2002) made one of the first attempts toward analyzing EAs with recombination and with a population size greater than 1. That study provided a general framework for the computational complexity of EAs considering mutation, crossover and selection. The computational time is either polynomial or exponential depending on the nature of the problem. Based on the optimization problem defined in 4.2.1, the size of the problem spanning the whole time horizon is nu^h , assuming h is the optimization time horizon. Obviously, it is exponential, with $O(u^h)$. Hence, the computational time of GA in this study is exponential as well (He and Yao, 2002).

The complexity of DP has been discussed by Papadimitriou and Tsitsiklis (1987). Their results show that for a finite horizon problem, the complexity to find the optimal policy is in polynomial time. In this study, it is $O(hu)$. Apparently, it is much less complexity than the one from GA.

4.1.4 Comparisons of Optimization Results

Since DP has computational time in polynomial comparing to exponential time of GA and GA is global optimization by its nature, it is interesting to compare the optimization results from both. These two algorithms are tested on October 16, 2009, for heating energy optimizations. The prediction horizon is 16 hours with 1 hour control time step. Figure 4.6 shows the comparison results between DP and GA. The energy consumption from DP is 36.4 kWh, while GA is 35.6 kWh. The absolute difference is only 2%, which is considered small. Hence, DP has the similar optimization result compared with GA, while much less computational time step.

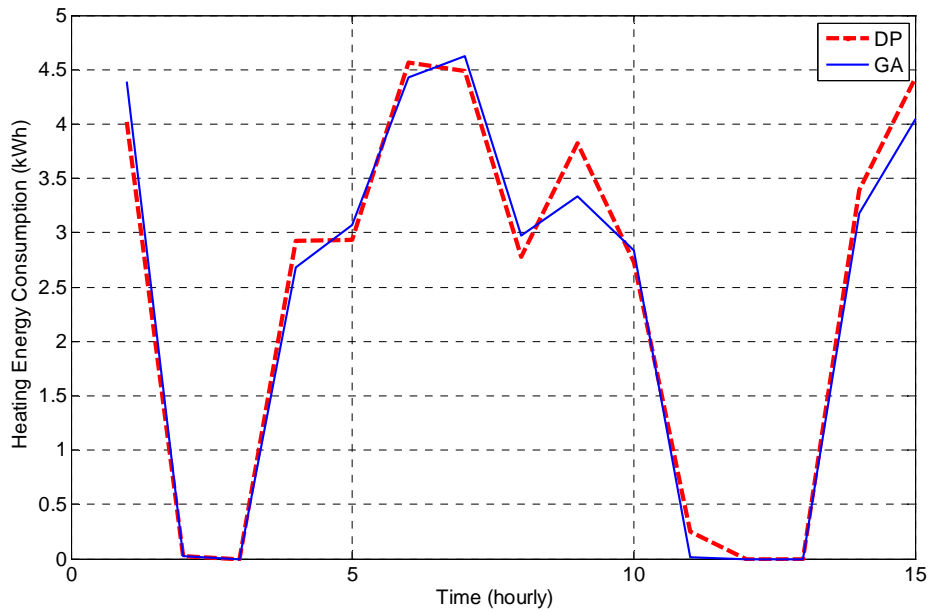


Figure 4.6 Results of energy optimization comparisons between DP and GA

4.2 Optimal Control Implementation

4.2.1 Overview

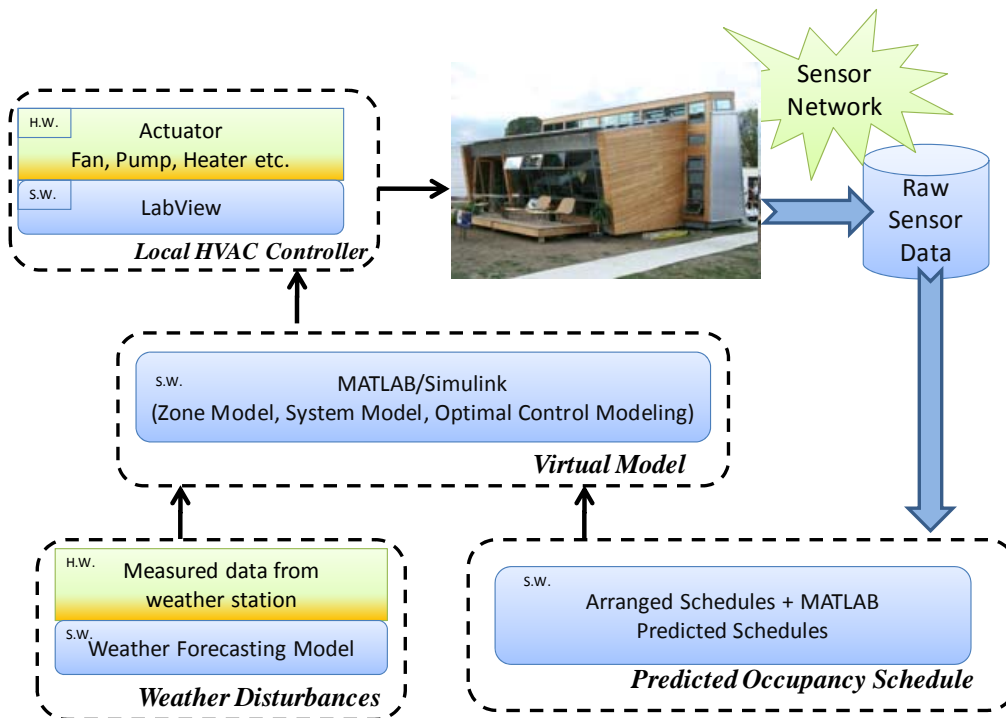


Figure 4.7 Overview of optimal control implementation schema

(Note: S.W. means software, H.W. means hardware.)

Figure 4.7 shows the overview of optimal control implementation schema in this study. Starting from the sensor network inside the house, the raw sensor data are as inputs into occupancy pattern prediction algorithms discussed in Chapter 2. At the same time, the weather forecasting model makes predictions of outdoor temperature, solar radiation and wind speed for the next time horizon (Jiang and Dong, 2010). The resultant weather and occupancy information are then used as inputs into the virtual model in MATLAB/Simulink. The virtual thermal model is the dynamic heat transfer model developed in Chapter 3. The optimal control results from the virtual model are then implemented through LabVIEW on local HVAC actuators for pumps, water heater and fans.

4.2.2 Heating Season

4.2.2.1 Experiment Setup

The heating season experiment is first setup on a day of October, 2009 and then setup through the first week of February, 2010. During the experiment period, the windows are all closed because outside temperature is range from -20°C to 10°C . Building occupants include staff from Remaking City Institute, visitors from outside of campus and students of School of Architecture. The training data set for occupancy and weather prediction is previous one month continuously collected data. The heating set-point while occupied is 21°C at day time.

4.2.2.2 Results and Discussion

The results have three parts: weather prediction, occupant behavior pattern prediction and measured energy consumption profile from integrated control.

Weather prediction

The evaluation criteria for weather prediction accuracy are based on RMSE defined in section 3.5.2 and Mean Absolute Percentage Error (MAPE). MAPE defined the deviation of errors from measured value. It is defined as:

$$MAPE = \frac{1}{n} \sum_{t=1}^n \left| \frac{A_t - P_t}{A_t} \right| \quad (4.17)$$

where

n Total number of data points

A_t Measured data points

P_t Predicted data points.

- 1) Outdoor temperature prediction:
 - a. Overview

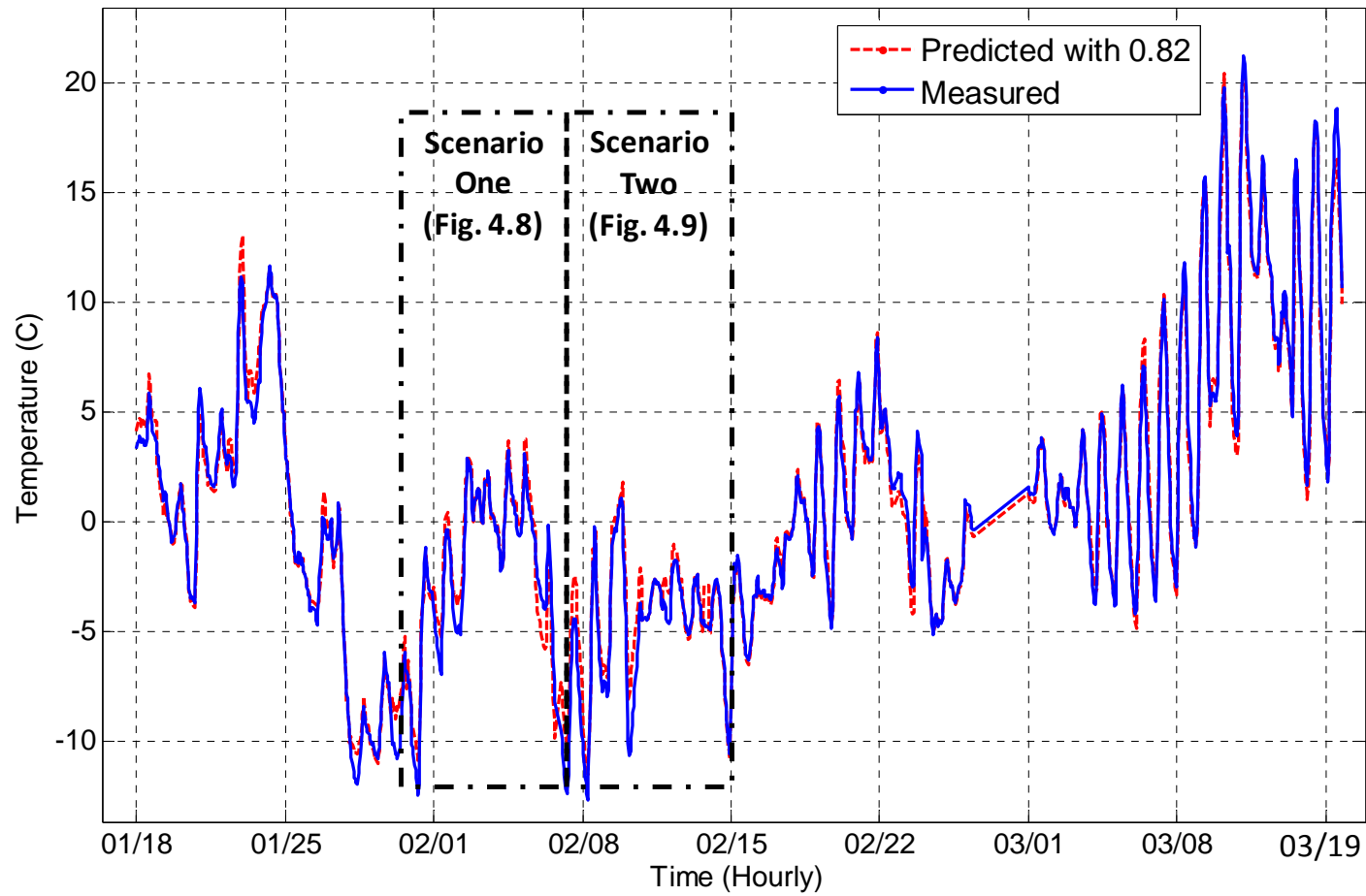


Figure 4.8 Results of hourly local outdoor air temperature prediction from January 18 to March 19, 2010

Figure 4.8 shows the results of outdoor air temperature prediction from January 18 to March 19, 2010. The overall prediction accuracy is with RMSE of 0.82. Two scenarios are selected: one has higher prediction accuracy than the average value; another one is during the lowest temperature period in winter. There is also a period from February 28 to March 1, when there is no data recorded.

b. Scenario One

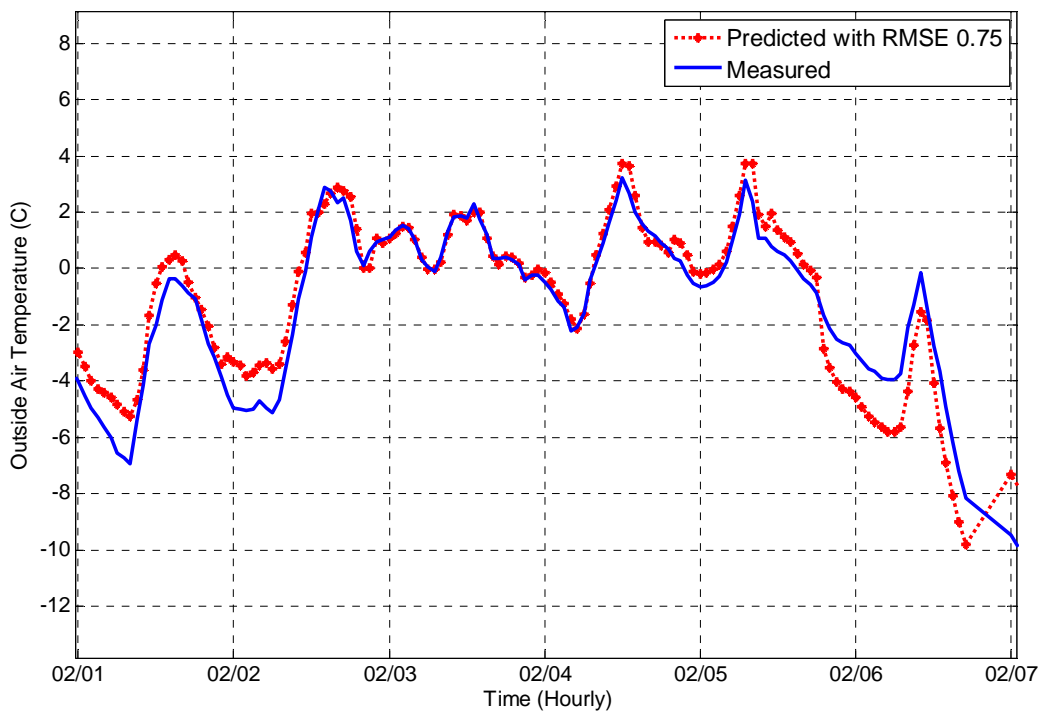


Figure 4.9 Results of hourly local outdoor air temperature prediction from February 1 to February 7, 2010

Figure 4.9 shows the results of outdoor air temperature prediction. The RMSE is 0.75 and MAPE is 12%. The maximum point difference is 2.4 °C and minimum is 0.2 °C. Overall, the prediction tracks the measured data quite well. The hourly prediction is implemented in real time and the training data is the previous one month hourly measured data.

c. Scenario Two

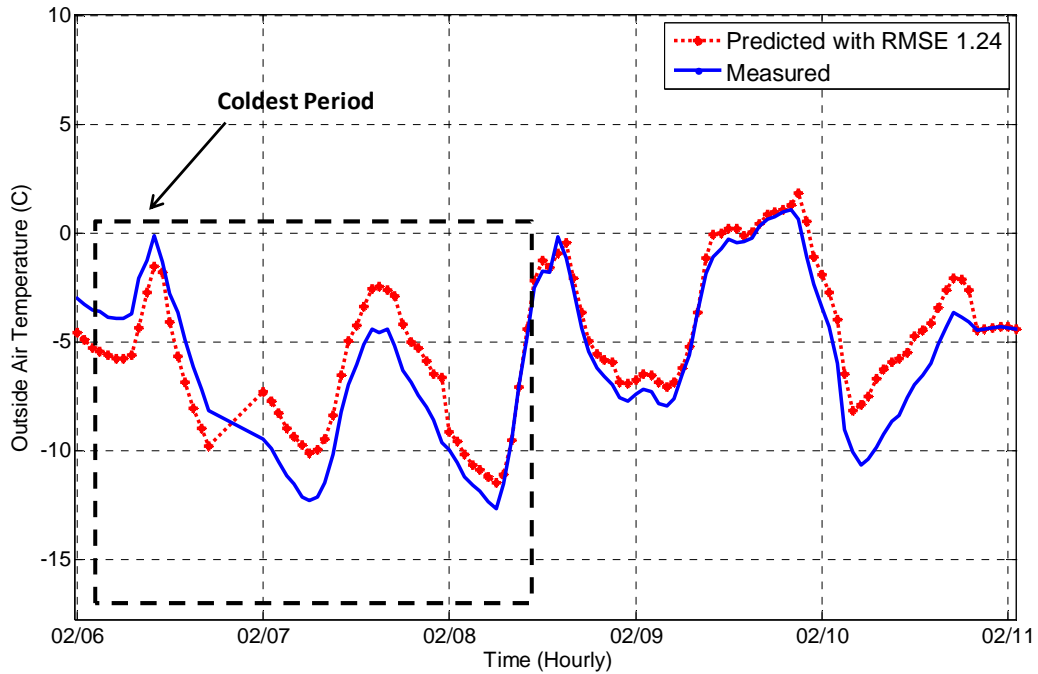


Figure 4.10 Results of hourly local outdoor air temperature prediction from February 6 to February 11, 2010

Figure 4.10 shows that during the coldest period, the predicted outdoor temperature has an average of 2 degree difference from the measure one. The prediction on February 8 seems better than February 7 and February 6. This is could be that once the new training data set is available the prediction algorithm can learn from the low temperature data.

2) Solar radiation prediction

a. Overview

Figure 4.11 shows the results of hourly global solar radiation prediction from January 18 to March 19. The average prediction accuracy is with RMSE of 97.79. Two scenarios are selected, which are within the same selected periods of outdoor air temperature.

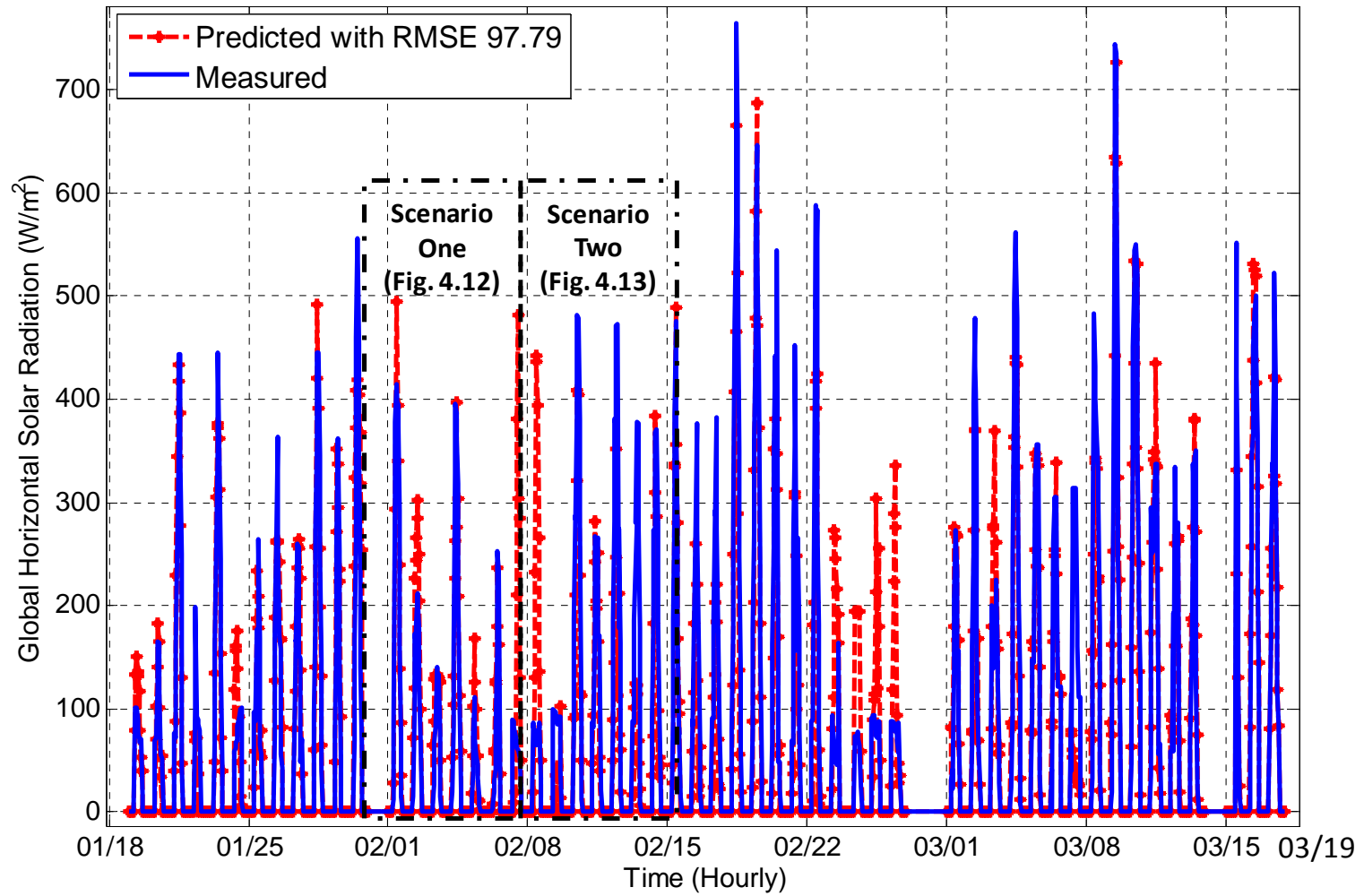


Figure 4.11 Results of hourly local global horizontal solar radiation prediction from January 18 to March 19, 2010

b. Scenario One

Figure 4.12 shows the results of hourly global horizontal solar radiation prediction for the whole week. The RMSE is 50.15 and MAPE is 20%.

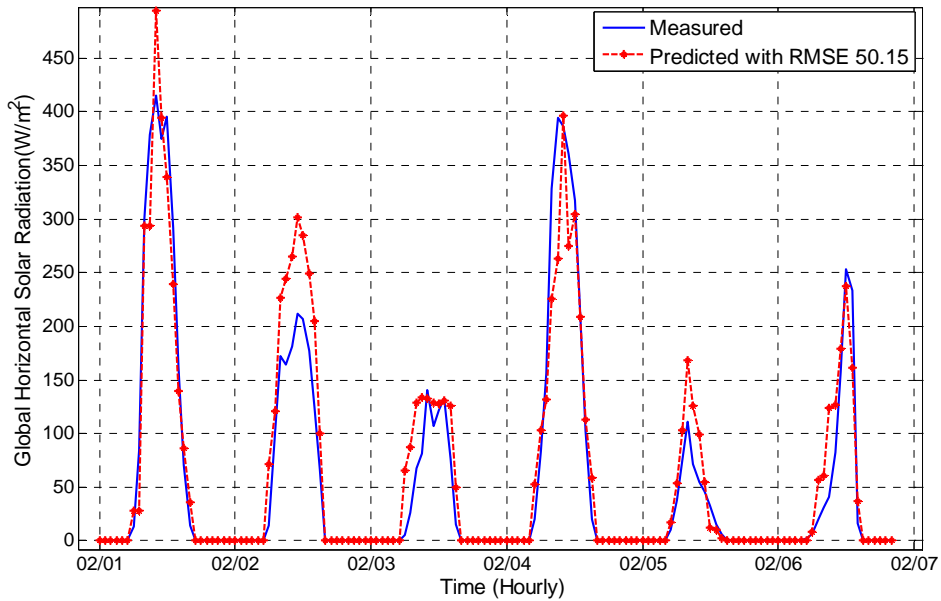


Figure 4.12 Results of hourly local global horizontal solar radiation prediction from February 1 to February 7, 2010

b. Scenario Two

Figure 4.13 shows the solar radiation prediction during the snow storm period. On the night of February 6, Pittsburgh had a snow storm and the sensor is covered by snow. The sensor then did not function for the following three days until the snow on the sensor is melted by Sun. The same thing happened to the sensor again during the week of February 25 as shown in Figure 4.11.

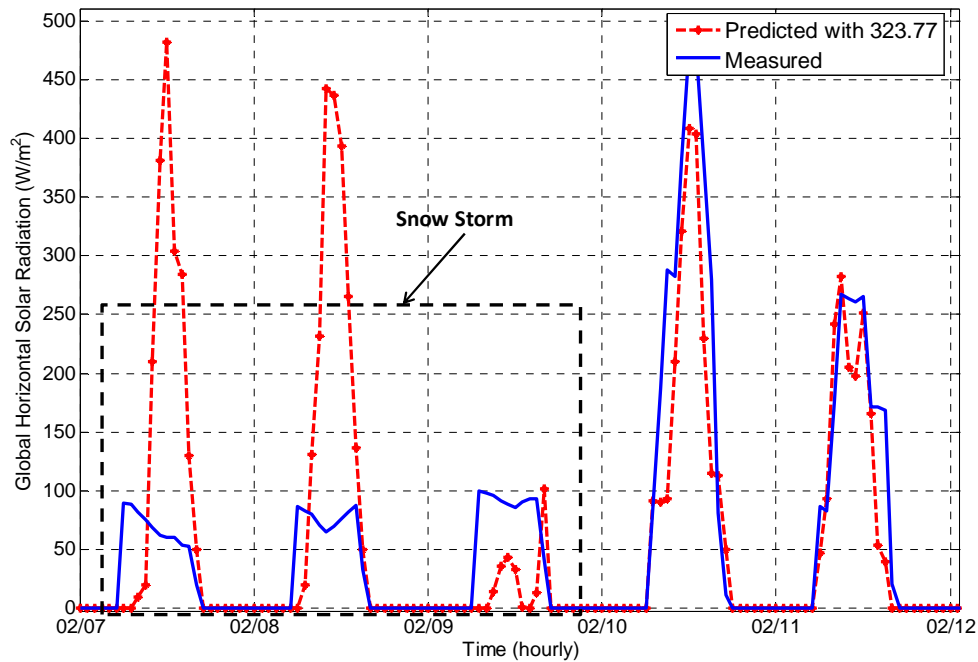


Figure 4. 13 Results of hourly local global horizontal solar radiation prediction from February 7 to February 12, 2010

3) Wind speed prediction

a. Overview

Figure 4.14 shows results of hourly local wind speed prediction from January 18 to March 19, 2010, with RMSE 0.85. The wind speed changes faster than outdoor air temperature and solar radiation, which makes the prediction difficult. Overall, the prediction algorithm correctly predicts 80% of the experimental time. Two scenarios are selected to further illustrate the results of wind speed prediction.

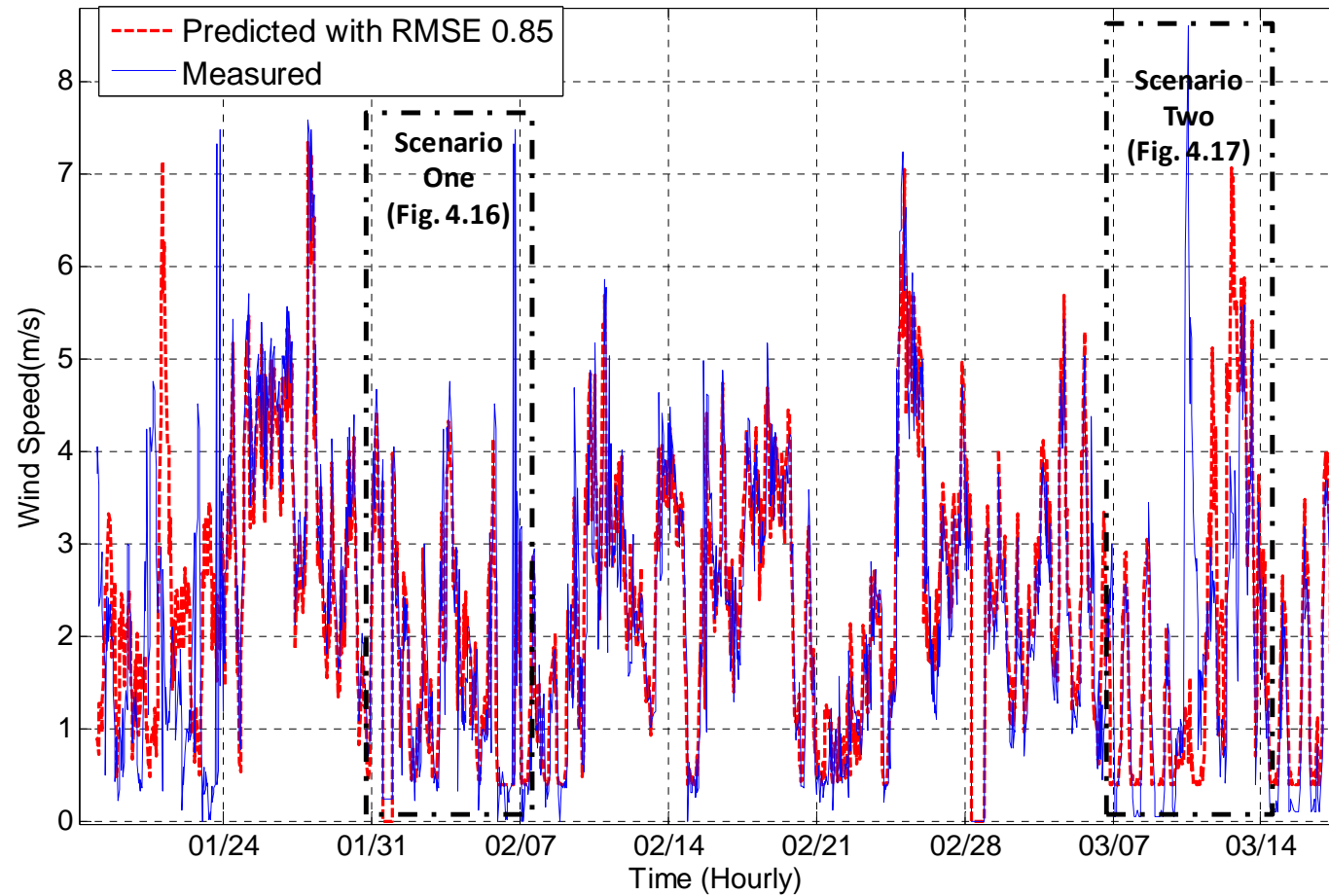


Figure 4.14 Results of hourly local wind speed prediction from January 18 to March 19, 2010

b. Scenario One

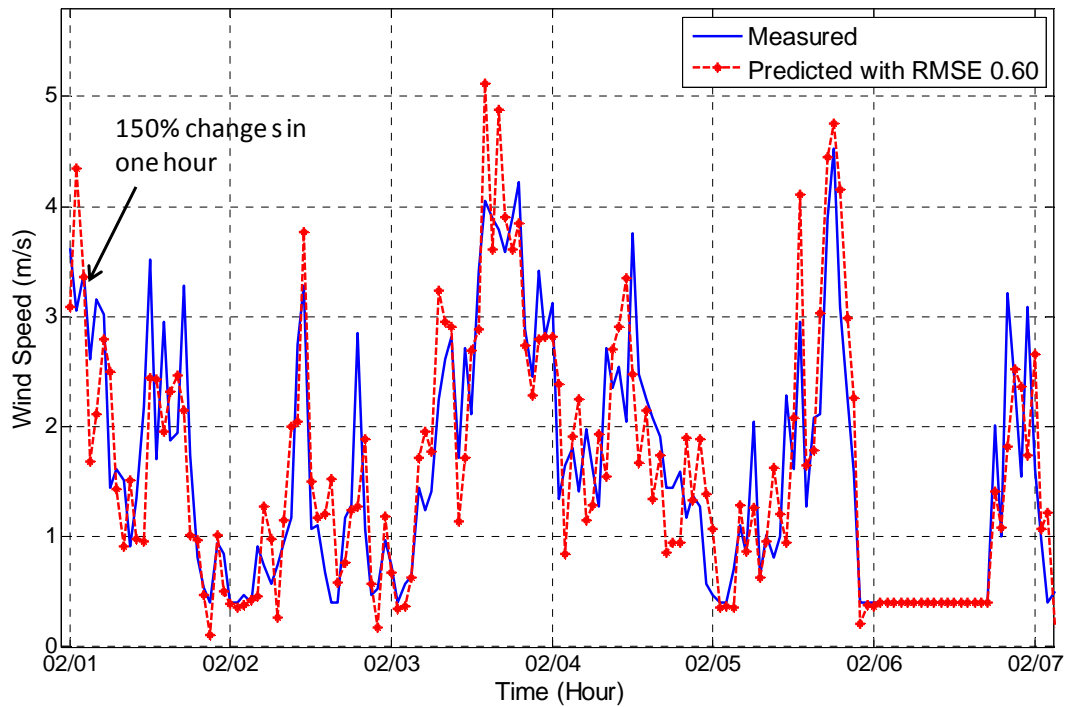


Figure 4.15 Results of hourly local wind speed prediction from February 1 to February 7, 2010

Figure 4.15 shows the results of hourly prediction of wind speed from February 1 to February 7, 2010. The accuracy is with RMSE of 0.6 and MAPE of 15%. The hourly wind speed value changes quite often and the maximum wind speed is 5 m/s. The difficult part for the prediction is when the wind speed changes by 150% in just one hour, for example, from 0.7 m/s to 1.9 m/s on February 1.

b. Scenario Two

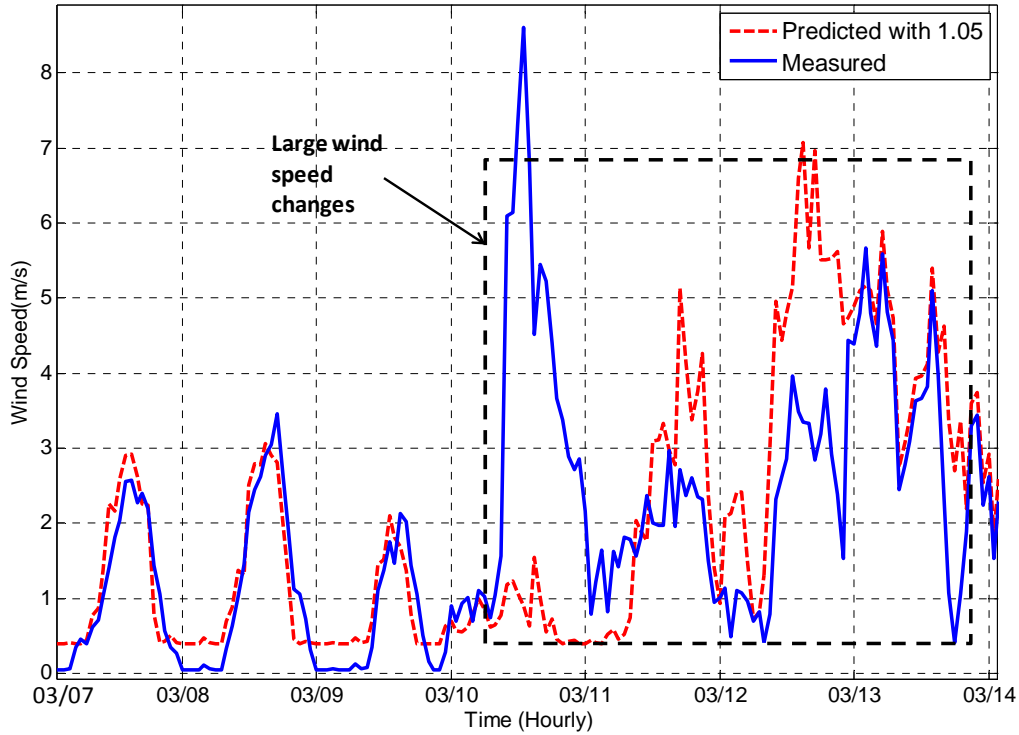


Figure 4.16 Results of hourly local global horizontal solar radiation prediction from March 7 to March 14, 2010

In scenario two, the wind speed has large changes in short time period on March 10, when the prediction did not catch such changes. On the following two days, the algorithm starts to learn the new training data sets from the past one month. Until March 13, the algorithm can predict the wind speed closer to the measured ones.

Occupant behavior pattern prediction

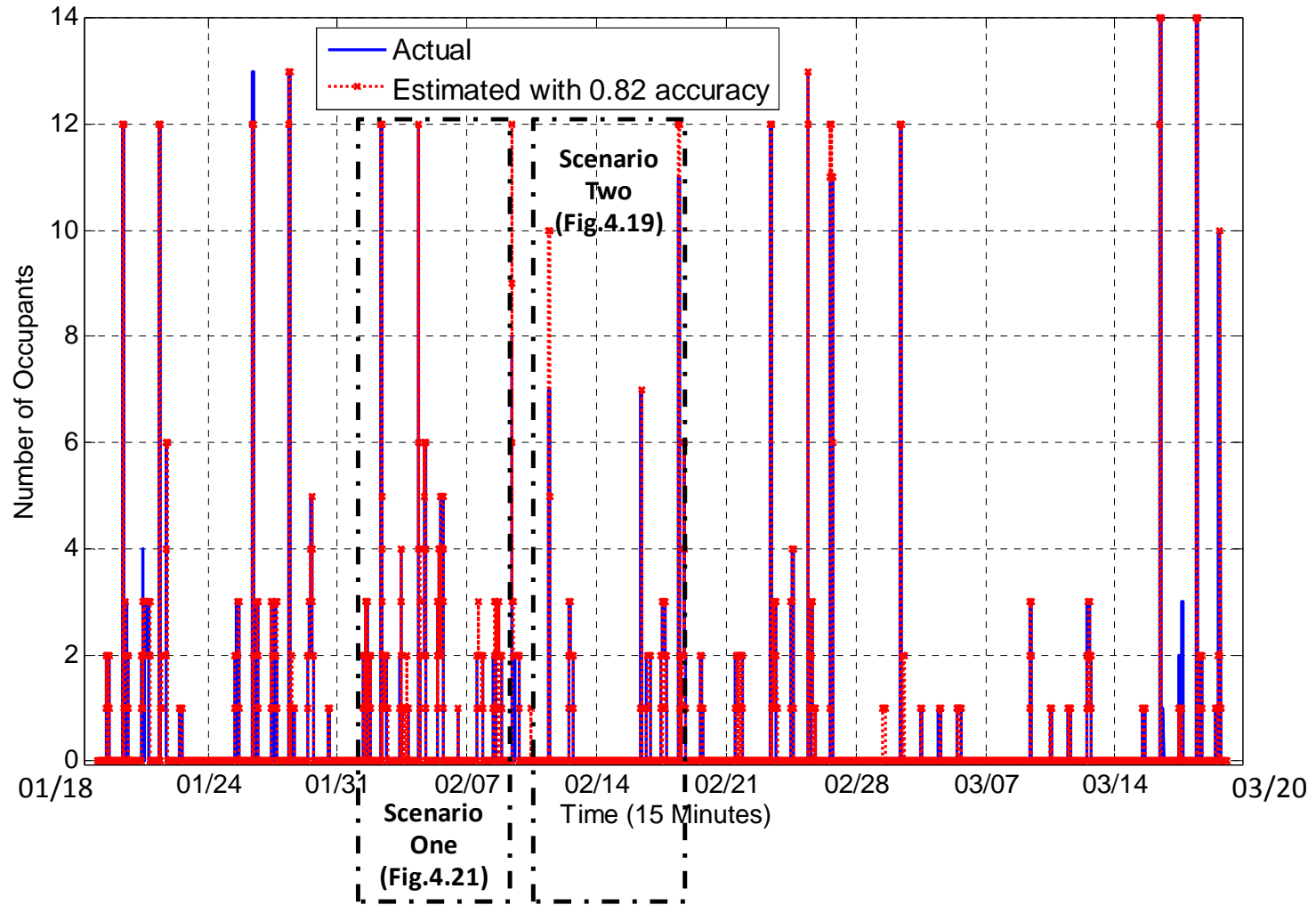


Figure 4.17 Results of occupancy pattern prediction from January 18 to March 20, 2010

Figure 4.17 shows the results of occupant pattern prediction from February 1 to February 7, 2010. As described in Chapter 2, the occupancy pattern prediction includes occupancy number and duration:

1) Occupant number estimation

The number of occupants during the testing period time ranges from 0 to 14.

a. Scenario one

When integrated with scheduled meetings and classes, the accuracy for the week of scenario is 88%, as shown in Figure 4.18. The selected feature CO₂ has a delay effect of 15 to 20 minutes. However, acoustics and motion does not. Hence, one strategy is to compensate the time CO₂ concentration building up with motion and acoustics data. Figure 4.19 shows one day prediction to further investigate the prediction accuracy. It is found that when the occupants stay in the room for a short time such as 10 minutes, the prediction cannot catch it.

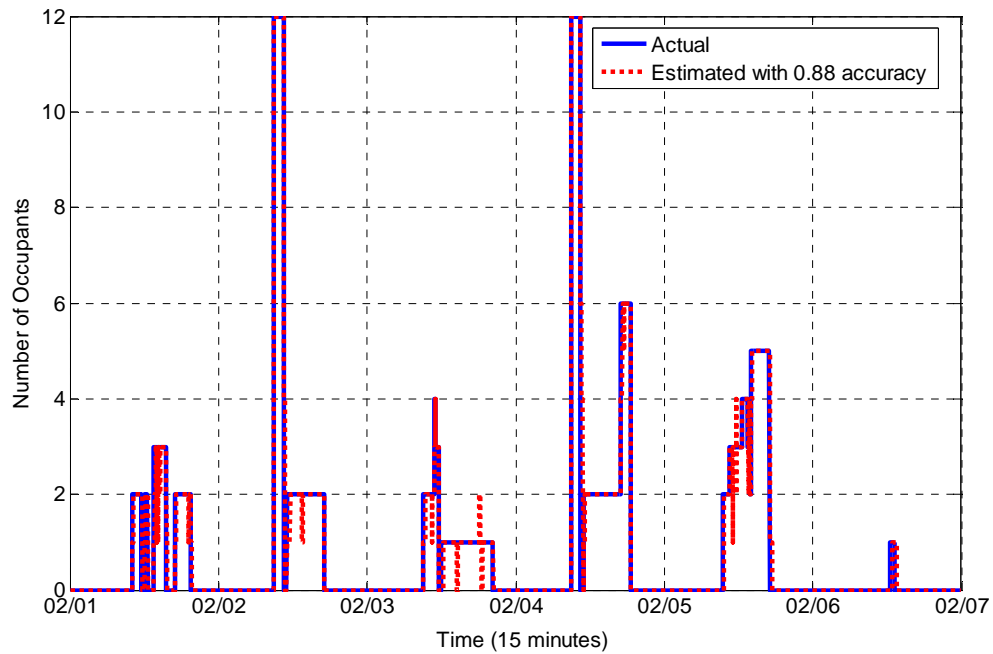


Figure 4.18 Results of occupancy pattern prediction from February 1 to February 7, 2010

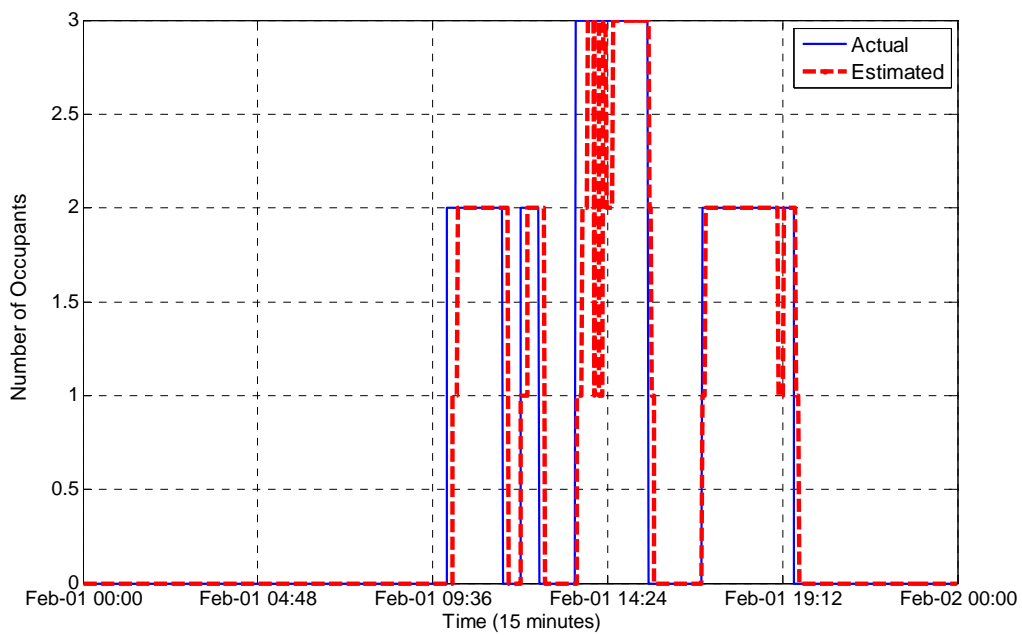


Figure 4.19 Results of occupant pattern prediction on February 1, 2010

b. Scenario two

The number of occupant detection failed when the occupant pattern never happened before. Figure 4.20 shows the results of occupant pattern prediction from February 7 to February 14, 2010. The whole week prediction accuracy is 0.65, which is lower than the average. On February 11, the number of occupants is 7. However, those numbers of occupants did not appear in the training data sets. For example, Figure 4.21 further illustrates the prediction algorithm chooses the possible closest number of occupants, 10, instead of 7 on February 11, 2010.

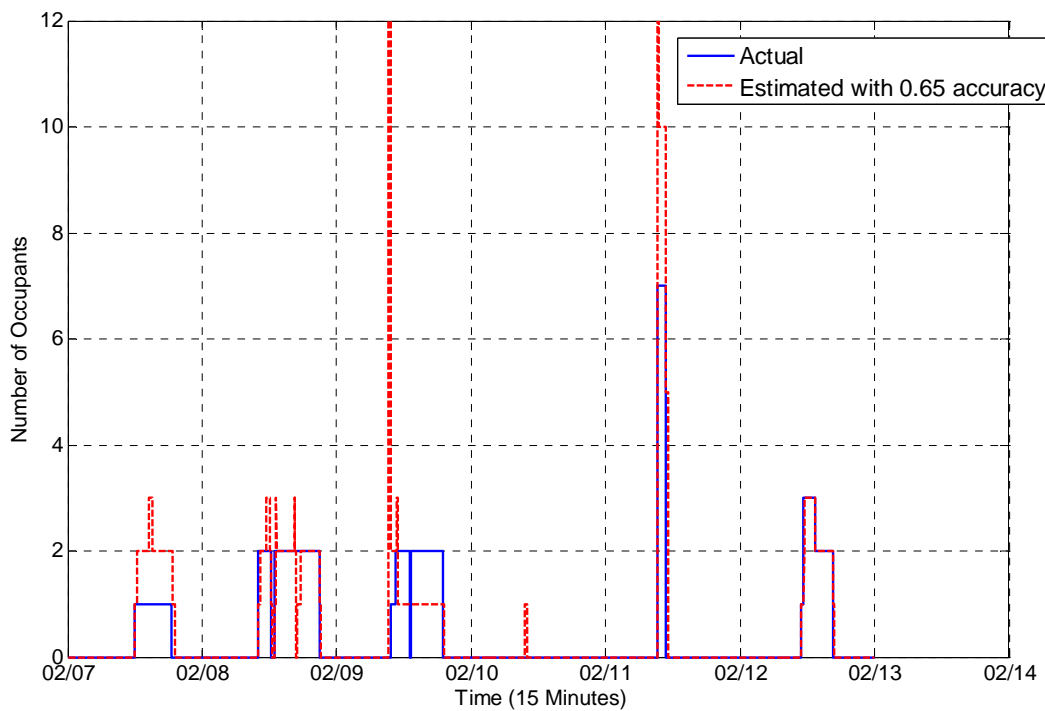


Figure 4.20 Results of occupant pattern prediction from February 7 to February 14, 2010

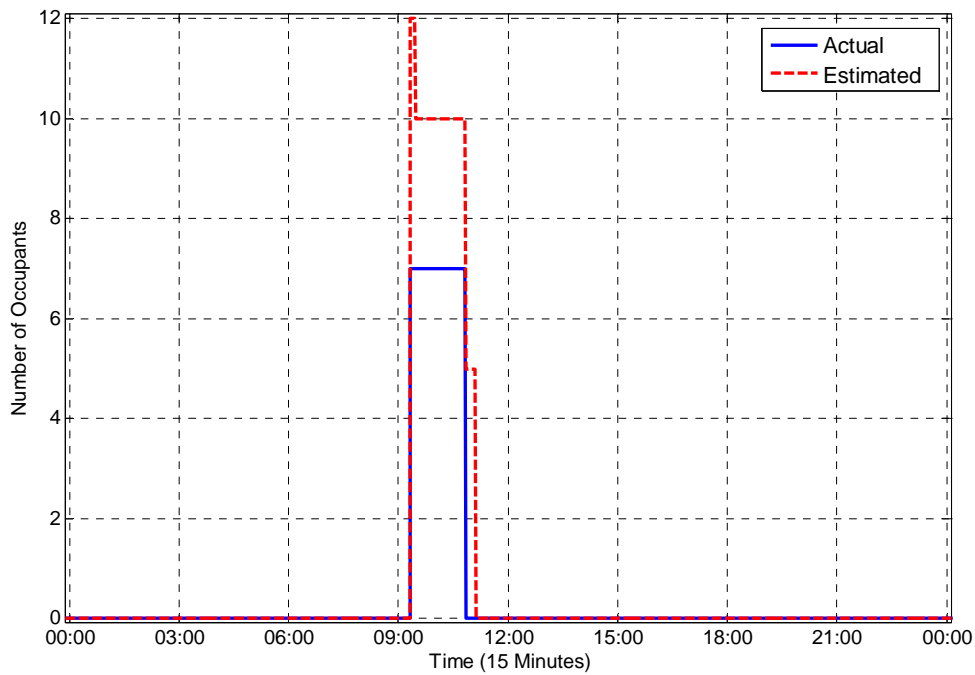


Figure 4.21 Results of occupant pattern prediction on February 11, 2010

c. Special Scenario: Window Open

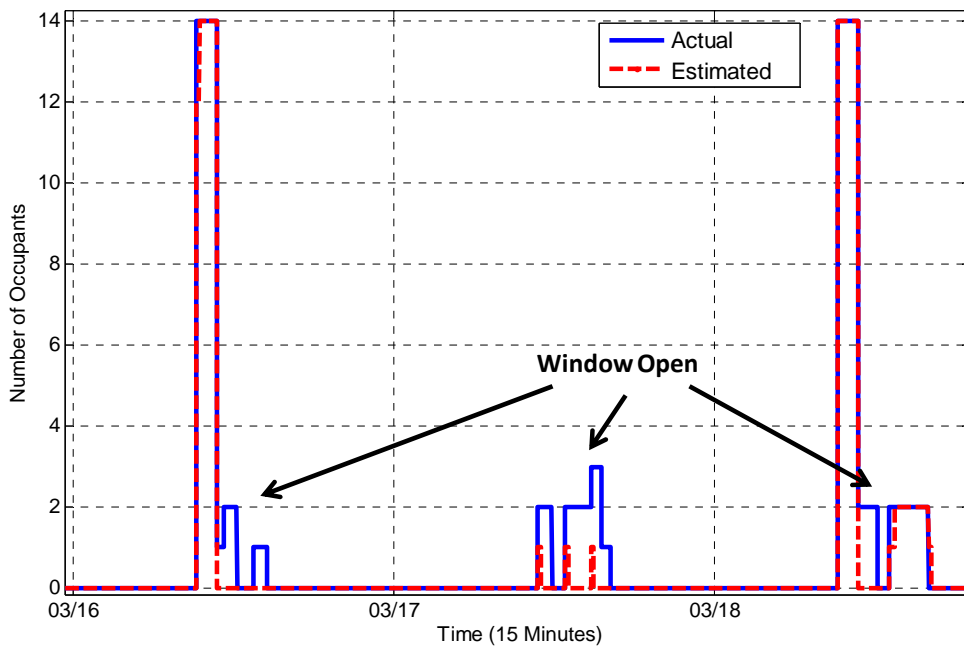


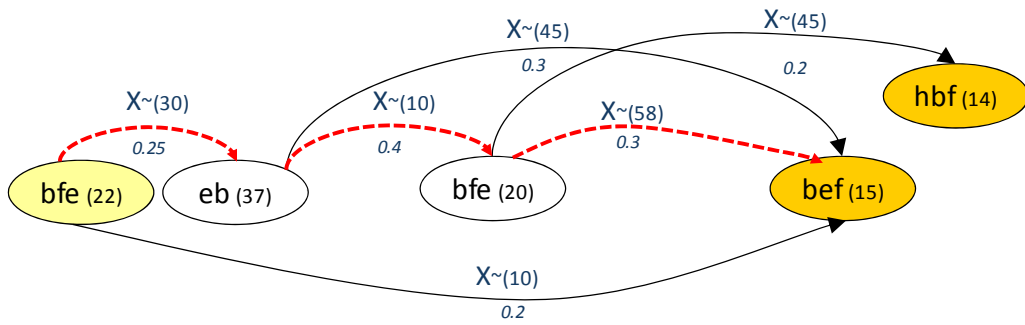
Figure 4.22 Results of occupant pattern prediction from March 16 to March 19, 2010

In some cases, when the window is open, the occupant pattern prediction does not work at all because the level CO₂ is not as comprehensive as closed space. Figure 4.22 shows the results of occupant pattern prediction from March 16 to March 18. All these three days have window open for certain amount of time. When the window is open, the prediction algorithm would predict nobody in the space. This is because one of the important features for occupant pattern prediction is the differences of CO₂ level between indoor and outdoor.

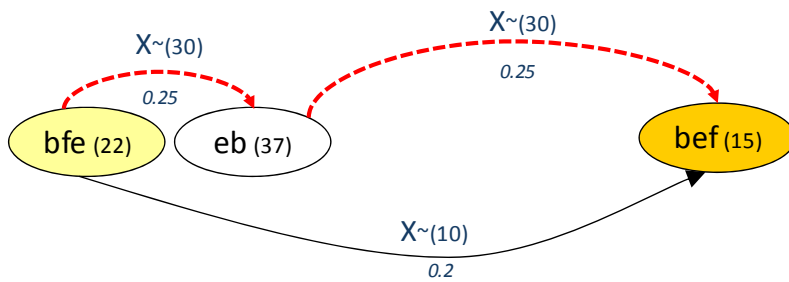
2) Occupancy duration prediction

The duration prediction is to find out daily occupancy patterns, based on Hidden Semi Markov model and estimation of duration as an Exponential function. For the whole testing period, the prediction accuracy is 78%±16 minutes. This means the method developed in this thesis can predict correctly 78% of the time, while with an offset of 16 minutes.

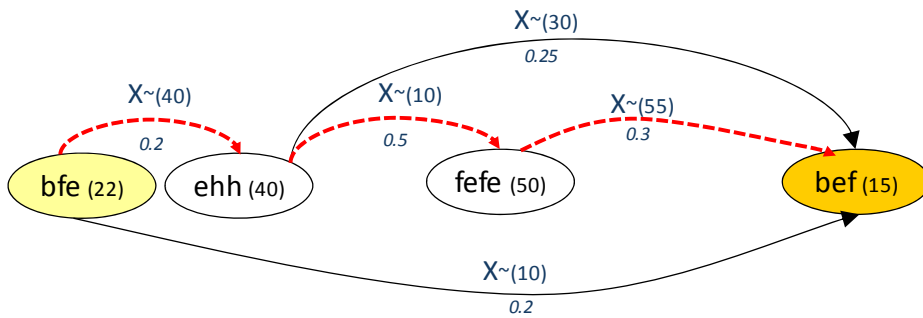
Since the found patterns are developed from the same training data sets for all testing data, the results from Scenario 1 is shown below. Figure 4.23 shows daily event patterns on February 1, 2010, discovered in this study. Event code letters are as defined in Chapter 2, Table 2.4. On that day, there are four occupancy durations happened. Figure 4.23 shows a standard Markov model with numbers on the arcs indicating the transition probability between states, Transitions with relatively low probabilities (less than 15%) are not shown. Parentheses indicate number of occurrences of the pattern in the training period. As an example, state “*bef*” has a 25% transition probability to state “*eb*” and a 20% probability to state “*bef*”, with “*bef*” occurring 22 times, “*eb*” 37 times and “*bef*” 15 times during the month. Figure 4.23 also shows the results of including duration in the model. Each duration distribution is denoted as $X \sim (time)$, where *time* is the expected duration for the exponential model. For example, “*bef*” has an expected duration of 30 minutes before it transitions to state “*eb*” and 10 minutes before transiting to state “*bef*”. The red-dotted line in Figure 4.23 a) indicates a typical 98 minute meeting scenario where an occupant enters the room, triggers the motion sensor “*e*”, triggering sound on “*b*”, and sits down, triggering the motion off “*f*”. The occupant continues to stay in the room, generating acoustics “*b*” and moving around generating motion “*e*”. Upon leaving, the occupant moves towards the door “*e*” and departs “*f*”.



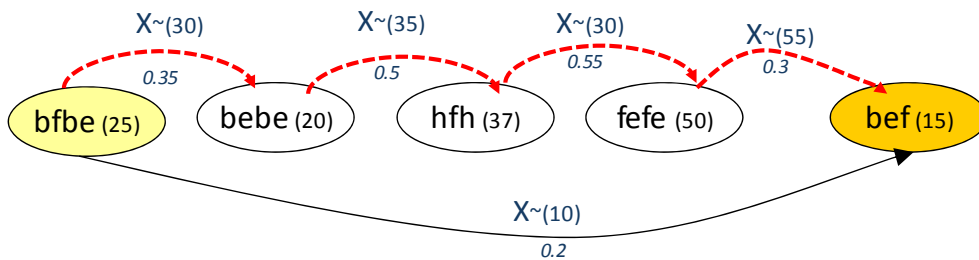
a) Actual: 110(min); Predicted: 98(min)



b) Actual: 50(min); Predicted: 60(min)



c) Actual: 121(min); Predicted: 105(min)



d) Actual: 153(min); Predicted: 150(min)

Figure 4.23 Markov model of discovered patterns on 10 minutes maximal window

Energy consumption from NMPC

a. Two months' continuous data

Figure 4.24 shows the comparison of energy profile between NMPC and scheduled temperature set-point for the whole heating testing period. The overall energy saving is 26.2% as shown in Table 4.2. The set-point not met by NMPC for the occupied time is 15 hours for the two months, which is only 6% of the total occupied time.

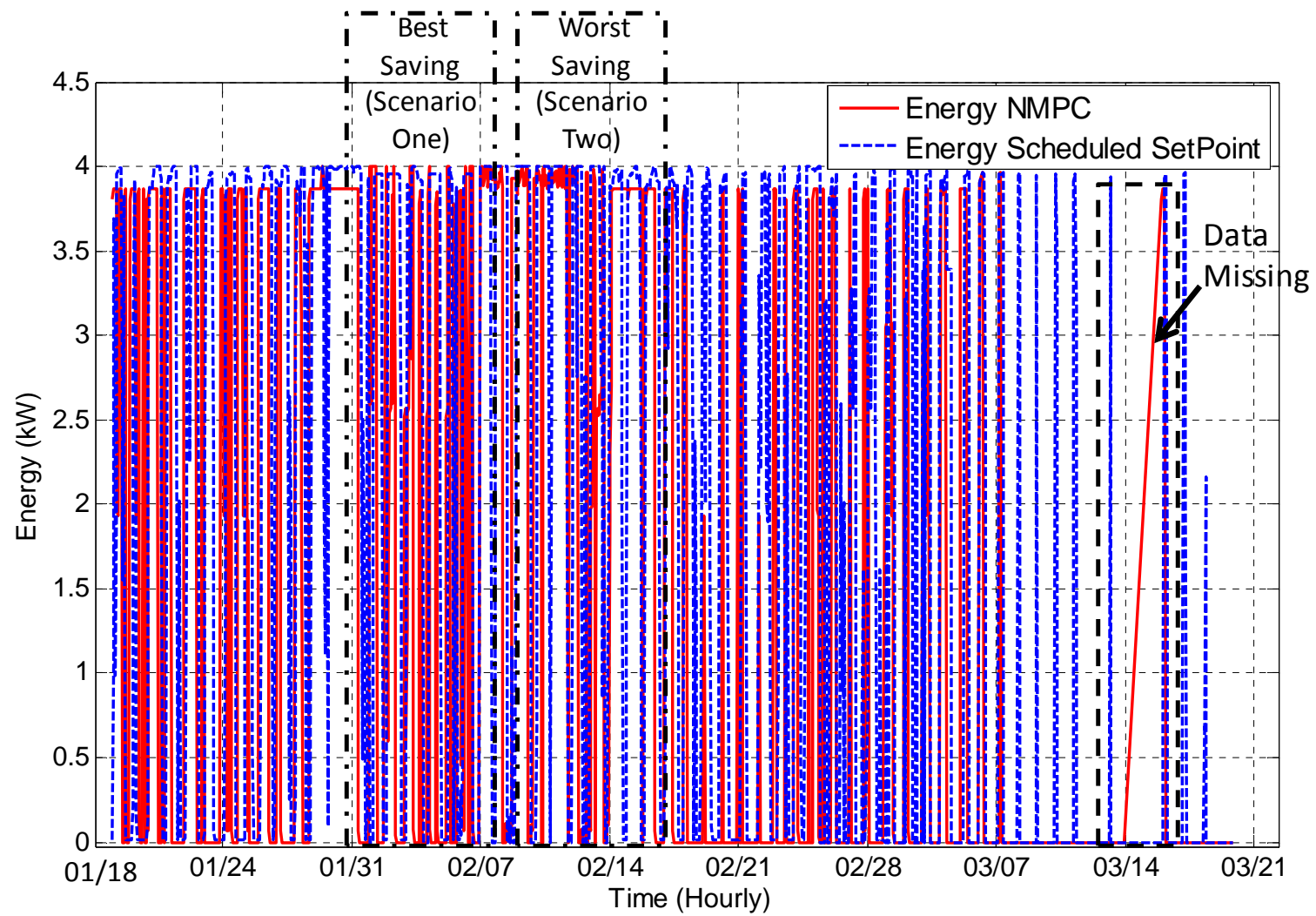


Figure 4.24 Comparison of energy profile between NMPC and scheduled temperature set-points from January 18 to March 20, 2010

Two scenarios are selected to represent “Most Energy Saving” and “Least Energy Saving” periods. There is also a period from March 14 to March 15 when the data is missing due to the failure of the sensors.

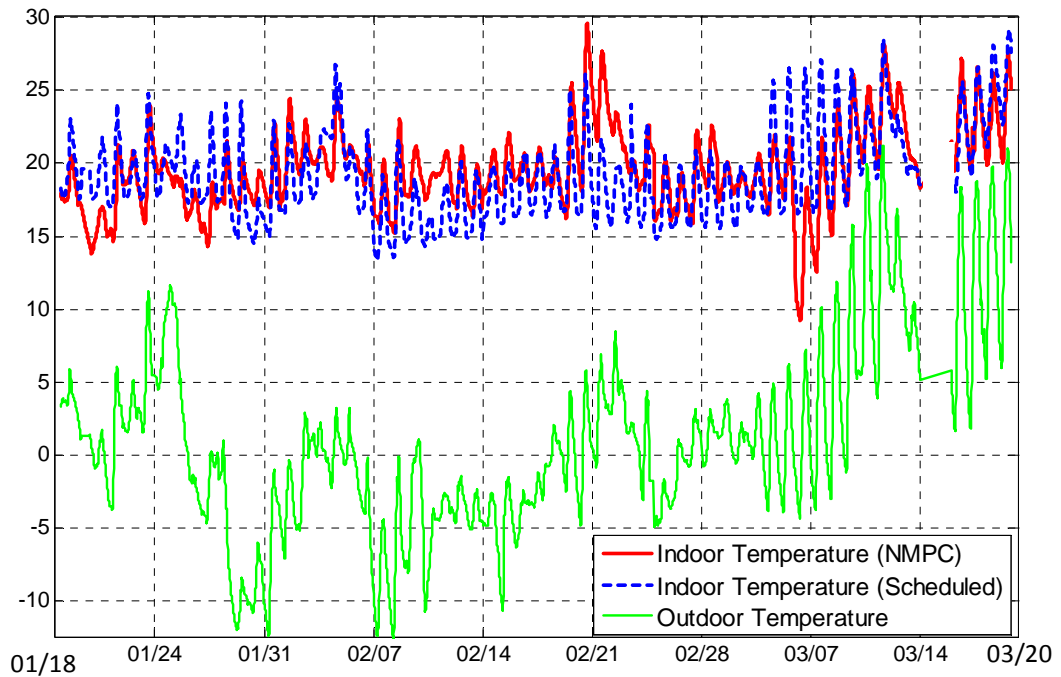


Figure 4.25 Temperature profile from February 1 to February 7, 2010

Table 4.2 Comparison of total heating energy consumption and set-point not met hours

Energy Consumption (kWh)		Energy Saving (%)
Scheduled Set-points	2752	26.2
NMPC Optimization	2032	
Temperature Set-point not met while occupied (Hrs)		Improved Set-point Met Time (%)
Scheduled Set-points	40	62.5
NMPC Optimization	15	

b. Scenario one

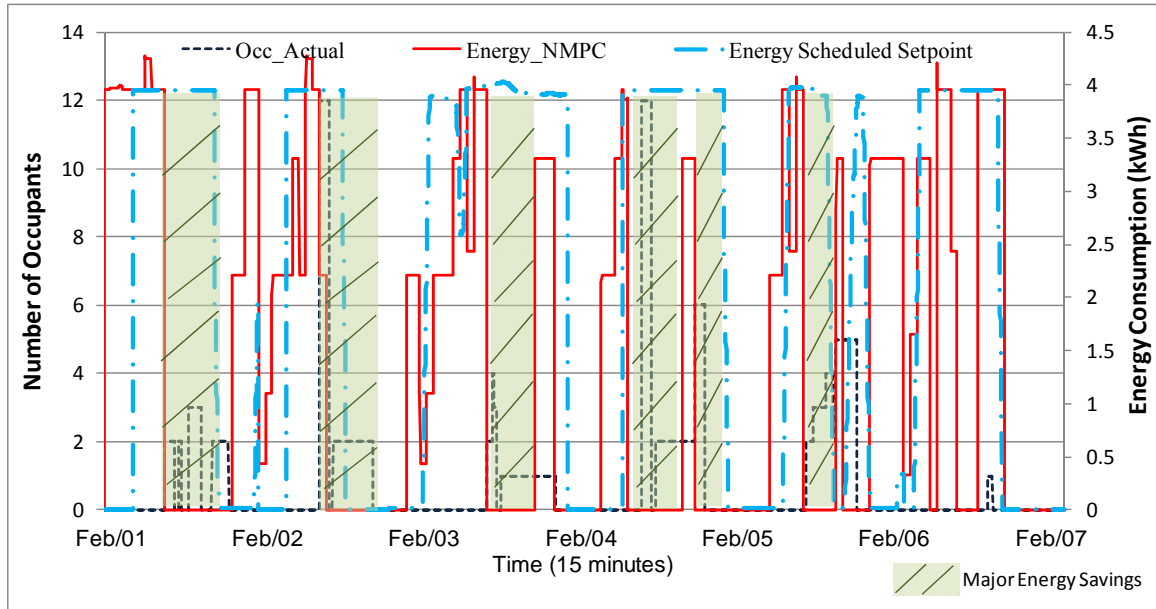


Figure 4.26 Comparison of energy profile between NMPC and scheduled temperature set-points of scenario one

Figure 4.26 shows the measured results of energy consumption profile of NMPC, which integrates the weather forecasting and occupant behavior pattern prediction. Due to the thermal mass effect of the concrete floor slab, there is often no need for additional heating during day time, while maintaining the set-point temperature band ($21^{\circ}\text{C}\pm 2$) as shown in Figure 4.27. In addition, the occupancy prediction can provide the information on the occupant's arrival time on the next day. This information helps to predict an optimized energy profile of the next day.

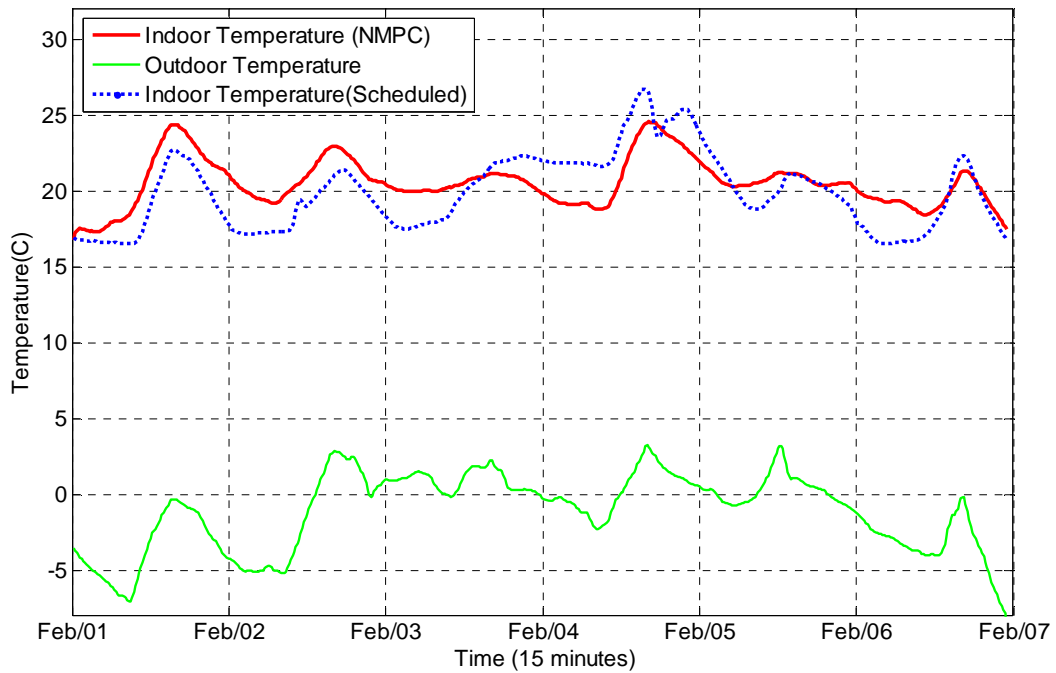


Figure 4.27 Temperature profile from February 1 to February 7, 2010

Table 4.3 Comparison of heating energy consumption and set-point not met hours in scenario one

Energy Consumption (kWh)		Energy Saving (%)
Scheduled Temperature Set-points	343	30.1
NMPC Optimization	240	
Temperature Set-point not met while occupied (Hrs)		Improved Set-point Met Time (%)
Scheduled Temperature Set-points	8	75
NMPC Optimization	2	

Figure 4.26 also compares the energy profile between NMPC and scheduled set-points. The scheduled temperature set-point normally has a night setback, which is 17°C in this study. The heating system remains off until the indoor temperature falls below the setback temperature. Hence, the heating system often starts after the mid-night and at its full capacity to reach the set-point in the morning. In addition, the predicted occupant arrival time is often not within the range of scheduled daily temperature set-point period. This results in more energy consumption.

The energy saving from the NMPC compared to scheduled set point is further illustrated in dashed boxes in Figure 4.26. Table 4.3 Comparison of heating energy consumption shows the comparison of total energy consumption for the whole week. The NMPC can save 30.1% of energy compared with the scheduled start. Furthermore, the NMPC does not meet the temperature set-point for 2 hours, compared to 8 hours from schedule temperature set-point control. This is because during some cold nights, if the indoor air temperature is around the night set-back (17 °C), the daily set-point in the morning cannot be met. Instead, the NMPC keeps the indoor air temperature warm enough at night to meet the set-point in the morning.

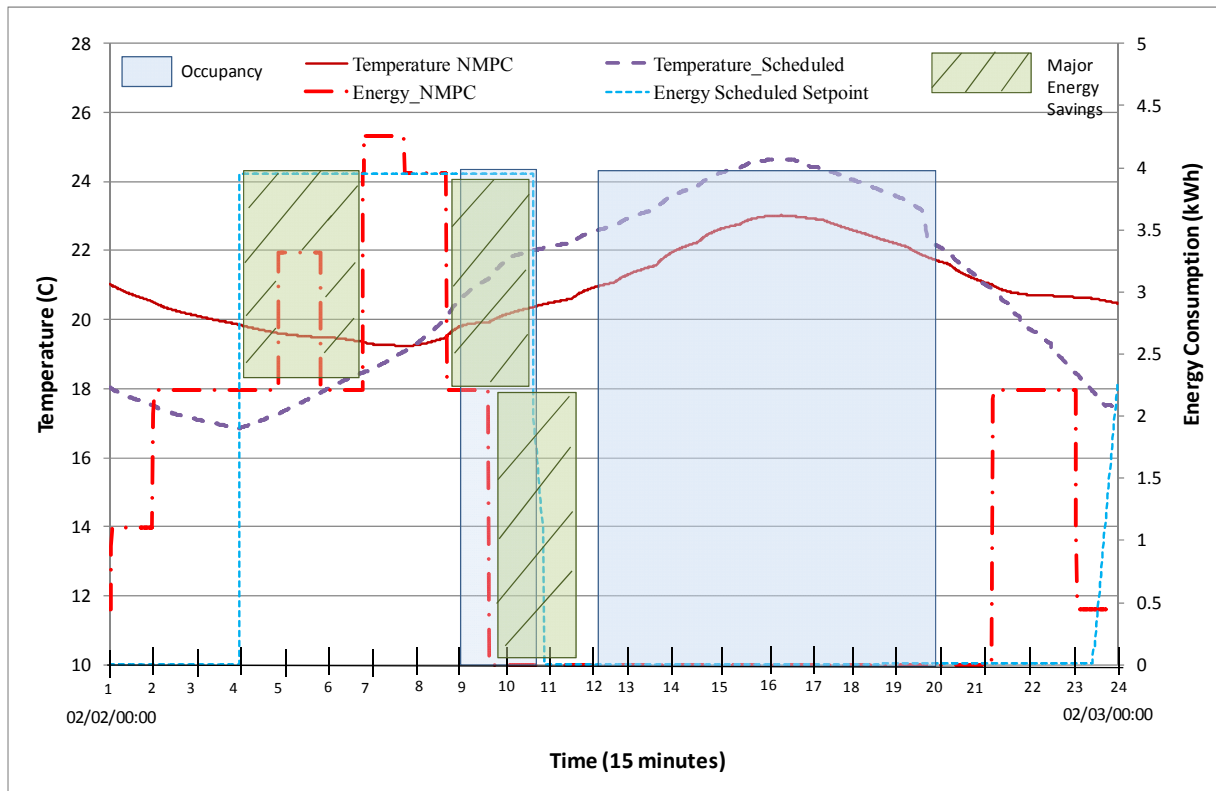


Figure 4.28 Comparison of energy profile between NMPC and scheduled temperature set-points on February 2, 2010

Figure 4.29 shows the results from the one day test on February 2, 2010. The major energy saving from NMPC is heating control at night where it dynamically adjusts the set-points, while reaching the set-point temperature when the occupant arrived. NMPC maintains the indoor air temperature at a certain level after the occupant leaves. In this case, the instant water heater does not need to operate at the maximum power.

c. Scenario Two

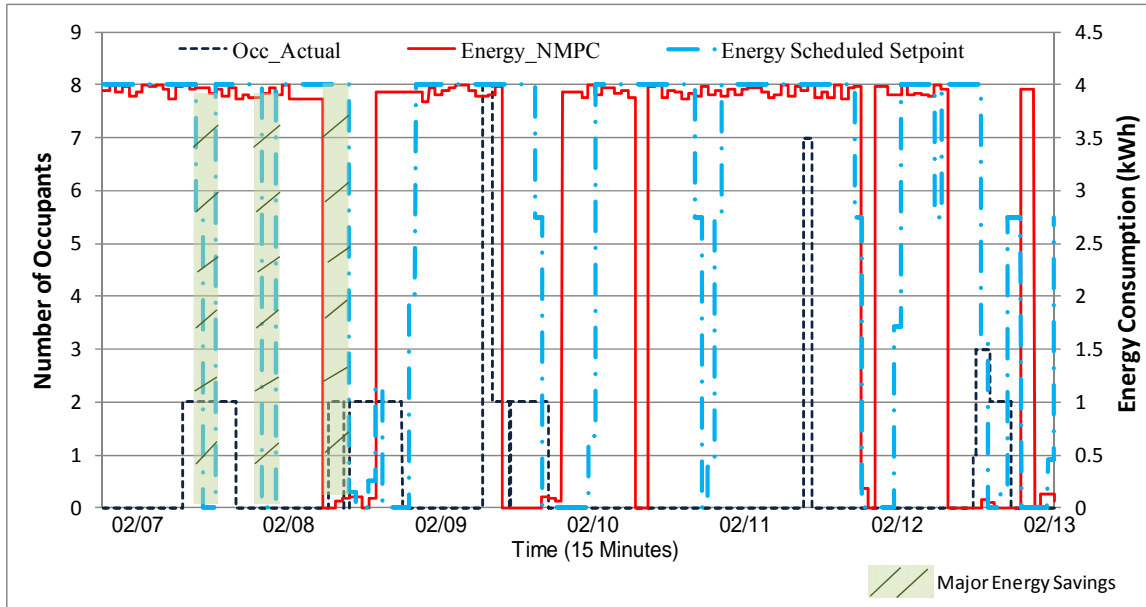


Figure 4.29 Comparison of energy profile between NMPC and scheduled temperature set-points of scenario two

Figure 4.29 compares the energy consumption between NMPC and schedule temperature set-points of scenario two. The outdoor temperature reaches the coldest point (-17°C) in this winter. The heating is on all the time from NMPC. Hence, the energy consumption from these two control methods is almost the same as shown in Table 4.4. In other words, dynamic occupancy schedules do not impact the heating energy consumption in this scenario. Table 4.4 also shows in such cold period, scheduled temperature set-point control is difficult to meet daily set-points.

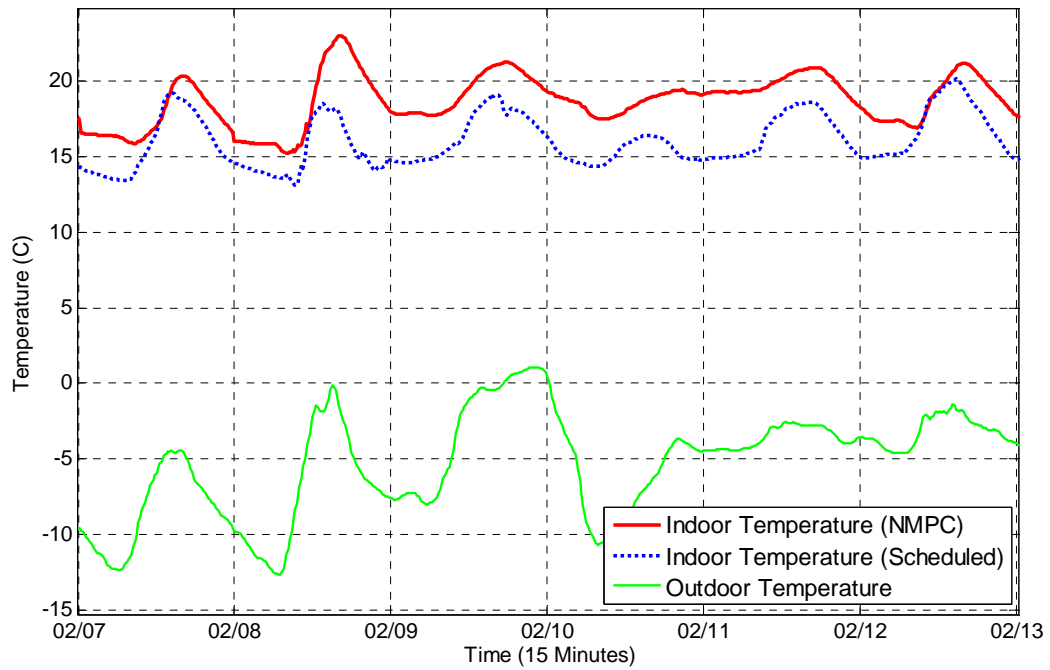


Figure 4.30 Temperature profile from February 7 to February 13, 2010

Table 4.4 Comparison of total heating energy consumption of scenario two

Energy Consumption (kWh)		Energy Saving (%)
Scheduled Set-points	482	2
NMPC Optimization	473	
Temperature Set-point not met while occupied (Hrs)		Improved Set-point Met Time (%)
Scheduled Set-points	20	70
NMPC Optimization	6	

4.2.2.3 Sensitivity Analysis of Heating Controls

Figures 4.31 to 4.33 show the heating energy consumption for different levels of occupancy changes as defined in Table 4.5. The heating energy consumption does change much with the occupancy level change. Instead, the outdoor air temperature becomes the dominant factor for the energy consumption. For example, the daytime temperature profiles on February 4 and February 5 are similar as shown in Figure 4.23 and 4.24. However, on the February 5 night, the temperature suddenly dropped 10 degrees, which caused high heating energy consumption during the evening in order to meet the temperature set-point on the morning of February 6.

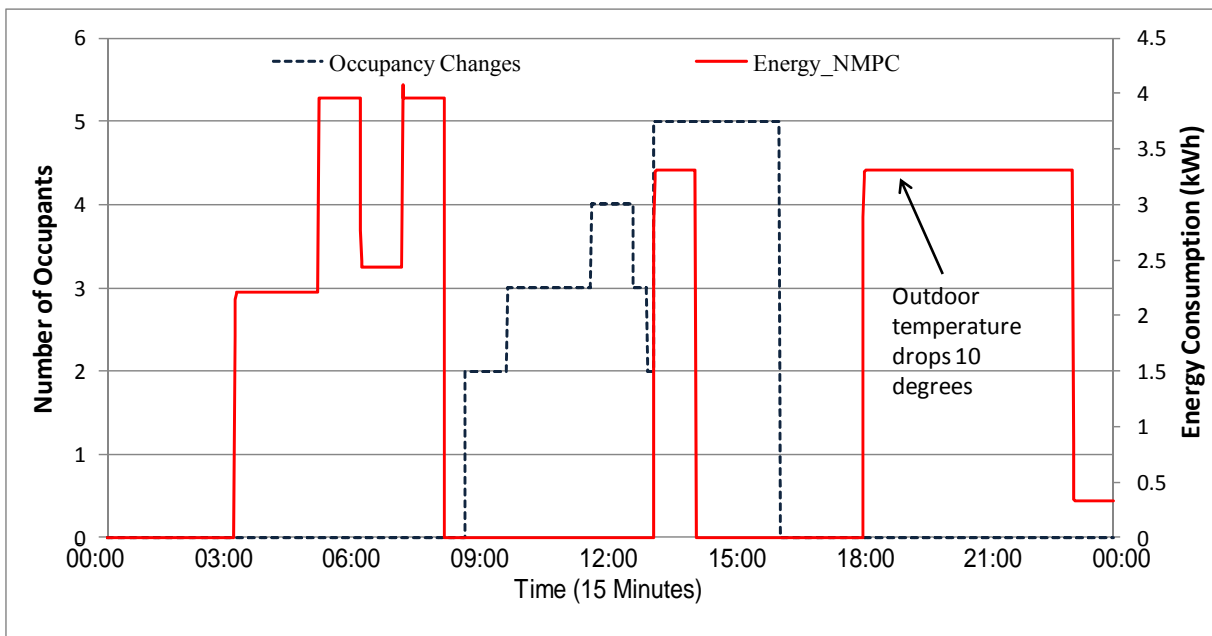


Figure 4.31 Heating energy profile of high occupancy changes on February 5, 2010

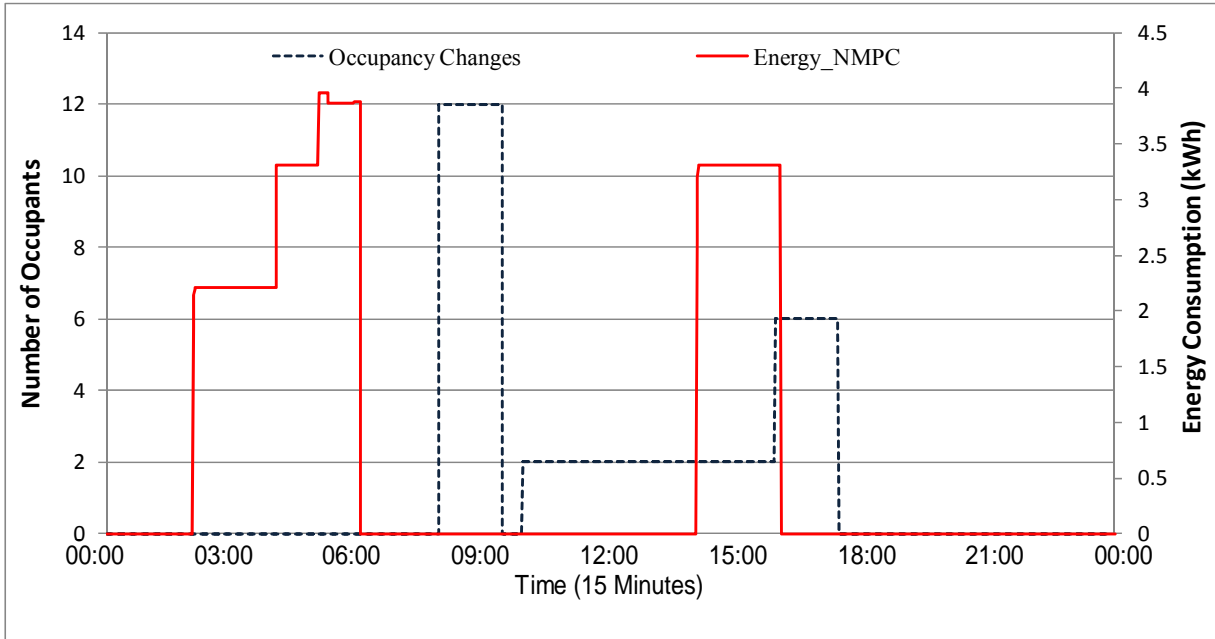


Figure 4.32 Heating energy profile of moderate occupancy changes on February 4, 2010

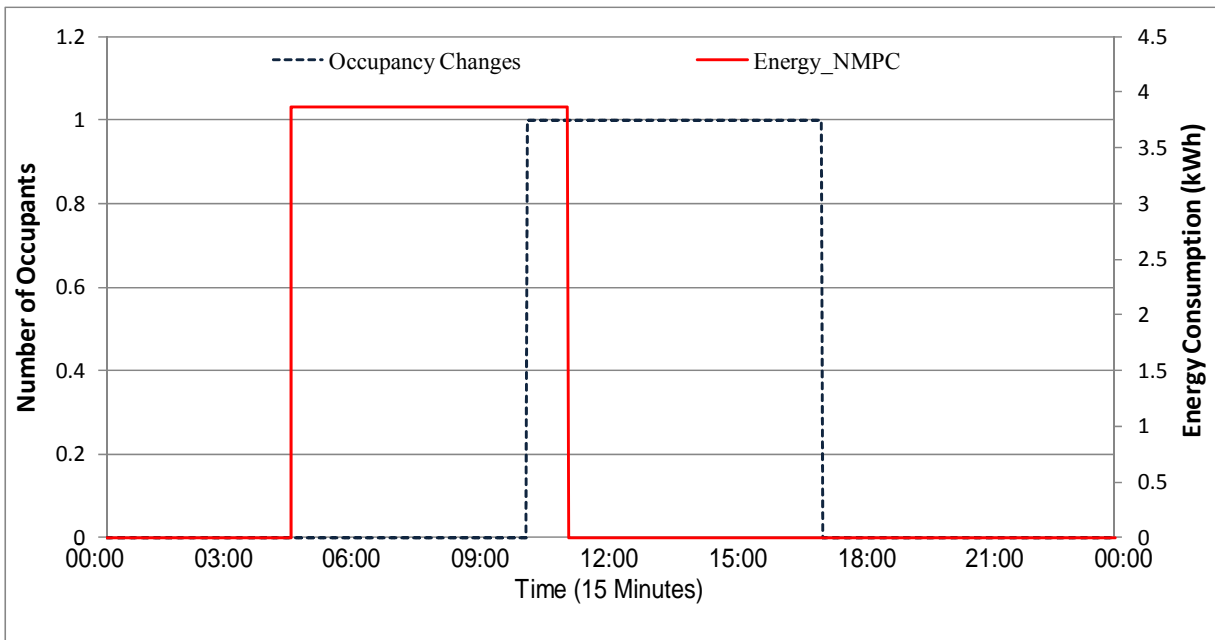


Figure 4.33 Heating energy profile of low occupancy changes on March 5, 2010

Table 4.5 Heating energy consumption and daily occupancy changes

Energy Consumption (kWh)		Differences (%)
Low Occupancy Changes (1 change)	24	Baseline
Moderate Occupancy Changes (2~3 changes)	25	4%
High Occupancy Changes (>3 changes)	35	45%

4.2.3 Cooling Season

4.2.3.1 Experiment Setup

The cooling season experiment is setup through the week from July 5 to July 10, 2010. Since there is no automatic control for the cooling equipment, this is just a demonstrative experiment based on a short period of data and availability. During this experiment period, the windows are all closed because outside temperature ranges from 25 °C to 35 °C. Occupants are visitors from outside of campus and students of the School of Architecture. The occupant activities include meetings, lunch break and normal office hours. The training data set for occupancy and weather prediction uses continuous data collected from the previous month data. During the cooling season, the time step for control is 15 minutes because the heat pump system can cool down the space from 29 °C to 25 °C in 15 minutes. The cooling setpoint while occupied is 25 °C in the day time.

4.2.3.2 Results and Discussion

Weather prediction

Figure 4.34 to Figure 4.36 show the 15-minute prediction results of outdoor air temperature, global horizontal solar radiation and wind speed. As shown in the Figures, the RMSEs are 0.62, 60.02 and 0.37 respectively, which are all as low as the results for the heating season. The MAPEs are 8%, 25% and 12%. Only the solar radiation prediction is worse than the 60-minute

time step during the heating season. This is because the cloud coverage has only hourly data and the values within the hour are assumed to be constant.

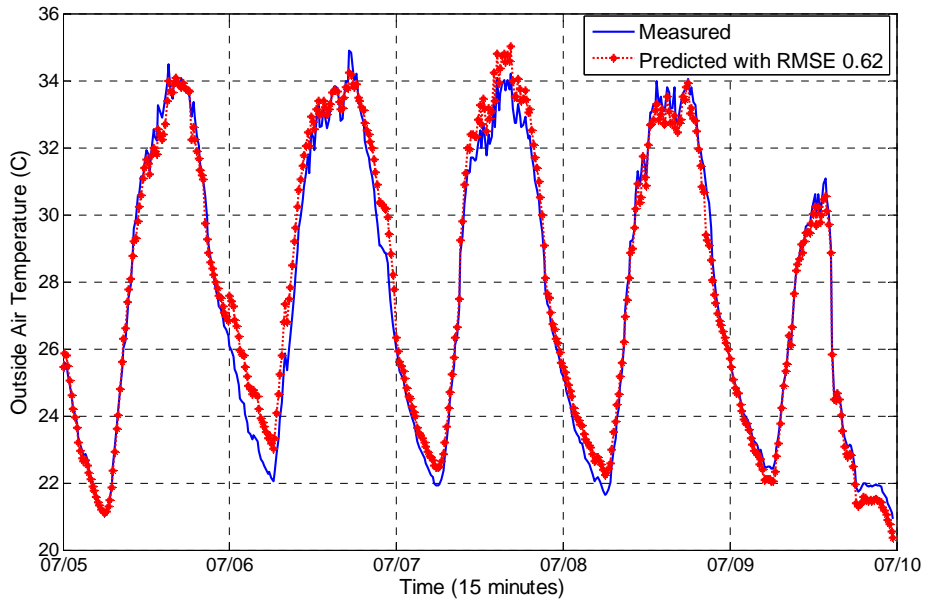


Figure 4.34 Results of 15-minute local outdoor air temperature prediction from July 5 to July 10, 2010

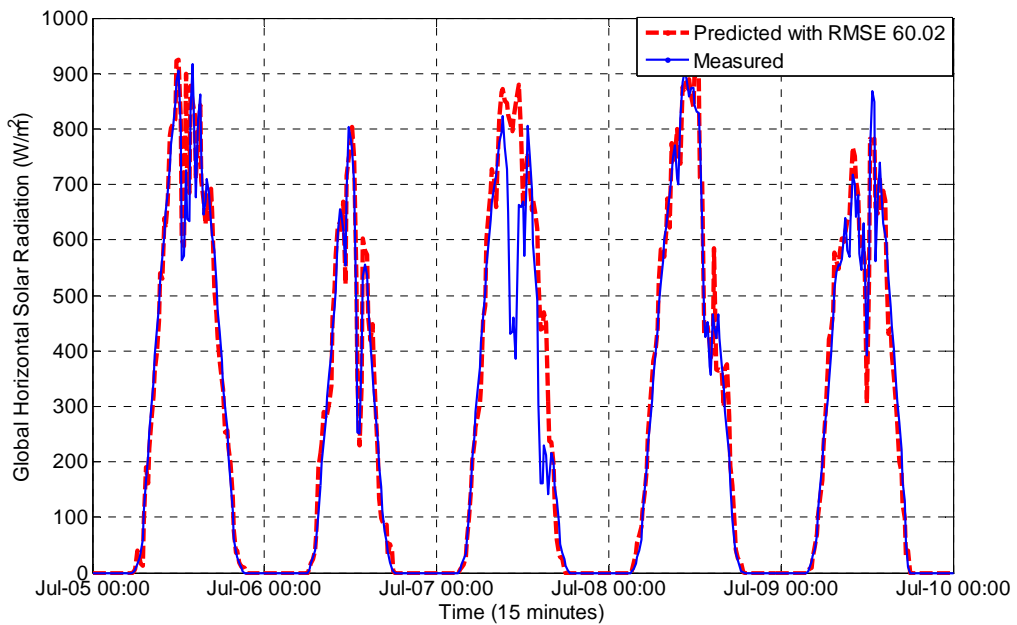


Figure 4.35 Results of 15-minute local global horizontal solar radiation prediction from July 5 to July 10, 2010

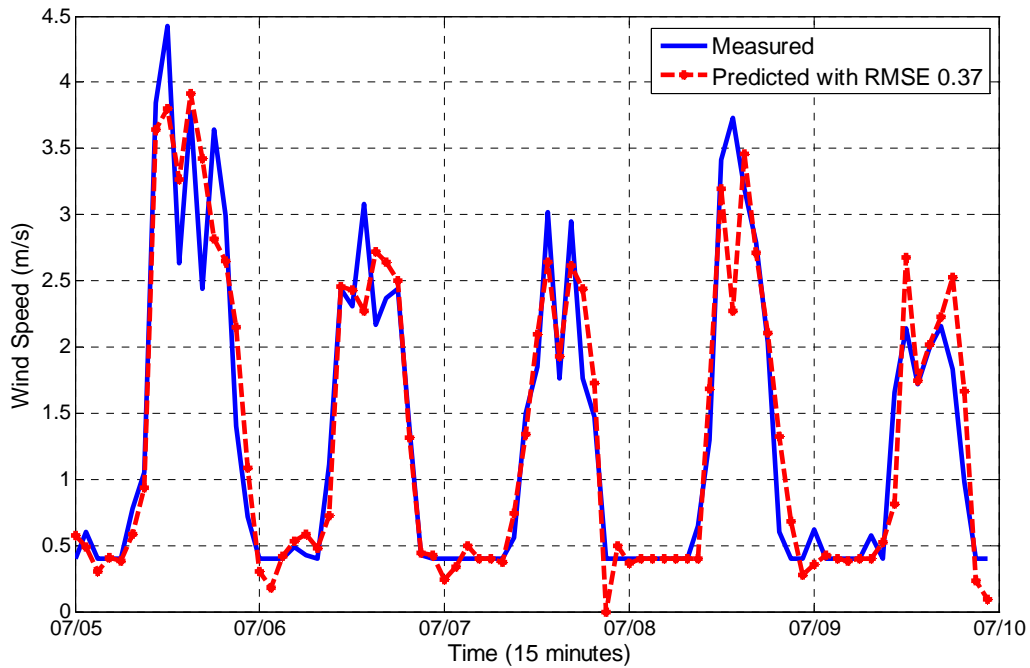


Figure 4.36 Results of 15-minute local wind speed prediction from July 5 to July 10, 2010

Occupant behavior pattern prediction

As described in heating season, the occupancy pattern prediction during cooling also includes two parts: (1) occupant number estimation; (2) occupancy duration prediction. Figure 4.37 shows the results of occupancy pattern prediction from July 5 to 10, 2010. The number of occupants during the testing period ranges between 0 and 7. The prediction accuracy for the whole week is 92%. During this testing period, 15 minutes moving average of CO₂ is changed to 5 minutes as one of the training features. As shown in Figure 4.38, the daily profile of predicted occupancy shows a prediction delay. In addition, a sudden change of occupancy number within 5 minutes cannot be detected.

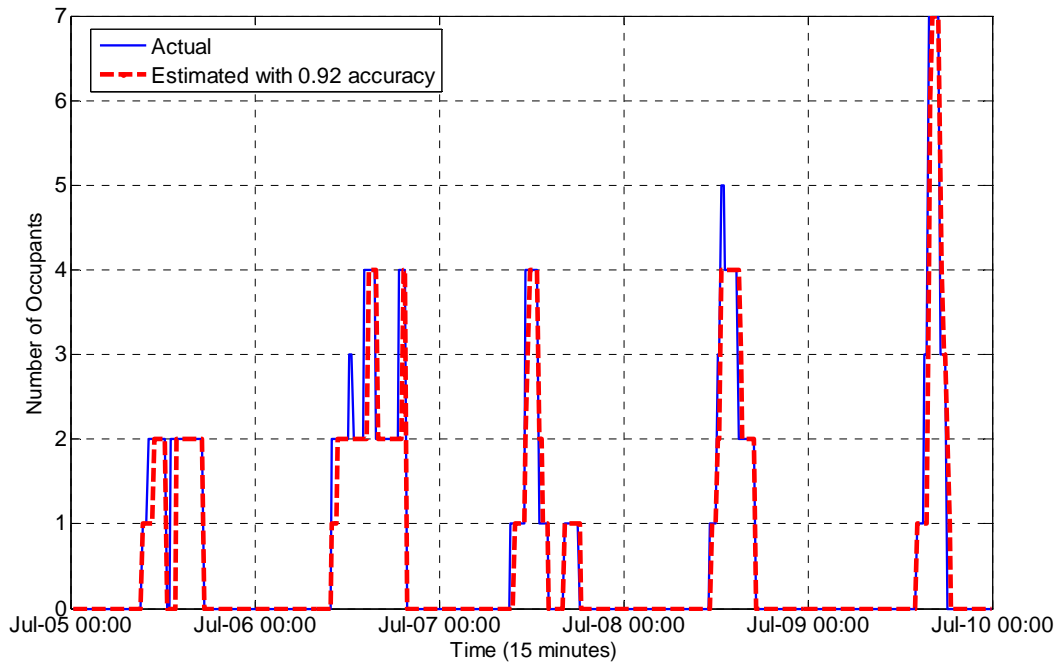


Figure 4.37 Results of occupancy pattern prediction from July 5 to July 10, 2010

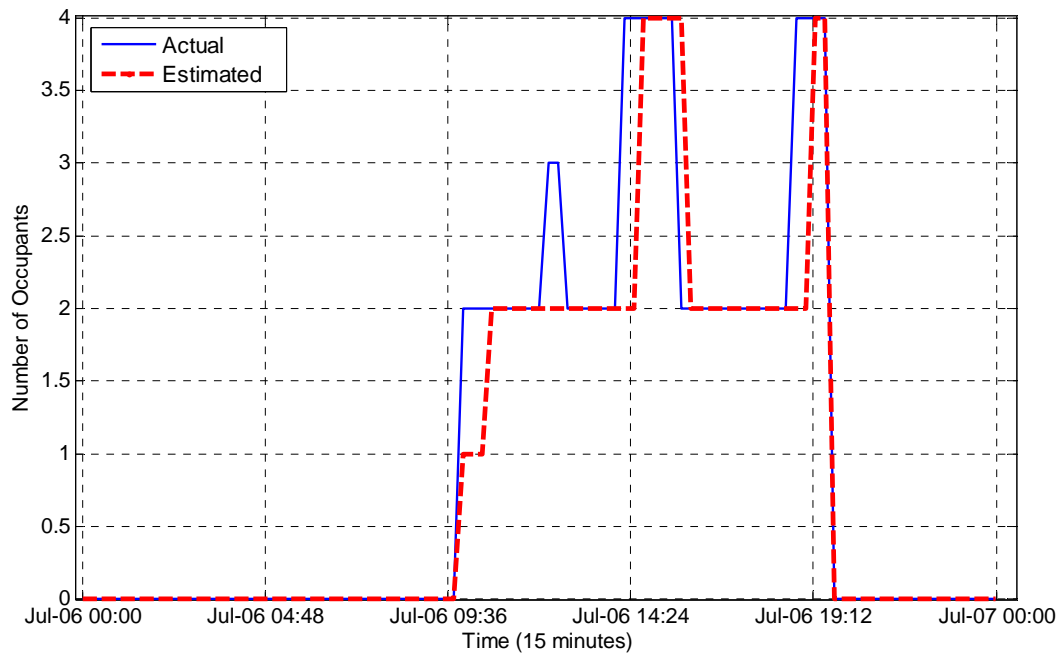
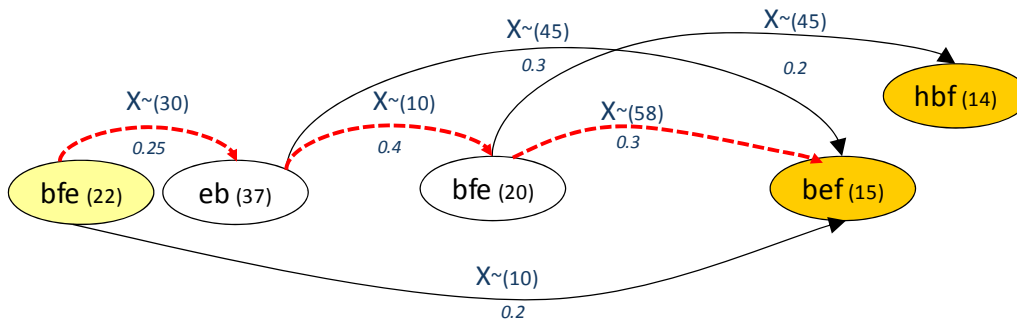
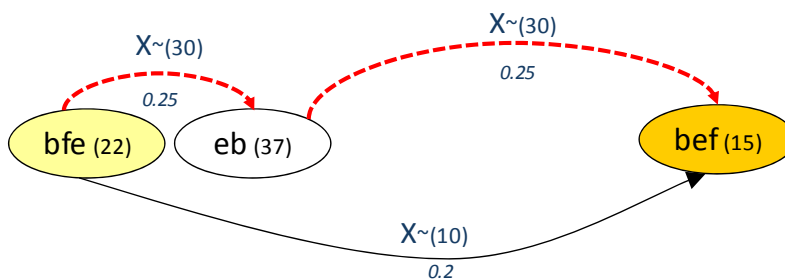


Figure 4.38 Results of occupancy pattern prediction on July 6, 2010



a) Actual: 90(min); Predicted: 98(min)



b) Actual: 60(min); Predicted: 60(min)

Figure 4.39 Markov model of discovered patterns on 10 minutes maximal window

Figure 4.39 shows the daily event patterns on July 5, 2010. There are two patterns representing the durations of 90 minutes and 60 minutes. The overall prediction accuracy is 90%±10 minutes.

Supply air flow rate

Figure 4.40 shows cooling supply air flow rates with different levels of occupancy. In this study, these values are 0.19 m³/s, 0.12 m³/s and 0.08 m³/s. According to ASHRAE 62.1 (ASHRAE, 2004), a flow rate of 0.08 m³/s is enough for 10 people. Hence, the supply air flow rate is working together with return and supply air temperature to have minimum energy consumption. One interesting finding is that the system turns on only one time step (15 minutes) before the occupant's arrival and with maximum supply air flow rate. This is because the cooling system is oversized and it only takes 15 minutes to cool down the space to set-point.

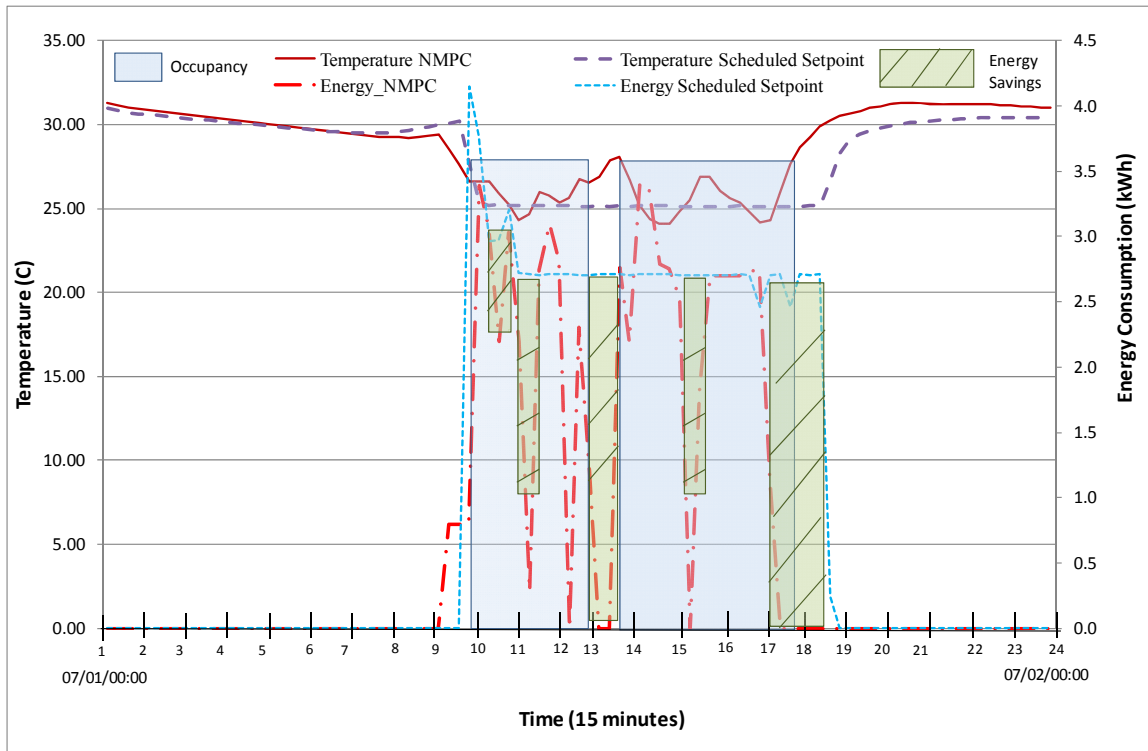


Figure 4.41 Comparison of energy profile between NMPC and scheduled temperature set-points on July 1, 2010

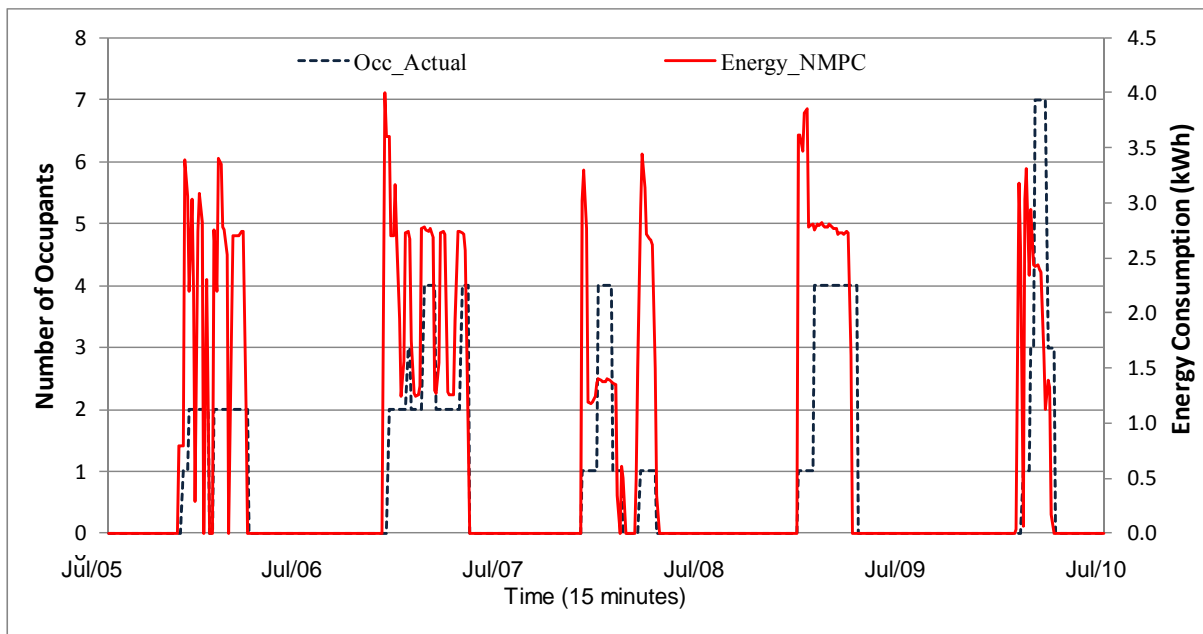


Figure 4.42 Energy consumption profile of NMPC from July 5 to July 10, 2010

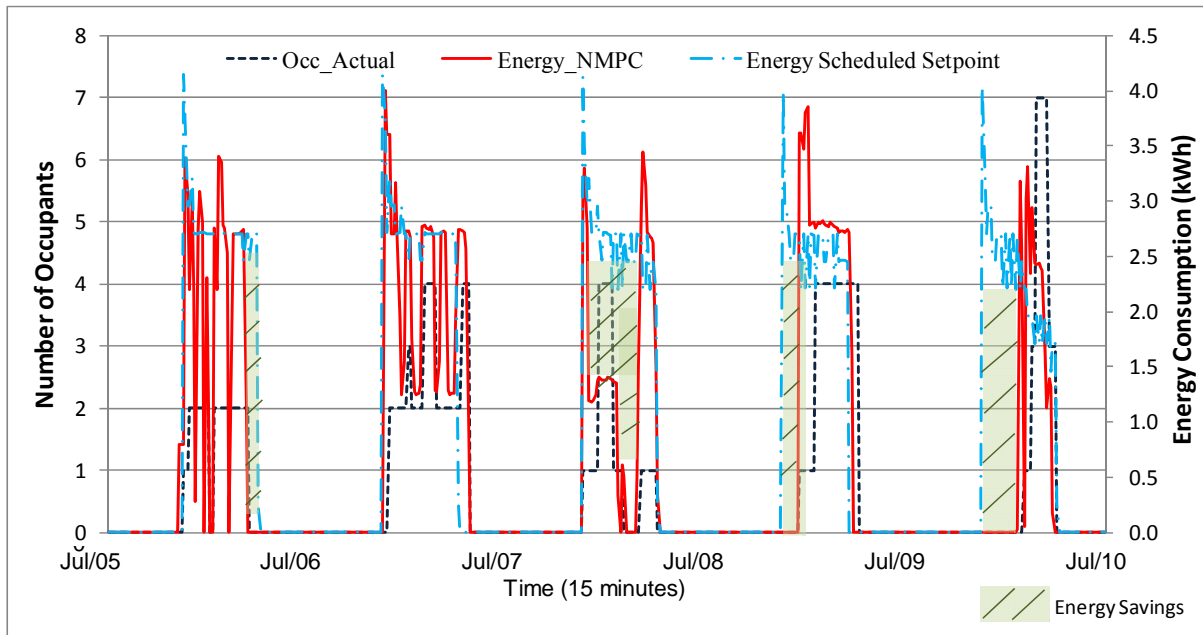


Figure 4.43 Comparison of energy profile between NMPC and scheduled set-point

Figure 4.42 shows the measured results of cooling energy consumption based on the predicted dynamic occupancy schedule. The cooling energy fluctuates with the level of occupancy during day time. This demonstrates the robustness of the control that it can track the changes of occupant numbers and meet the temperature set-point while the space is occupied. Figure 4.43 compares the energy consumption between NMPC and scheduled set-points. The energy saving mainly comes from the dynamic occupancy scheduling, while the scheduled control set-point method tries to maintain the set-point regardless of whether there is any occupant in the space.

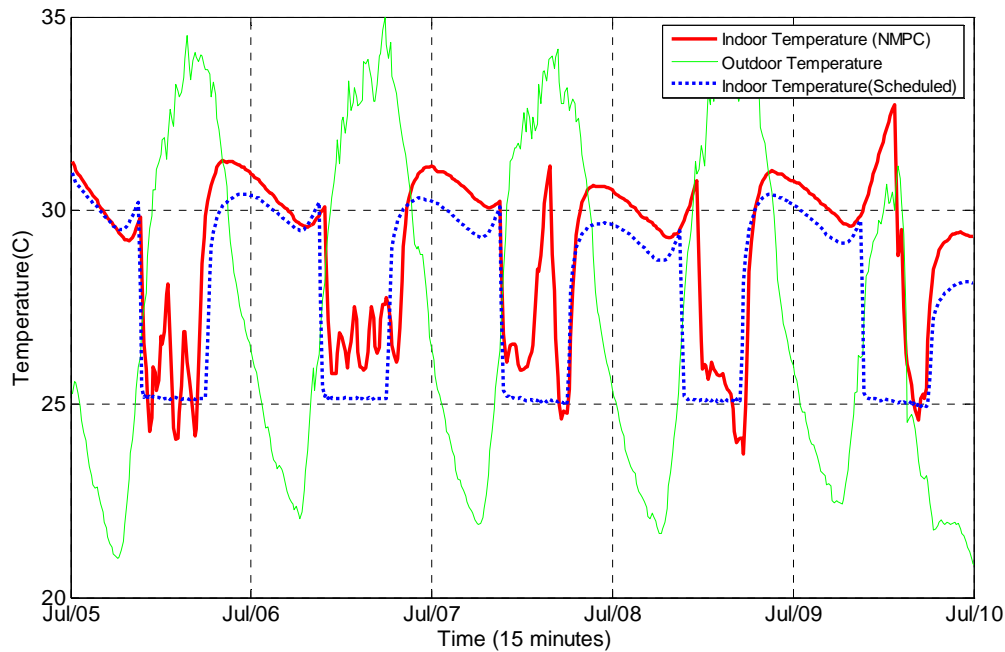


Figure 4.44 Indoor temperature profile based on NMPC from July 5 to July 10, 2010

Table 4.6 Comparison of total cooling energy consumption

Energy Consumption (kWh)		Energy Saving (%)
Scheduled Temperature Set-points	96.83	
NMPC Optimization	79.62	17.8
Simulated NMPC Optimization with Less Infiltration	77.3	20.2
Temperature Set-point not met while occupied (Hrs)		Improved Set-point Met Time (%)
Scheduled Set-points	3	
NMPC Optimization	2	33%
Simulated NMPC Optimization with Less Infiltration	1	66%

Figure 4.44 shows the indoor air temperature changes under NMPC control. When the space is not occupied, the indoor temperature does not maintain at the 25 °C set point. Table 4.6

compares the simulated energy consumption of schedule set-points and measured NMPC optimization. The total cooling energy saving for one week is 17.8%. Although the dynamic occupancy schedule varies with cooling set points in the space, the temperature of the space changes quickly so that the energy saving is only realized over a short duration of about an hour (four 15-minute time-steps).

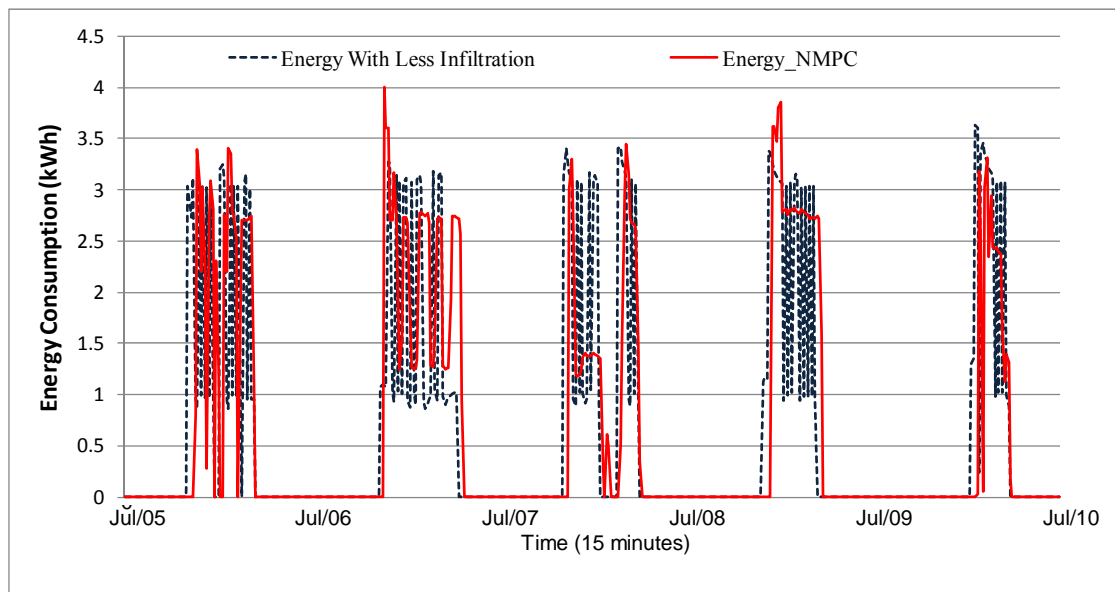


Figure 4.45 Comparison of energy profile between NMPC and simulated energy from better envelope

In order to investigate the further saving possibilities, a model with better insulation value is conducted. As mentioned in Chapter 3, the identified air infiltration rate for meeting room is 0.6 ACH. However, the benchmark models from EnergyPlus states that a tight envelope should have 0.3 ACH. Hence, 0.3 is used and the whole week is optimized again. Figure 4.45 compares the simulated results with measured NMPC results. With less air infiltration, the pre-cooling time became longer with 3 to 4 time step ahead of occupant's morning arrival instead of 1 time step. In addition, the cooling system shut down several time steps earlier over leaving time of the occupancy.

4.2.3.3 Sensitivity Analysis of Cooling Controls

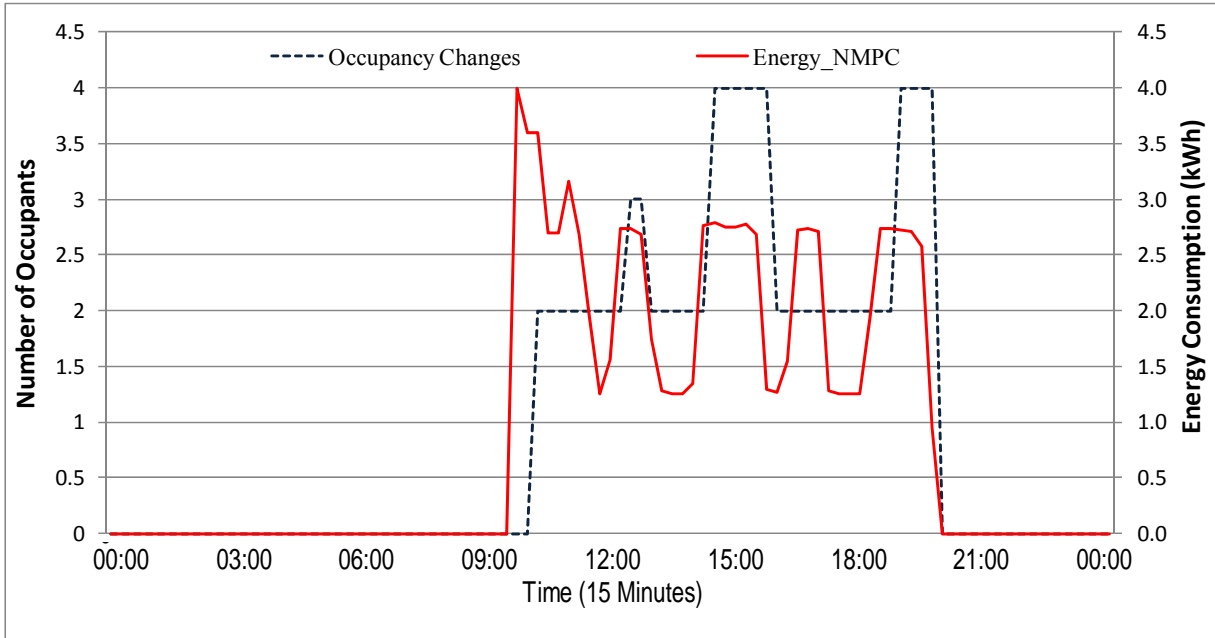


Figure 4.46 Cooling energy profile of high occupancy changes on July 6, 2010

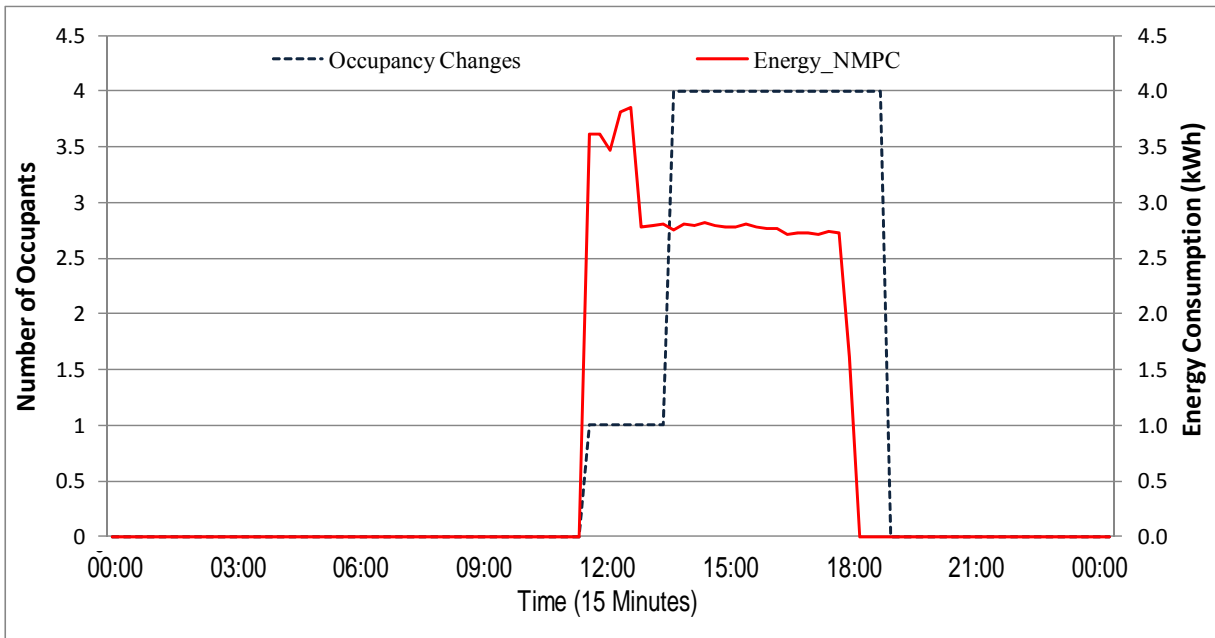


Figure 4.47 Cooling energy profile of moderate occupancy changes on July 8, 2010

Figure 4.46 and Figure 4.47 show the cooling energy consumption profiles with high and moderate occupancy changes, respectively. The cooling energy consumption changes while the occupancy level changes. This is because the cooling system is an air-based system, which can provide almost instant cooling into the space. Figure 4.46 shows that cooling energy consumption changes with the changes of level of occupancy. However, between 15:00 and 16:00 in the afternoon, although the occupant number does not change, the cooling energy consumption increases. This is because the outdoor temperature increases and the cooling system tries to meet the temperature set-point in the next few hours. Figure 4.47 shows that when the occupancy level is constant, the cooling energy consumption is also constant to maintain the indoor temperature set-point.

4.3 Summary

In this chapter, a nonlinear model predictive control is designed and implemented in the Solar Decathlon House test bed in real time. This NMPC integrates weather forecasting model and occupant behavior pattern models. Both predictions have within 80% of accuracy. The real time optimization is solved based on the dynamic programming algorithm. The outputs are then implemented through LabVIEW in the test-bed. The results show that the heating energy consumption is saved by 26% compared with usual daily set-point and night setback temperature control strategy, while cooling energy is saved by 17.8%. The saving during the heating season are mainly from the thermal lag effects of radiant floor heating system while estimating the morning arrival time of occupants. The heating energy is not sensitive to the occupancy level changes. The saving during the cooling season are from the fast dynamic set-points' changes from the cooling system while estimating the duration of the occupants in the space. The cooling energy is sensitive to the occupancy level changes. The measured indoor temperatures for both cases are within set-point temperature bands.

5.1 Contributions

The major contribution of this thesis is the introduction of an HVAC real time control strategy which integrates real time weather forecasting and dynamic occupant behavior pattern predictions based on environmental sensors.

Based on this approach, the conventional HVAC system control changes in two fundamental ways:

First, the control of NMPC-based HVAC systems becomes active instead of passive, where the conventional HVAC system only responds to the scheduled indoor set-point temperature without knowing any other information. The integrated HVAC control can actively predict the control profile and state variables (e.g., indoor air temperature) based on the validated building HVAC models and weather forecasting information. Thus, with the predicted information, the energy consumption of HVAC system can be optimized.

Second, the real time occupant behavior patterns are integrated with HVAC controls, which change the conventional control from a single set-point temperature to a dynamic occupancy based schedule. Thus, when the space is unoccupied, there is no need to maintain the conventional temperature set-point. In addition, the operation of HVAC at night is also integrated with the prediction of occupants' arrival time of the second day. Furthermore, the ventilation rate can be adjusted according to the number of occupants in the space. Thus, such control can operate the HVAC system dynamically and result in energy saving while maintaining desirable set-point temperature. The new features of the integrated HVAC control contributes to

the next generation of building energy management systems in both residential and commercial buildings.

5.2 Summary of Findings

This study presents an HVAC control strategy integrating weather forecasting and occupant behavior pattern predictions. In this approach, a comprehensive heat transfer and thermal dynamic model for the test-bed is developed. The occupancy pattern models are developed based on Hidden Markov Models and Hidden Semi Markov Model to estimate both number of occupants and occupancy duration in the space. The real-time local weather forecasting models are developed as well to have future weather information as inputs for the building model. A nonlinear model predictive controller is designed for the HVAC systems based on dynamic programming.

The feasible implementation of the proposed HVAC control is proven through a two-month heating, and a week of cooling and ventilation experiment in a Solar Decathlon House test bed. A large scale sensor network is setup to measure environmental parameters including temperature, humidity, CO₂, lighting, motion and acoustics and power consumptions from plugs, computers, HVAC equipment and appliances. The building model is then validated through measured data. The occupancy data is collected through paper-based time logs. The occupancy models are also calibrated and validated through almost half of year data collection.

Finally, the implementation of the HVAC control is through LabVIEW and its DAQ control board for the heating season and manually programmed in the remote controller for the cooling season. Following is a summary of the findings in this study:

- 1) The most important sensors for the accurate occupant behavior pattern prediction are CO₂, acoustics and motion. However, there is always a time delay for the number of occupancy estimation because indoor CO₂ level takes time to build up. Thus, the abrupt changes of occupancy cannot be estimated. The overall accuracy achieves up to 90% in a closed space. In addition, when the window is open, the developed algorithm for occupancy detection does not

work because indoor CO₂ is mixed up with outdoor CO₂ and no longer an important feature to indicate number of occupant in the space. Hence, the developed occupant behavior pattern algorithm only works for a closed space.

2) The sensitivity analysis of system identifications of building zone and system models shows that the overall heat transfer coefficients between indoor air and building internal surfaces such as internal walls and concrete slab vary from 30% to 50% with different training and test data sets. Building material properties such as resistances and capacitances are relatively constant.

3) During the heating season, the result from NMPC shows a 26% energy reduction compared to the scheduled temperature set-point control. This saving is mainly from the predicted occupancy arrival time on the next day compared with the pre-defined schedules. It is interesting to find that the NMPC maintains the indoor temperature at certain level without turning off the heating system at night, which saves energy, instead of maintaining a night set-back. Since the response of radiant floor heating system is slow, the sensitivity analysis shows that the predicted daily dynamic occupancy schedule does not impact on the heating energy consumption significantly. In addition, when the outdoor temperature is below -10 °C, the heating has to be on all the time to meet the temperature set-point. In that case, NMPC performs similarly as the schedule temperature set-point control.

4) During the cooling season, the result from NMPC shows a 17.8% energy saving. Since the cooling system is over-sized and brings down the temperature very quickly, the pre-cooling period is normally one time step (15 minutes). The saving is mainly from the dynamic control of cooling set-point based on the real-time occupancy schedules. In addition, the ventilation rate for different occupancy level is also contributed.

5.3 Future Work

This research contributes to the next generation of the HVAC control to further save energy consumption in buildings. The developed NMPC based on dynamic occupant patterns have

demonstrated its benefits through actual implementations in a single zone of one building. The research findings of this study point to the further research directions:

a. Multi-zone full-scale implementation

In this study, only one zone in the Solar Decathlon test bed is controlled. The developed NMPC can be further implemented in a multi-zone building fully equipped with necessary sensors, with more varied levels of occupancy. The algorithms developed in this study can then be tested to catch the dynamics of occupancy as much as possible in a whole building level.

b. Integration with mix-mode operation

This current study does not consider the interaction between occupancy and window opening to take advantage of passive design. Those interactions will generate another control problem within the so-called mix-mode building operation which requires further investigation.

c. Development of a fast global optimization algorithm

In this study, a dynamic programming algorithm is implemented. However, dynamic programming still cannot guarantee a global optimal point all the time. A new fast global optimization algorithm should be developed. There are some pioneering studies of dynamic optimization applied in building energy studies (Zava, et al. 2010). However, there is no demonstration case study which actually implements this in real buildings.

References

Akesson, J. 2008. Optimica—an extension of modelica support dynamic optimization. *Proceedings of Modelica*.

Andreas, W. and L. T. Biegler. 2005. Line search filter methods for nonlinear programming: motivation and global convergence. *SIAM Journal of Optimization*, 16, 1, pp. 1-31.

Abushakra B., J. Haberl and D.E. Claridge. 2004. Overview of existing literature on diversity factors and schedules for energy and cooling load calculations (1093-RP). *ASHRAE Transactions* 110(1).

ASHRAE SSPC 135. Last reviewed: 01/31/2008. <http://www.bacnet.org/WG/XML/>.

ASHRAE. 2009. *Handbook of Fundamentals*. ASHRAE.

ASHRAE. 2004. Standard 62.1 Ventilation for acceptable indoor air quality. ASHRAE

Augenbroe, G. 1992. Integrated building performance evaluation in early design stages. *Building and Environment*. Vol. 27, pp.149-161.

Anderson, B. and A. Moore. 1998. AD-trees for Fast Counting and for Fast Learning of Association Rules. *Knowledge Discovery from Databases Conference*.

Barney, L.C. and C.C. Lynne. 2007. *Web-based Enterprise Energy and Building Automation Systems*. Fairmont Press, Inc.

Bellman, R. and R. Kalaba. 1965. *Dynamic programming and modern control theory*, Academic Press, New York.

- Bourgeois, D., C. Reinhart and I. Macdonald. 2006. Adding Advanced Behavioural Models in Whole Building Energy Simulation: A Study On the Total Energy Impact of Manual and Automated Lighting Control. *Energy and Buildings* Vol. 38, pp.814-823
- Bazjanac, V. 2004. Building Energy Performance Simulations as Part of the Interoperable Software Environments. *Building and Environment*. Vol. 39, pp. 879-883.
- Brambley, M., D. Hasen, P. Haves, D. Holmberg, S. McDonald, K. Roth and P. Torcellini. 2005. *Advanced Sensors and Controls for Building Applications: Market Assessment and Potential R&D Pathways*. Pacific Northwest National Lab. Report No. 15149.
- Braun, J. and N. Chaturvedi. 2002. An inverse gray-box model for transient building load prediction. *HVACR Research* : 8, 72~99.
- Braun, J. 2007. Intelligent building systems- past, present, and future. *Proceedings of American Control Conference*. July 11-13. New York. USA.
- Bathorn, R., A. Koopman and S. Siebes. 2006. *A. Frequent Patterns that Compress*, Technical Report, Utrecht University.
- Camocho, E.F. and C. Bordons. 2003. *Model Predictive Control*. Springer.
- Clark J A, 2001. Control in building energy management systems: the role of simulation, *Proc. of the 7th Conference on International Building Performance Simulation Association*.
- Coffey, B. 2008. *A Development and Testing Framework for Simulation-Based Supervisory Control With Application to Optimal Zone Temperature Ramping Demand Response Using a Modified Genetic Algorithm*. Master Thesis, Concordia University, Quebec, Canada, 2008.
- Claridge, D.E., B. Abushakra, J. Haberl and A. Sreshthaputra. 2004. Electricity Diversity Profiles for Energy Simulation of Office Buildings. *ASHRAE Transactions* 110(1).

Capehart, B. 2007. *Web-based Enterprise Energy and Building Automation Systems*. Fairmont Press, Inc.

Coleman, T.F. and L. Yuying. 1994. On the convergence of interior-reflective Newton methods for nonlinear minimization subject to bounds. *Mathematical Programming*. Vol. 67, pp 189-224.

Cook, D. and S. Das. 2004. *Smart Environments: Technology, Protocols and Applications*. Wiley.

Clarke, J.A. 2001. *Energy simulation in building design*. Butterworth Heinemann, London.

Crawley, D.B., Lawrie, L.K. Pedersen, C.O., Liesen, R.J., Fisher, D.E. Strand, R.K. Taylor, R.D. Winkelmann, R.C. Buhl, W.F. . Huang, Y.J. Erdem, A.E. 1999. ENERGYPLUS, A New-Generation Building Energy Simulation Program, *Proceedings of Building Simulation '99, an IBPSA Conference*, Kyoto, Japan, pp. 81- 88

Degelman L.O. 1999. A Model for Simulation of Daylighting and Occupancy Sensors as an Energy Control Strategy for Office Buildings, in: *Proceedings of Building Simulation '99, an IBPSA Conference*, Kyoto, 571-578.

Dong, B., K.P. Lam, Y.C. Huang, G. M. Dobbs. 2007. A comparative study of the IFC and gbXML informational infrastructures for data exchange in computational design support environments. *Proc. of the 10th Conference on International Building Performance Simulation Association*. Beijing, China.

Duong, T.V. D.Q. Phung, H.H. Bui and Venkatesh, S. Human. 2006. Behavior Recognition with Generic Exponential Family Duration Modeling in the Hidden Semi-Markov Model. *In Proceedings of the 18th international Conference on Pattern Recognition*. Vol. 3.

Droste, S., T. Jansen, I. Wegener. 2002. On the analysis of the (1 + 1) evolutionary algorithms. *Theoret. Comput. Sci* 276: 51–81.

Diane J.C. and Sjal K.D. 2005. *Smart Environments, Chapter 9*. John Wiley & Sons, Inc.

Dodier, R.H., Henze, G.P., Tiller, D.K., Guo, X. 2006. Building occupancy detection through sensor belief networks. *Energy and Buildings*, Vol.28 (9), pp 1033-1043.

eBIDS. <http://cbpd.arc.cmu.edu/ebids/pages/home.aspx>, latest access on 08/11/2010/

Emmerich, S.J. and Persily A.K. 2001. “State-of-the-art review of CO2 demand controlled ventilation technology and application”, *NISTIR 6729*.

Engineering ToolBox, <http://www.engineeringtoolbox.com/>. Last accessed, 2009.

Eiben, A.E. and G. Rudolph. 1999. “Theory of evolutionary algorithms: A bird’s eye view”. *Theoret. Comput. Sci.* vol 299.

EIA. 2009. <http://www.eia.doe.gov/emeu/cbecs/>. Commercial buildings energy consumption survey data.

Elfeky, M. G. and Lemagarmid, A.K. 2005. Periodicity Detection in Time Series Databases. *IEEE Trans. on Knowl. and Data Eng.* Vol.17, 875-887.

Fritsch R., Kohler A., Nygard-Ferguson M. and Scartezzini J.-L. 1990. A Stochastic Model of User Behaviour Regarding Ventilation. *Building and Environment* 25 (2): 173-181.

Gauchel, J., S. Hovestadt, V. Wyk, and R. Bhat. 1992. Building modeling based on concepts of autonomy. *Proceedings of AID*, Pittsburgh, PA. USA.

Federspiel, C.C. 1997. Estimating the inputs of gas transport processes in buildings, *IEEE Transactions on Control Systems Technology* Vol.5, pp 480–489.

He, J., and X. Yao. 2007. Drift analysis and average time complexity of evolutionary algorithms. *Artificial Intelligence*. Vol.127. pp.57–85.

Henze, G. P., R. H. Dodier, and M. Krarti. 1997b. Development of a predictive optimal controller for thermal energy-storage systems. *Int. J. of HVAC&R Res.*. Vol.3. pp. 233–264.

Henze, G.P., F. Clemens and K. Gottfried. 2004. Evaluation of optimal control for active and passive building thermal storage. *International Journal of Thermal Sciences*. Vol. 43: 173-183.

Henze, G.P., D.E. Kalz, S. Liu and C. Felsmann. 2005. Experimental analysis of model-based predictive optimal control for active and passive building thermal storage inventory. *HVAC&R Research* 11(2):189-214.

He, J. and X. Yao. 2002. From an individual to a population: An analysis of the first hitting time of population-based evolutionary algorithms, *IEEE Trans. Evolutionary Comput.* Vol. 6 pp.495–511.

Hunt, K. and G.P. Nason. 2001. Wind speed modeling and short-term prediction using wavelets, *Wind Engineering*. vol. 25. pp. 55–61.

Hocaoglu, F., M. Fidan, and O. Gerek. 2009. Mycielski approach for wind speed prediction, *Energy Conversion and Management*. Vol.50, pp.1436–1443.

Hagras, H., V. Callaghan, M. Colley, G. Clarke, A. Pounds-Cornish, and H. Duman. 2004. Creating an ambient-Intelligence environment using embedded Agents. *IEEE Intelligent Systems* 19, 6.

Heierman, H., G.M. Youngblood and D. Cook. 2004. Mining Temporal Sequences to Discovery Interesting Patterns, *KDD Workshop on Mining Temporal and Sequential Data*.

Hassoun, M.H. 1995. *Fundamentals of Artificial Neural Network*. MIT Press.

Jimenez, M., H. Madsen and K. Andersen. 2008. Identification of the main thermal characteristics of building components using MATLAB. *Building and Environment* 43, 170-180.

Jiang, X.Q. and B. Dong. 2010. Adaptive Gaussian process for short-Term wind speed forecasting *Proceedings of 19th European Conference on Artificial Intelligence - ECAI 2010*. Lisbon, Portugal. September.

Kummert, K. and P. Andre. 2005. Simulation of a model-based optimal controller for heating systems under realistic hypotheses. *Proceedings of 9th IBPSA 2005*. Montreal, Canada.

Lawrence Berkeley National Laboratory. 2006b. Simulation problem analysis and research kernel (SPARK). Available online from: <http://gundog.lbl.gov/VS/spark.html> Berkeley, Calif.: Lawrence Berkeley National Laboratory.

Lymberopoulos, D. A. Bamis, T. Teixeira and A. Savvides. 2008. BehaviorScope: Real-Time Remote Human Monitoring Using Sensor Networks. *Proceedings of International Conference on Information Processing in Sensor Networks*.

Lam, K.P. M. Höynck, Dong, B., Andrews, B. Chiou, Y.S. Zhang, R. and Benitez, D. 2009. Occupancy detection through an extensive environmental sensor network in an open-plan office building. *Proceedings of Building Simulation '2009, an IBPSA Conference*, Glasgow.

Lam, K.P. M. Höynck, Zhang, R., Andrews, B. Chiou, Y.S. Dong, B. and Benitez, D. 2009. Information-theoretic environmental features selection for occupancy detection in open offices. *Proceedings of Building Simulation 2009* Glasgow.

Lam, K.P. 1994. *A computational design support system for interactive hygro-thermal analysis of building encloures*. Ph.D. Thesis. Carnegie Mellon University.

Lesser, V., M. Atighetchi, B. Benyo, B. Horling, A. Raja, R. Vincent, T. Wagner, X. Ping and S.X. Zhang. 1999. The intelligent home testbed. *In Proceedings of the Autonomy Control Software Workshop.*

Liu, S. and G.P. Henze. 2006. Experimental analysis of simulated reinforcement learning control for active and passive building thermal storage inventory. Part 2. Experimental results, *Energy and Buildings*, 38. pp.148–161.

Ma, Y., F. Borrelli, B. Hencsey, A. Packard and S. Bortoff. 2009. Model predictive control of thermal energy storage in building cooling systems. *48th IEEE Conference on Decision and Control.*

Magni, L. G.D. Nicolao, R. Scattolini¹, and F. Allgöwer. 2003. Robust model predictive control for nonlinear discrete-time systems. *Internal Journal of Robust and Nonlinear Control*. Vol.13 (4). pp.229-246.

McKinley, T. and A. Alleyne. 2008. Identification of building model parameters and loads using on-site data logs. *SimBuild*. 2008.

Mechaqrane, A. and M. Zouak. 2004. A comparison of linear and neural network arx models applied to a predication of the indoor temperature of a building. *Neural Comput and Appliccation*.13, 32-37.

Mendes, N., G.H.C. Olivera, H.X. Araujo, and L.S. Coelho. 2003. A Matlab-based simulation tool for building thermal performance analysis. *Proceedings of Building Simulation '2003*, an IBPSA Conference.

Mitchell, T.1997. *Machine Learning*, McGraw-Hill. Mozer M. 1998. The neural network house: An environment that adapts to its inhabitants. In *Proceedings of the AAAI Spring Symposium on Intelligent Environments*, pp 110–114.

Mohammadian, M., X. Yao. 2002. *Evolutionary Optimization*, Chapter 14, Kluwer Academic, Boston. pp. 349–370.

Moore, B.J. and D.S. Fisher. 2003. Pump differential pressure setpoint reset based on chilled water valve position. *ASHRAE Transactions* 109(1): 373-79.

Murphy, K. 2002. Hidden semi-Markov Models. Technical Report. University of British Columbia.

Nassif, N., S. Kajl, and R. Sabourin. 2005. Optimization of HVAC control system strategy using two-objective genetic algorithm. *HVAC&R Research* 11(3):459-86.

Rabiner, L.R. 1989. A Tutorial on hidden markov models and selected applications in speech recognition. *Proceedings of the IEEE*, Vol.77 (2), pp. 257–286.

Palomares, J. C., J. J. G. Rosa, J. G. Ramiro, J. Melgar, A. Aguera, and A. Moreno. Comparison of models for wind speed forecasting. *Proc. of International Conference on Computational Science* (2009).

Page, J., D. Robinson, N. Morel and J. L. Scartezzini. 2007. A Generalised Stochastic Model for the Simulation of Occupant Presence. *Energy and Buildings*. Vol. 40 (2). pp. 83-98.

Reinhart, C. 2004. Lightswitch-2002: A Model for Manual and Automated Control of Electric Lighting and Blinds. *Solar Energy*. Vol. 77, pp. 15-28.

Russell, M. J. and Moore, R. K. 1985. Explicit modelling of state occupancy in hidden Markov models for automatic speech recognition. *In Proceedings of IEEE Conference on Acoustics Speech and Signal Processing*, pp. 5–8.

Roy, A., Das, S.K. and Basu, K. 2007. A Predictive Framework for Location-Aware Resource Management in Smart Homes. *IEEE Transactions on mobile computing*, Vol. 6 (11).

Rink, R.E. N. Li. 1995. Aggregation/disaggregation method for optimal control of multizone HVAC systems. *Energy Conversion and Management* 36(2): 79-86.

Sane, H. and M. Guay. 2008. Minmax dynamic optimization over a finite-time horizon for building demand control. *Proceedings of American Control Conference*. June 11-13, Seattle, Washington, USA.

Shamshad, A. M., A. Bawadi, W. W. Hussin, T.A. Majid, and S. Sanusi. 2005. First and second order Markov chain models for synthetic generation of wind speed time series. *Energy*. vol. 30, pp.693–708.

Sherman, M.H. and Grimsrud, D.T. 1980. Measurement of infiltration using fan pressurization and weather data. *1st Symposium of the air infiltration centre on instrumentation and measurement techniques*, Windsor, England.

Steftos, S. 2000. A comparison of various forecasting techniques applied to mean hourly wind speed time series. *Renew Energy*. 21, 23–35.

Smaton, A. and McHugh, M. 2006. Event Detection in an Audio-based Sensor Network. *Multimedia Systems*. Vol. 12 pp179-194.

Stanislav, F., G. Carlos, P. Mark, and S. Rahul. 2006. Distributed Localization of Networked Cameras, *In the Fifth International Conference on Information Processing in Sensor Networks*.

The MathWorks. 2010a. MATLAB. Natick, MA.

TRNSYS. 2009. <http://sel.me.wisc.edu/trnsys/index.html>

Tore, M.C., P. Poggi, and A. Louche. 2001. Markovian model for studying wind speed time series in corsica, *Renew Energy*, 3, 311–319.

Trivedi, M., K. Huang and I. Mikic. 2000. Intelligent environment and active networks. *Proceedings of IEEE International Conference on Systems, Man, and Cybernetics*.

Torrance, M.C. 1995. Advances in human-computer interaction: The intelligent room. *In Working Notes of the CHI 95 Research Symposium*.

Underwood, C.P. 1999. *HVAC Control: Modeling, Analysis and Design*. Taylor & Francis Group.

Vapnik, V.N. 1995. *The Nature of Statistical Learning Theory*, Springer.

Wetter, M. 2005. BuildOpt - A new building energy simulation program that is built on smooth models. *Building and Environment*, 40:1085--1092.

Wetter, M. and C. Haugstetter. 2006. Modelica versus TRNSYS -- A Comparison Between an Equation-Based and a Procedural Modeling Language for Building Energy Simulation. *Proc. of the 2nd SimBuild Conference*, Cambridge, MA, USA, August 2006.

Wetter, M. 2006. Multizone Building Model for Thermal Building Simulation in Modelica. *Proc. of the 5th International Modelica Conference*, Vienna, Austria.

Weiss, M.A. 2007. *Data Structures and Problem Solving Using Java Data Structures and Problem Solving Using Java*. Addison-Wesley.

WBCSD. 2009. "Transforming the Market: Energy Efficiency in Buildings". *World Business Council for Sustainable Development*.

Wächter, A. and L. T. Biegler, 2005. Line Search Filter Methods for Nonlinear Programming: Motivation and Global Convergence, *SIAM Journal of Optimization*, 16, 1, pp. 1-31.

Wegener, I. 2000. *Methods for the analysis of evolutionary algorithms on pseudo-Boolean functions*. Technical Report. University of Dortmund.

Wang, D., Federspiel C. and Rubinstein F. 2005. Modelling occupancy in single person offices. *Energy and Buildings* 37: 121-126.

Wang, S.W. and Jin, X.Q. 1998. CO₂-based occupancy detection for on-line outdoor air flow control. *Indoor+Built Environment*. Vol. 7 pp 165-181.

Wang, S.W. and Jin, X.Q. 2000. Model-based optimal control of VAV air-conditioning system using genetic algorithm. *Building and Environment*. 35(6): 471-87.

Wang, S. and X. Xu. 2006. Simplified building model for transient thermal performance estimation using ga-based parameter identification. *International Journal of Thermal Sciences* 45, 419~432.

Xu, P. and P. Haves. 2004. A simulation-based testing and training environment for building controls. *Proceedings of SimBuild*, Boulder, Colorado, 2004.

Xing, H.Y. 2004. *Building load control and optimization*. Ph.D.Thesis, MIT.

Youcef, F., H. Sauvageot, and A. Adane. Statistical bi-variate modeling of wind using first order markov chain and weibull distribution,. *Renew Energy*. 28, 87–80, (2003).

Youngblood, G.M. and D. Cook, 2007. Data Mining for Hierarchical Model Creation. *IEEE Transactions on system, man and cybernetics*. Vol. 37, No.4.

Yu, S.Z. and H. Kobayashi. 2003. An Efficient Forward-Backward Algorithm for an Explicit-duration HMM, *IEEE Signal Processing*.

Zaheer-uddin, M. and R.V. Patel. 1995. Optimal tracking control of multi-zone indoor environmental spaces. *ASME transactions on dynamic system, measurement and control*.

Zaheer-uddin, M. and G.R. Zheng. 2001. Multistage optimal operating strategies for HVAC systems. *ASHRAE Transaction* 107(2), pp346-52, 2001.

Zava, J., J. Wang, S. Leyffer, E. Constantinescu, M. Anitescu, and G. Conzelmann. 2010. Proactive energy management for next-generation building systems. *SimBuild 2010*, New York. U.S.A.

Zheng, G.R., and M. Zaheer-uddin. 1996. Optimization of thermal processes in a variable air volume HVAC system, *Energy, the Int. Journal*, Vol.21 (5), pp.407-420.

Zhang, Y. and V.I. Hanby. 2006. HVAC & R research. Model-based control of renewable energy systems in buildings. *HVAC&R Research Vol (12)*.pp. 577-598.